National Library of Canada

Acquisitions and Bibliographic Services

395 Wellington Street
Ottawa ON K1A 0N4
Canada

Bibliothèque nationale du Canada

Acquisitions et services bibliographiques

395, rue Wellington
Ottawa ON K1A 0N4
Canada

Your file Votre référence

Our file Notre référence

The author has granted a non-exclusive licence allowing the National Library of Canada to reproduce, loan, distribute or sell copies of this thesis in microform, paper or electronic formats.

L'auteur a accordé une licence non exclusive permettant à la Bibliothèque nationale du Canada de reproduire, prêter, distribuer ou vendre des copies de cette thèse sous la forme de microfiche/film, de reproduction sur papier ou sur format électronique.

The author retains ownership of the copyright in this thesis. Neither the thesis nor substantial extracts from it may be printed or otherwise reproduced without the author's permission.

L'auteur conserve la propriété du droit d'auteur qui protège cette thèse. Ni la thèse ni des extraits substantiels de celle-ci ne doivent être imprimés ou autrement reproduits sans son autorisation.

0-612-69709-6

Canada

The University of Alberta

Library Release Form

Name of Author: Jim John Fuite

Title of Thesis: The Effects of the Fractal Structure of the Liver Upon the Pharmacokinetics of Mibefradil

Degree: Master of Science

Year the Degree Granted: 2002

Permission is hereby granted to the University of Alberta Library to reproduce single copies of this thesis and to lend or sell such copies for private, scholarly, or scientific purposes only.

The author reserves all other publication and other rights in association with the copyright in the thesis, and except as herein before provided, neither the thesis nor any substantial portion thereof may be printed or otherwise reproduced in any material form whatever without the author's prior written permission.

Jim John Fuite
P.O. Box 4784
Ponoka, AB
T4J 1S5

10 April, 2002

The University of Alberta

Faculty of Graduate Studies and Research

The undersigned certify that they have read, and recommend to the Faculty of Graduate Studies and Research for acceptance, a thesis entitled **The Effects of the Fractal Structure of the Liver Upon the Pharmacokinetics of Mibefradil** submitted by **Jim Fuite** in partial fulfillment of the requirements for the degree of Master of Science.

J. A. Tuszynski (Supervisor)

M. W. Radomski (External)

Richard Sydora

R. D. Sydora

M. Y. Li

Date: 6 December, 2001

Abstract

Classical mass action kinetics are generally so assumed to occur that its basic tenets are rarely questioned. However, elementary chemical kinetics are quite different when reactions are dimensionally restricted. The compact Brownian motion of the drugs leads to anomalous diffusion and to atypical rate laws. Under these conditions, the conventional rate law exhibits a characteristic reduction of the rate constant with time. These anomalous macroscopic rate laws are a manifestation of the entropic self-ordering of reacting molecules on a mesoscopic scale.

This report is an attempt to describe the pharmacokinetics of the drug mibefradil utilizing these physical arguments. A physiologically motivated model is designed with the goal of improving the accuracy of the data descriptions and to provide mechanistic insights into the pharmacokinetics of mibefradil. The heterogenous interpretation of drug kinetics within the liver is adopted by the inclusion of a time-dependent rate coefficient, while the liver itself was argued to be fractal like. As an outcome of the implementation of the model, an experimental value for the spectral dimension of a dog liver is produced. Along the way, the basic principles of pharmacokinetics, and scientific modeling, philosophy, and statistics are contemplated.

The Table of Contents

Abstract

Table of Contents

List of Tables

List of Figures

List of Symbols

Foreword 1

1. A Few Pharmacokinetic Forethoughts for Physicists 3
    - •An Overture of Basic Pharmacokinetic Concepts 3
    - •A Reminder of Classical Kinetics 6
        - ○A Brief Explanation of Michaelis-Menten Kinetics 10
    - •A Review of Classical Pharmacokinetic Models 12
    - •A Synopsis of Physiologically Based PharmacoKinetic (PBPK) Models . . 15
        - ○Some Theoretical Context 15
        - ○The Mathematical Framework for a Flow-Limited Lumped-Parameter PBPK Model 20
    - •A Note on Noncompartmental Analysis 21

2. Certain Remarks on Scientific Modeling 25
- •Some Comments on the Philosophy of Modeling 25
- •A Concrete Proem to Modeling in Pharmacokinetics 28
- •The Practicalities of Modeling in Pharmacokinetics 32

3. An Initial Consideration of the Biological Model System 41
- •A Summary of Relevant Knowledge on Mibefradil 41
- •A Scrutiny of the Data by Empirical Curve Fitting 44
    - ○A Brief Rationale 44
    - ○The Debut of a Modified Prony's Method to Include Weighted Datum Points for Curve Fitting in Pharmacokinetics . . . 45
    - ○A Justification for Restriction of the Data 56
    - ○A General Technique of Nonlinear Fits with a Global Optimization Method 57
    - ○A Second Study of the Sums of Exponentials 61
    - ○The Analytical Equations Implied by Michaelis-Menten Kinetics . . 64
    - ○A Fit by a Single Power Function 66
    - ○Several Illations from Empirical Curve Fitting 67

4. A Furtherance of the Metabolic Context of Mibefradil 69
- •A Curt Overview of Liver Physiology 69
    - ○The Liver as a Fractal 72
- •An Introduction to Fractals 74
- •The Implications of Fractal Kinetics 82
- •Phenomenological Issues 84
- •The Thesis 86

5. The Development of a Theoretical Model 87
- An Approximate Analytical Solution by Perturbation Methods 91

6. Model Predictions & Comparison to Data 95
- The Spectral Dimension of the Dog Liver 100
- Model Adequacy 104

7. Discussion 106

8. Conclusions 109

References 111

Appendix 117
- An Introduction to Lambert's W Function 117
- A Recapitulation of the Method of Least-Squares Approximation Over Discrete Sets of Points 118
- A Brief Definition of the Gaussian Distribution 120
- Coda of Pharmacokinetic Concepts 121
  - Volume of Distribution 121
  - Additional Noncompartmental Analysis Formulas 122
- Expounders of the Development of the PBPK Model 122
  - An Introduction to the Matrix Exponential 123
  - The Definition of the Method of Variation of Parameters 124
- Expounders of the Solution of the Multicompartmental Mathematical Model 124

Glossary of Scientific, Literary, and Biographical Vocabulary . . 125

List of Tables

Table 3.1: A comparison of empirical fits to the pharmacokinetic data by equations utilizing three distinct types of functions as measured by the chi-squared figure-of-merit function. 68

List of Figures

Figure 1.1: A didactic diagram introducing indicative pharmacokinetic concentration time course data, (t_i, C_i), $i=1,2,\ldots,n$, fit by a function, $C[t]$ 4

Figure 1.2: A notional diagram of the microscopic conditions nearby an single annihilating trap. Whenever movements caused by diffusion bring two distinct species together closer than R, annihilation of C occurs. 8

Figure 1.3: A schematic of a general 2-compartment model where the sources enter, and measurements are taken from, the central compartment. The ith-compartment is considered open if it looses drug to the environment, $k_{0i}>0$, otherwise it is closed, $k_{0i}=0$. A multicompartmental model is considered mammillary if the secondary compartments are connected to the central compartment in a parallel arrangement, and is considered catenary if the secondary compartments are connected in a series alignment 13

Figure 1.4: An abstract representation of a Physiologically-Based Pharmacokinetic (PBPK) Model indicating: a structural interrelationship between organs and tissue groupings, a possible internal arrangement within an organ, and an indication of some biochemical and physicochemical concerns within an organ or a part thereof 16

Figure 1.5: A general mass balance equation for a lumped-parameter compartment 18

Figure 1.6: An illustration of the possible internal structures of a compartment depending on the speculated rate limiting transport process in the subcompartments 19

Figure 1.7: The basic physical model structure implied by noncompartmental analysis when a scientific physiological interpretation is made. 22

Figure 2.1: An abstract block diagram indicating the distinction and relations between the biological model system, the measurement system, and the variables used to construct the mathematical model 30

Figure 2.2: A hypothetical two-dimensional confidence region ellipse centered at $\bar{a}$ corresponding to values of chi-square larger than the fitted minimum. The one-dimensional confidence intervals for the parameters are indicated by the appropriate projections of the region onto the axes 36

Figure 2.3: An abstract block diagram sketching the Monte Carlo simulation of an experiment. Computer generated random numbers are used to synthesize many simulated data sets from the single experimental realization. It is assumed that the statistical distribution of synthetic Monte Carlo parameters, ${}^{i}_{S}\hat{\mathbf{a}}$, $i = 1, \ldots, N$, around the fitted parameters, ${}^{0}\hat{\mathbf{a}}$, is similar to the distribution of hypothetical parameters, ${}^{i}\hat{\mathbf{a}}$, $i = 1, \ldots, \infty$, around the true parameters, ${}^{\text{true}}\hat{\mathbf{a}}$ 39

Figure 3.1: A representative concentration verses time data set from the dog model system studied with a characteristic sharp peak and elongated tail. The measured concentrations are of Mibefradil in the plasma of the number two dog taken at various times from the portal vein after an intravenous dose (IV-PV-D2). The uncertainty of the concentration measurements was calculated to be 9%. 42

Figure 3.2: A curve generated using a sum of six exponential terms fit by the standard Prony's method compared to the concentration time-course data taken after an intravenous dose from the portal vein of dog number two (IV-PV-D2) 48

Figure 3.3: A plot of the weighted residual squared for each of the real datum points separated in time to indicate their relative contribution to the disparity with the curve produced by Prony's method as measured by the chi-squared figure-of-merit function for the trial IV-PV-D2 49

Figure 3.4: A plot of the calculated aggregate weight values assigned to each of the N-M equations of (3.7) for the IV-PV-D2 data. Large values cluster around real datum assigned large weights whereas zero values indicate equations constituted entirely of interpolated data given no weight 52

Figure 3.5: A curve generated using a sum of six exponential terms determined by the weighted Prony's method to the IV-PV-D2 concentration time-course data exhibiting an improved fit, but where arrows indicate anomalous behavior 54

Figure 3.6: An inspection of the very early time behavior of the concentration time-course data for each dog model indicating the initial increase in drug concentration occurs over a shorter time than the resolution of the experiment. 57

Figure 3.7: A heuristic illustration along one-dimension of the first two stages of the AGR procedure for minimization of a hypothetical merit function with many local minima starting with a grid size of seven over a defined domain 60

Figure 3.8: A Semi-Log plot of [Mibefradil] verses time shows an intuitive estimation of the domain of the linear elimination before curve stripping for the IV-PV-D2 data. The graph and associated buttons below are from an original curve stripping program designed to provide first estimates of parameter values for the original nonlinear fit program Model Maker 62

Figure 3.9: Mibefradil time course data fit with a single exponential term, ■, a sum of two, ■, and a sum of three exponential terms, ▪, for trial IV-PV-D2 63

Figure 3.10: Mibefradil time course data fit with a single term analytical function implied by Michaelis-Menten enzyme kinetics for trial IV-PV-D2 using the original program Model Maker. The calculated value of the chi-square merit function is no better than that of a single exponential term 65

Figure 3.11: Mibefradil time course data fit with a single power term for the trial IV–PV–D2 using the original program Model Maker. The ostensibly apt way a function with so few parameters seems to deftly shift from early to late-time behavior to match the data was impressive 67

Figure 4.1: A picture of the macroscopic branching of the intrahepatic portal vein throughout the liver of a human. Additionally, there are vertebrae (V) visible in the background that offer scale and the catheter (C) that provided a contrast medium. A slightly altered photo taken from ⟨54⟩ 69

Figure 4.2: Two levels of microcirculatory structure within the monkey liver. A tiny near peribiliary portal vein (PPV, arrow) branches from the plexus below to supply blood to a small sinusoid region (S) of a lobule. Magnification ≈ ×500. Photo taken directly from ⟨53⟩ 70

Figure 4.3: A picture of the decidedly structured microvillar surface of the sinusoidal face of and isolated liver cell. Magnification = ×6 000. Photo taken directly from ⟨53⟩ 71

Figure 4.4:. The porous endothelial lining of a sinusoid containing fenestrae (pores or holes) on different scales of size (but all smaller than the diameter of an erythrocyte). The two faint black arrow heads point to hepatocyte microvilli (see Figure 4.3) protruding through the larger fenestrae into the sinusoid lumen (space). Magnification= ×10 000. Photo taken directly from ⟨53⟩ 72

Figure 4.5: A cross-section of a liver cell bordering a sinusoid. Numerous irregularly oriented microvilli project into the narrow space of Disse between the hepatic cell and the endothelium lining the sinusoid. A black arrow indicates a small fenestra in the the sinusoid lining. Magnification = ×18 000. Photo taken directly from ⟨53⟩ 73

Figure 4.6: Levels 0-8 of a dichotomously branching "tree" in two dimensions generated by a trivial recursive rule: for each generation pairs of branches are added with a length and at an angle relative to the terminal segments of the previous generation. Qualitatively, compare to some aspects of the branching network of microcirculatory structure of Figure 4.2 . . . 75

Figure 4.7. Levels 0-5 of the Sierpinski Gasket. Qualitatively, compare to some aspects of the porous endothelial lining of a sinusoid containing fenestrae on different scales of size in Figure 4.4 76

Figure 4.8: Illustrated calculations of the fractal dimension based on self-similarity considerations for a line, square, and Koch curve. Calculated values for the more general Hausdorff dimension would be similar for the above examples. See Figure 6.1 to view an example of a further developed Koch curve (snowflake) 78

Figure 4.9. My own tentative attempts to construct a knobby fractal. The topological dimension is $d_T = 1$ and the Euclidean space in which the fractal structure is embedded in is $D=2$. Instead of alterations of a one-dimensional line, imagine similar protrusions of a two-dimensional surface and qualitatively, compare to aspects of the microvillar structure on the surface of a hepatocyte in Figure 4.3 79

Figure 4.10: Geometric figures with equal fractal dimensions $d_f \approx 1.65$, but with different spectral dimensions arising from the differences in the connectivity of the geometric objects. The connectivity of the top fractal is equal to six, while for the lower fractal, the connectivity is twelve. Picture taken directly from ⟨68⟩ 80

Figure 4.11: Two identical fractal containers, with identical macroscopic concentrations of reacting molecules, but with different instantaneous reaction rates. The probability for instantaneous reaction is obviously higher in the container on the left. In specifying a concentration, a uniformly random distribution in space of the reactants is implicitly assumed. Only under such an assumption can two containers with the same concentration have identical reaction rates - this seems not to be the case with fractal containers. 85

Figure 5.1: A simple flow limited Physiologically-Based Pharmacokinetic (PBPK) Model where clearance of the drug occurs only in the liver by fractal kinetics 88

Figure 5.2: A comparative graph indicating that the series expansion (5.4) rapidly converges over the domain of t spanning the experimental abscissal data for an experimentally relevant value of ζ 92

Figure 6.1: A diagram of a 2-compartment model where the i.v. bolus source enters, and measurements are taken from, the central compartment. The secondary compartment is considered fractal with a time dependent rate of elimination. Compare to Figure 1.3 96

Figure 6.2: A numerical plot sketch using experimentally relevant numerical values for the parameters to qualitatively suggest the perturbative affects of fractal kinetics on the trajectory in the phase plane for the model system using equations (6.1) and (6.2) (Dr. Li, Associate Professor of Mathematics, University of Alberta, personal communication, 10 September, 2001) 97

Figure 6.3: Comparative graphs of the first three terms impelled by the series of equalities in (6.7) for the pharmacokinetic model employing illustrative values of *a*, *b*, *k*, and **Ӿ**. Notice that the initial conditions for the higher order perturbation terms are met at the origin (✓). The solution implied is $\phi[t] \approx \phi_0[t] + \zeta\phi_1[t] + \zeta^2\phi_2[t]$ 100

Figure 6.4: Mibefradil time course data fit with a three term perturbation series implied by a 2-compartment model with fractal kinetics in the eliminating compartment for trial IV-PV-D2 101

Figure 6.5: The confidence region intersecting the k-ζ plane in parameter space for trial IV-PV-D2, indicating an ellipse of 90% confidence 103

Figure 6.6: The ad hoc chi-square distribution for the model to which a chi-square value may be compared to estimate the probability that such a model could give rise to that data set or to one that fits at least as poorly. The probability is simply the ratio of the statistical weight of the bins to the right of the observed chi-square value to the total number of all observations ($N=300$). Relevant to IV-PV-D2 105

Figure a.1: A graphical comparison of the obscure product log function, $W[z]$, with the related ubiquitous natural logarithm function, ln[z] 117

Figure a.2: (a) The administration of a drug into the body produces a specific plasma concentration. The apparent volume of distribution, $V_{distribution}$, is the volume that accounts for the total dose administered based upon the observed plasma concentration, $C_{concentration}$. (b) Any factor that suppresses the drug plasma concentration will increase the apparent volume of distribution. (c) Conversely, any factor that increases the plasma concentration will decrease the apparent volume of distribution (5) 121

The List of Symbols

A_{el}	the culmulative amount of drug eliminated from the body.
AGR	Adaptive Grid Refinement.
a_j	one of M model parameters.
$\vec{a}$	a vector in M-dimensional parameter space with components a_j.
B	a neighborhood in a topological space.
$\mathcal{B}$	fraction of free unbound drug in the blood or tissue.
C	drug concentration or mass density in the systemic circulation or in a tissue as indicated by a subscript, exempli gratia mg/ml.
C_δ	unit impulse response of the biological model system.
CL	clearance, a flow, exempli gratia ml/s.
D	a region of descent surrounding a local minimum, or the dose given in a biological model system, or the dimension of an embedding Euclidian space - not easily confused.
$\mathcal{D}$	diffusion constant, usually relative between two reactants.
χ^2	chi-squared figure-of-merit statistical function, unitless.
d	dimension, or, a function defining a metric space.
$\boldsymbol{d}$	differential.
δ_{ij}	Kronecker delta.
E	as a subscript to indicate Euclidian dimension.
$\boldsymbol{e}$	Euler's constant ≈ 2.718.
ε	a small positive real number.
$\vec{e}$	data measurement uncertainties.
ER	extraction ratio.
f	a mathematical function; as a subscript to indicate the term fractal.
F	bioavailability, or a name given to a shape as a set.
Γ	the gamma function.
H	a closed surface, or as a subscript to indicate the Hausdorff dimension.

HPLC	High Performance Liquid Chromatography.
i	$\sqrt{-1}$.
IV-PV-D2	intravenous-portal vein-dog two.
j	drug flow density into a tissue or organ, exempli gratia mg/(ml s).
$\vec{J}$	general particle flux.
k	a zero, first, or second order rate coefficient (usually constant).
K_M	Michaelis-Menten constant.
Ϙ	a number between zero and one.
λ_z	terminal rate constant in noncompartmental models.
m	number of state variables in a model, exempli gratia, mass of drug; equal to the number of compartments in a multicompartmetal model.
M	number of variable parameters in a model.
μ	a temporary variable used in Prony's method.
N	number of real datum points to which a model is compared.
n	a real number with local textual relevance, often the number of real datum points or the number of dimensions in a real vector space.
$\mathcal{N}$	number of synthetic Monte Carlo data sets to which a model is compared.
ν	number of degrees of freedom in a calculation.
P	partition coefficient, unitless.
$\mathcal{P}$	probability, unitless.
Ꝑ	incomplete gamma function.
Q	plasma flow rate into or out of tissue, exempli gratia ml/s.
R	rate of drug input reaching the systemic circulation; as a subscript to indicate probability of return.
R_o	zero order rate of constant drug input.
$\mathbb{R}$	the set of real numbers.
$\mathbb{R}^M$	M-dimensional real vector space.
ρ	the statistical residual of a ordinate value of a datum point.
r	rate of drug elimination density in a tissue, exempli gratia mg/(ml s).
s	as a subscritpt to indicate spectral dimension.
S	a compact set; or the mean number of sites visited by a random walker.

T	the subjective tolerance for the AGR method; as a subscript to indicate a topological dimension.
σ	standard deviation of a Gaussian distribution, often identified with the uncertainty of a measured quantity.
t	elapsed time from the start of drug administration or from the time of peak concentration of the drug.
t_z	time after the systemic drug concentration declines monoexponentially.
$\vec{u}$	biological model system "noise".
V_i, V	tissue volume; generalized volume.
V_d	volume of distribution of a drug.
V_{max}	maximum reaction rate for Michaelis-Menten kinetics, exempli gratia mg/s.
w	the statistical weight assigned to a corresponding residual for each datum point.
W	Lambert's W function or the product log function (see Appendix 1).
X	amount of drug in a tissue, exempli gratia mass of drug in grams.
$\vec{X}$	i.v. bolus dose to a compartment.
ζ	zeta, a constant equal to $1-d_s/2$.
$\vec{\nabla}$	del vector differential operator.
$\bullet$	multiplication when an explicit indication is required.
$*$	a convolution of two functions.
$\lVert\cdot\rVert$	the euclidian norm of a vector.
$\ni$	such that.
$\in$	is a member of.
$\forall$	for all; for any.
$\wedge$	logical and.
$\cap$	intersection of sets.
$\cup$	union of sets.
$\subseteq$	subset or equal to.
$\Rightarrow$	this implies.
$\Leftrightarrow$	if and only if.

⟨ ⟩	angle brackets are reserved to indicate reference numbers in the body of text.
( )	the use of round brackets is limited to indicate grouping of terms: $s(t-1) = s^*(t-1)$, as usual parentheses within regular sentences, to indicate an open interval, or cartesian coordinates.
[ ]	the use of square brackets are reserved to enclose variables of functions, such that, $f[t]$ denotes a function f of the variable t, and to denote a matrix or vector, exempli gratia, $\vec{v} = [v_1, v_2, v_3]$. But, could be used to indicate a closed interval.
⟦ ⟧	double square brackets are used in the context of chemical equations to indicate the concentration of a chemical, exempli gratia $[\![S]\!]$ indicates the concentration of a substrate S.

Within the body text of the thesis, all mathematical variables are italicized for recognition within sentences; within equations, variables are written plain for uncomplicated reading. Equations are numbered only if they are directly refered to later in the body of text.

Chapter One

Forward

Pharmacokinetics is the quantitative study of the fate of a drug in the body through time as the drug undergoes absorption, distribution, metabolism, and excretion. The term "Pharmacokinetics" was coined in 1953, by Professor Dost in Germany - a pediatrician ⟨1⟩ but the idea had been around for a long time before that. For example, a Swedish scientist, Widmark, published a paper where he introduced the idea now considered as the volume of distribution and noted that the elimination of ethanol from the blood followed an exponential law in its final phase, back in 1919 ⟨2⟩. Since then, Pharmacokinetics has maintained an emphasis on clinical applications, resulting in improvements in drug utilization for patients, and has firmly established a role within the huge science and industry of pharmacology concerning the design and development of new drugs and the reassessment of established drugs.

Traditionally, Pharmacokineticists have concerned themselves more with the integration of aspects of physiology, pharmacology, biochemistry, and physiochemistry that influence drugs and less with biophysics. This was proper considering the obvious importance and complications of the biological and chemical connections with pharmacokinetics. But as the boundaries of pharmacokinetic research, assisted by technological improvements in analytical chemistry, are edged towards the foundational facets of drug deportment, questions of a more physical nature arise necessarily. This, in turn, provides an opportunity for those with a physical science background and with the interest to contemplate systems unlike most traditionally studied under the rubric, Physics, to contribute. This thesis represents the author's attempts in this regard: to extend outside of physics, and even just the familiar comfort of the classroom.

Yet, true to my past, I did not escape from presenting what is essentially a Physics paper. The topic of pharmacokinetics remains mostly as the environment within which a hopefully coherently developed course of concepts were cultivated and presented. There are some redundancies of ideas inside the thesis, but they are deliberate attempts to illustrate an evolution of thought and a progression of complications that require occasional revisiting of issues. The arrangement of the ideas advanced is intended to: familiarize a reader with a physics background to a pharmacokinetics setting, introduce the reader to the biological model system[†] studied, and then accrue more knowledge and statistical tools within the thesis to properly build a theoretical model of the biological model system as a foundation upon which conclusions can be made.

[†] There are two definitions using the term "model" listed in the glossary at the end of the thesis - one with specific biological implications, the other with general conceptual implications. Let the reader's attention also be drawn to the word "linear" which is hereafter used in three different ways. Note that the glossary is comprehensive and could be useful for answering many questions of vocabulary throughout the report.

Chapter One

A Few Pharmacokinetic Forethoughts for Physicists

An Overture of Basic Pharmacokinetic Concepts

> **Before turning to those moral and mental aspects of the matter which present the greatest difficulties, let the inquirer begin by mastering more elementary problems.**
>
> **-Sherlock Holmes, *A Study in Scarlet***
>
> **Sir Arthur Conan Doyle**

Following administration of a given dose of pharmacologically active drug to human, dog, or some other biological model system, concentrations of that drug appear in various body tissues, and ultimately a physiologic effect is produced. Because of the relationship between the intensity and duration of action of a drug and the concentration of the drug present, plasma concentrations of drug are usually evaluated over time in Pharmacokinetic studies. A variety of descriptive pharmacokinetic parameters characterize the behavior of the drug, such as clearance, bioavailability, absorption rate, volume of distribution, etc. - only a few of which will be briefly explained ⟨3⟩. For an understanding of this thesis, it is most important to note that estimates of these parameters are facilitated by an accurate portrayal of the plasma concentration-time data by mathematical techniques that generate a concentration time-course curve, $C[t]$ ⟨4⟩ (see Figure 1.1).

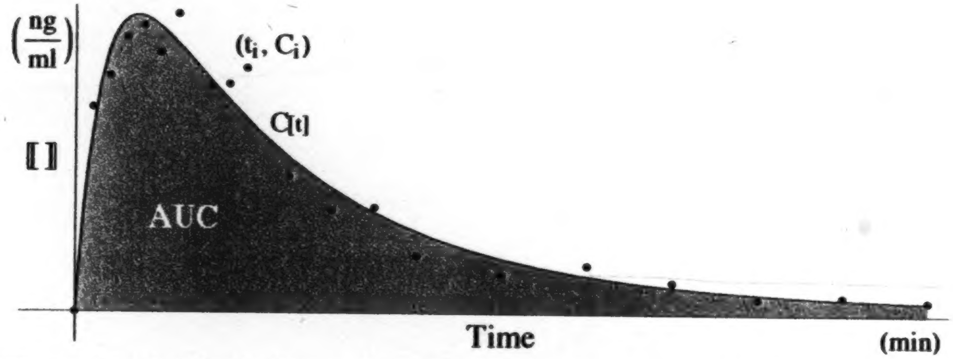

Figure 1.1: A didactic diagram introducing indicative pharmacokinetic concentration time course data, (t_i, C_i), $i = 1, 2, \ldots, n$, fit by a function, $C[t]$.

Plasma concentration data following intravenous injection provides partial characterization of drug disposition properties. Accurate assessment of volumes of distribution (V_d) and systemic clearance (CL) can best be attained with intravenous data. The volume of distribution is the apparent volume necessary to account for the total amount of drug in the body, X_{body}, if it were present throughout the body at the same concentration found in the plasma: $V_d = X_{\text{body}}/C_{\text{plasma}}$. Factors which tend to keep the drug in the plasma or increase C_{plasma}, such as escalated plasma protein binding, reduce the volume of distribution; while factors which decrease C_{plasma}, such as increased tissue binding or lipid solubility, increase the volume of distribution (see Appendix 4). The minimum value of the volume of distribution is the blood plasma volume (V_{plasma}). If the drug instantaneously and homogeneously equilibrated itself throughout the body, then $V_d = \text{Dose}/C_0$, where C_0 is the initial concentration immediately after intravenous bolus injection before any drug elimination. When the volume of distribution is time dependent, it may be estimated as

$$\mathrm{V_d[t]} = \frac{\mathrm{Dose} \cdot \mathrm{AUC}\Big|_t^{\infty}}{\mathrm{C[t]} \cdot \mathrm{AUC}\Big|_0^{\infty}}, \qquad \mathrm{AUC}\Big|_t^{\infty} = \int_t^{\infty} \mathrm{C}[\tau]\, d\tau,$$

where $AUC_0^{\infty} = AUC$ is unimaginatively called the Area Under the Curve. The clearance can be imagined as the intrinsic ability of the body and its organs of elimination to remove drug from the plasma, expressed as a volume per time. The total amount of drug removed depends on the plasma concentration of drug as well as the clearance. Consider a biological model system at steady state when the drug plasma concentration, $C_{\text{steady state}}$, is stable, such that the rate of sustained intravenous drug administration, $R_{i.v.}$, is equal to the rate of drug elimination. Clearance can then be measured as a proportionality constant at steady state ⟨5⟩:

$$\mathrm{R}_{\text{i.v.}} = \mathrm{R}_{\text{elimination}} = \mathrm{CL} \cdot \mathrm{C}_{\text{steady state}},$$

where systemic clearance is equal to the sum of all organ clearance processes:

$$CL = CL_{\text{hepatic}} + CL_{\text{renal}} + CL_{\text{other}} .$$

Plasma concentration data following oral doses of the drug in solution and common dosage forms provides additional pharmacokinetic parameters related to absorption and intrinsic clearance. These data permit assessment of bioavailability (F) and of the mean absorption time (MAT). Bioavailability refers to the fraction of an oral dose that actually reaches the systemic circulation of the biological model system. Since the availability of an intravenous dose is usually unity, bioavailability can be estimated by comparison, adjusted for differences in the oral and intravenous doses, as follows ⟨6⟩:

$$\mathrm{F} = \frac{\mathrm{AUC}_{\text{oral}} / \mathrm{D}_{\text{oral}}}{\mathrm{AUC}_{\text{i.v.}} / \mathrm{D}_{\text{i.v.}}} .$$

Clinical pharmacokinetics is an applied health science focused primarily on the pharmacokinetic aspects of the individualized optimization of drug therapy for patients; an important study since there can be appreciable interindividual differences in pharmacodynamics (the study of the effects) of a drug ⟨7⟩. Pharmacokinetics proper is a biological science concerned with the characterization and mathematical description of the absorption, distribution, metabolism, and excretion of drugs and their metabolites through time. Especially when the research is focalized on the investigation of drug elimination mechanisms or equilibrium distribution mechanisms, pharmacokinetics may be quite theoretical.

The vulnerability of Pharmacokinetics to analysis and cogitation using the principals and approaches of physics originates from its dependence on drug metabolism, which is a function of the reaction kinetics, which is a function of reactant diffusion, which is part of the general problem of transport physics ⟨8⟩. The methods used to describe transport in general physical systems may be useful in the quantification of the progress of a drug throughout the body or the invasion of the drug in an isolated tissue. This topic now partially fits within the expanding scope of physics that includes more complex biophysical phenomena. . Physicists of the past tended to focus on simpler archetypical problems not only for the love of fundamentals but due to the practical simplicity of such problems and their susceptibility to deep understanding. Whereas, in relatively recent times, a better understanding of complex, often mathematically nonlinear, systems coupled with the employment of modern computers has allowed Physicists to consider solving complicated secondary problems with their particular physical approach. This has been encouraged by scientists in other fields, like the Biological sciences, who in a sense have met the physicists halfway by extending their fields of study towards a more fundamental physical understanding, thus providing convergent interests whereby a multidisciplinary thesis such as this may be made.

A Reminder of Classical Kinetics

When a bimolecular reaction proceeds in solution, two effects conspire to determine how brisk the reaction will be. Firstly, the intrinsic velocity is determined by the detailed molecular mechanism of the reaction and involves a knowledge of such things outside the scope of the thesis as the distribution of electrons as they rearrange during the reaction. Secondly, the statistical probability accounting for the existence of adjacent reactive pairs must be considered. In the language of statistical mechanics this probability factor is the pair distribution function for the reactive molecules. Generally, in an assemblage of particles, each particle moves about in a random way. The particles spread out from their nearest neighbors as a result of this irregular individual motion. When this microscopic irregular movement results in some macroscopic motion of the group, it is considered a diffusion process. When there is a bulk flow drift juxtaposed with the diffusion process, it is considered a biased diffusion process.

Consider the simple bimolecular annihilation chemical reaction

$$\mathrm{E} + \mathrm{C} \xrightarrow{\mathrm{k}} \mathrm{E}, \tag{1.1}$$

where E may be considered a sink or an unsaturable trap, and C a species of reactant or its concentration, $[\![C]\!] \leftrightarrow C$. The traditionally used Law of Mass Action says that the rate of a homogeneous reaction is proportional to the concentrations of each of the reactants, such that

$$\begin{aligned} &\frac{dC}{dt} \propto \mathrm{C} \quad \wedge \quad \frac{dC}{dt} \propto \mathrm{E} \\ \Rightarrow\ &\frac{dC}{dt} = -\mathrm{k}\,\mathrm{E}\cdot\mathrm{C} = -\mathrm{k}\,[\![\mathrm{E}]\!][\![\mathrm{C}]\!], \end{aligned}$$

where k is the second order rate constant of proportionality. From the turn of the last century, Smoluchowski has been widely regarded to have showed that for diffusion-limited homogeneous dilute reactions in three dimensions, the reaction rate is also proportional to the reactant diffusion rates: $k \propto \mathcal{D}$ ⟨9, 10, 11⟩. Thus establishing that diffusion is the transport process in solution that determines the encounter between the reacting pair, where $\mathcal{D}$ is the effective mutual diffusion coefficient.

Contemplate now diffusion in three dimensions and the exemplary differential mass conservation equation (equation of continuity)

$$\frac{dC}{dt} + \vec{\nabla} \cdot \vec{J} = f[C, \vec{r}, t],$$

where C is the reactant concentration, $\vec{J}$ is a general flux transport and let the source term, $f[C, \vec{r}, t] = 0$. If Fick's Law is used to describe the flux in terms of diffusion along a concentration gradient ⟨12⟩

$$\vec{J} \propto -\vec{\nabla}C \;\Rightarrow\; \vec{J} = -\mathcal{D}\vec{\nabla}C,$$

then the conservation equation becomes

$$\frac{dC}{dt} - \mathcal{D}\vec{\nabla}^2 C = 0. \qquad (1.2)$$

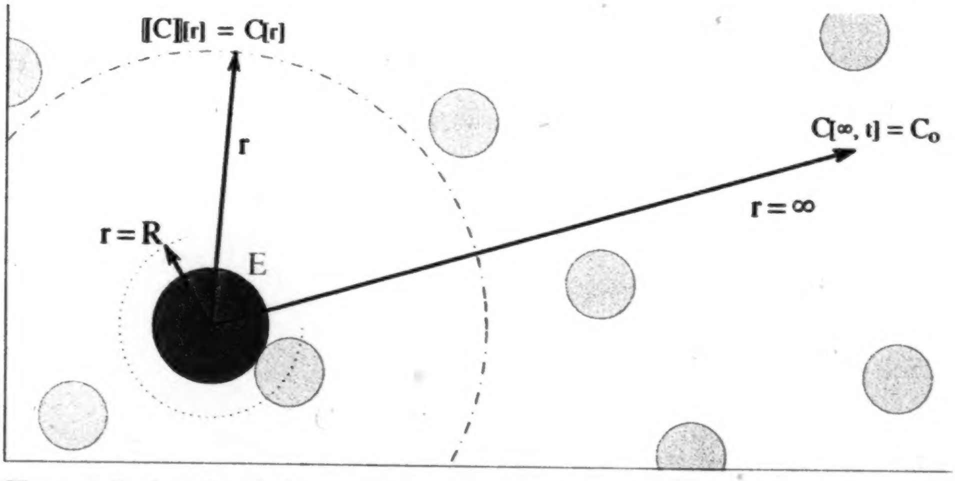

Figure 1.2: A notional diagram of the microscopic conditions nearby an single annihilating trap. Whenever movements caused by diffusion bring two distinct species together closer than R, annihilation of C occurs.

Applying the conservation equation to the bimolecular annihilation reaction (1.1), as shown in Figure 1.2, to the situation of an isolated sink, *E*, within an endless sea of reactant, *C*, the following boundary conditions may be proposed: $C[r{=}R,t]=0$, $C[r\to\infty,t]=C_o$, where $\mathcal{D}=\mathcal{D}_E+\mathcal{D}_C$ is the effective mutual diffusion coefficient, and *R* is the radial distance of closest approach of a molecule of reactant to the trap before annihilation. The boundary conditions and equation (1.2) are of the form of a homogeneous spherical heat equation and may be solved for using methods of separation of variables. For the steady state limit $t\to\infty$, the remaining radial solution is

$$C_{ss}[r]=C_o\left(1-\frac{R}{r}\right).$$

Now at steady state, the diffusion flux at the distance of closest approach is proportional to the observed reaction rate, kC_o, (remember that *E* is taken to be unity) so that

$$kC_o=\oint\!\!\oint\vec{J}\cdot d\vec{a}=-\mathcal{D}\oint\!\!\oint\vec{\nabla}C\cdot d\vec{a}\;=\;-4\pi R^2\,\mathcal{D}\,\frac{dC_{ss}}{dr}\bigg|_{r=R}=+4\pi R\,\mathcal{D}C_o$$

$$\Rightarrow\;k=4\pi R\,\mathcal{D}.$$

The significance of this derivation of classical mass-action kinetics for diffuse reactants in three dimensions is that a direct causal link is affixed between the macroscopic measurable quantities of concentration and reaction constants with the microscopic quantities of the size of the individual molecules and the diffusion of the molecules. Ergo, possessing a different understanding of the physics of diffusion allows for alternative macroscopic descriptions of reaction rates.

A Brief Explanation of Michaelis-Menten Kinetics

An aspect of life is the vital ability to induce, maintain, and manage multifarious chemical reactions that normally do not occur with significant rates at the temperatures and concentrations found in most environments. Subsequently, a preponderance of the metabolic reactions studied in Pharmacokinetics are enzyme-catalyzed reactions. The minimal chemical equation to describe a simple, one-substrate, one-product, reaction catalyzed by an enzyme is

$$E + C \underset{k_{-1}}{\overset{k_1}{\rightleftharpoons}} EC \xrightarrow{k_2} E + P,$$

where *E* denotes the conserved enzyme, *C* is the single substrate, *P* is the metabolite product of the reaction, k_i are the rate constants, and it is assumed that the reverse reaction between *E* and *P* is negligible. To derive a relatively simple expression for the reaction rate of the substrate, not in terms of the elusive or difficult to measure variables of

$[\![EC]\!]$ and k_i, consider the differential equation for the rate of change of the complex *EC*, such that

$$\frac{d\mathrm{EC}}{dt} = k_1\, E{\bullet}C - (k_{-1} + k_2)\,EC, \tag{1.3}$$

where now, and for the rest of this section, *E*, *C*, *EC* are concentrations of enzyme, drug substrate, and enzyme-drug complex respectively, exempli gratia $[\![EC]\!] \to EC$.

Accepting the Briggs-Haldane assumption, that the $[\![EC]\!]$ quickly builds, as the free enzyme is bound with the substrate, to a near constant value for most of the reaction time, a steady state, when $dEC/dt \approx 0$, is achieved such that,

$$\frac{E{\bullet}C}{EC} = \frac{(k_{-1} + k_2)}{k_1} = \text{constant} = K_M, \tag{1.4}$$

from (1.3), where K_M is the Michaelis-Menten constant. Since k_{-1} and k_2 are first-order rate constants and k_1 is a second-order rate constant, the Michaelis-Menten constant has the units of concentration.

The following differential equation describes the rate of change of the substrate *C* that is of most interest:

$$\frac{dC}{dt} = k_{-1}\,EC - k_1\,E\bullet C = -k_2\,EC, \tag{1.5}$$

by substitution from (1.3) at steady state.

Throughout the reaction, it is assumed that the total amount of the biological catalyst is conserved in the forms of bound and free enzyme, such that

$$\begin{aligned} E_{total} &= EC + E \\ \Rightarrow E_{total} &= EC + \frac{EC\,K_M}{C} = EC\left(1 + \frac{K_M}{C}\right) \end{aligned} \tag{1.6}$$

by substitution from equation (1.4).

In the presence of high drug substrate concentrations, the enzyme will be saturated or otherwise bound with the abundant substrate, such that $E_{total} \approx EC$, and the reaction will occur at a maximum zero-order rate of

$$\lim_{C\to\infty} \frac{dC}{dt} = \lim_{C\to\infty} -k_2\,EC \approx -k_2\,E_{total} = V_{max} \tag{1.7}$$

by substitution into (1.5). Therefore, generally

$$\frac{dC}{dt} = -k_2\,EC = -k_2\,\frac{E_{total}}{(1 + \frac{K_M}{C})} = \frac{V_{max}}{(1 + \frac{K_M}{C})} = \frac{V_{max}\,C}{K_M + C} \tag{1.8}$$

by substitution from equations (1.6) and (1.7), is the Michaelis-Menten equation that describes the rate of change of the concentration of a single drug substrate undergoing single enzyme catalysis. Unfortunately, biological reality ensures that most reactions entail complicating inhibitions, multiple substrates, multiple enzyme, and other reaction mechanisms, though the Michaelis-Menten description is still often used as an approximation ⟨13⟩. These complex reactions require extensive in vitro kinetic studies to accurately estimate all the appropriate kinetic constants.

A Review of Classical Pharmacokinetic Models

> Use the term *myth* for any theory that has been accepted by a society or some significant segment thereof primarily on the basis of the theory's attractiveness.
> -William S. Hatcher

In an attempt to interpret and quantify pharmacokinetic data, a commonly used model scheme, now termed "classical", was established. The biological model system under study is described by one, two, or more kinetically distinguishable interacting compartments. Each compartment represents a space of the body that is assumed to be kinetically distinct and homogeneously distributed with the drug ⟨2⟩. The movement of drug between the compartments and the elimination of drug are assumed to follow the law of mass action to the first-order with time independent rate constants, $k_{i,j}$. Their mammillary structure are intended to correspond with biological model systems composed of organ arrangements that receive blood circulation in parallel, as in humans. Source terms, R, are usually given as an initial condition for an effectively instantaneous bolus injection, as a zero-order (constant rate) i.v. infusion, or a first-order absorption of the drug from an oral dose (see Figure 1.3). Ordinarily, measurements of drug plasma concentration are taken from the "central compartment" which is assumed to contain most or all of the blood ⟨6, 14⟩. The basis for classical multicompartment exposition in Pharmacokinetics may be abstractly summarized as the conceptual model of stochastic transitions between states (spatial and chemical) of drug molecules behaving independently and with constant transition probability densities ⟨15⟩.

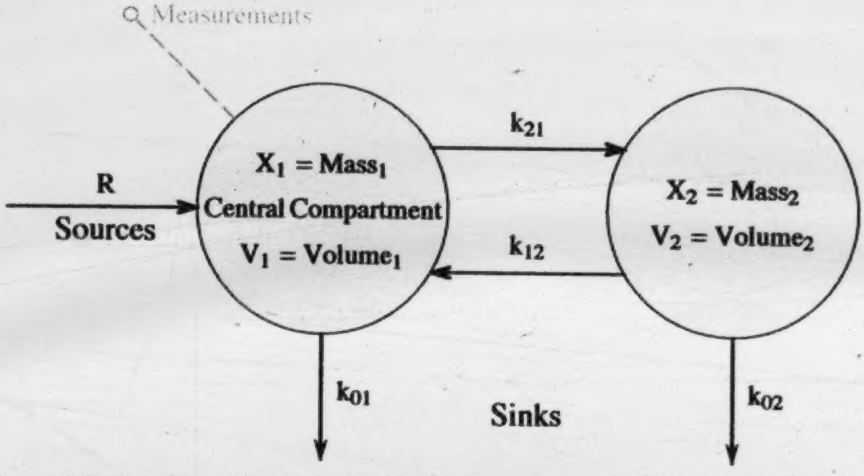

Figure 1.3: A schematic of a general 2-compartment model where the sources enter, and measurements are taken from, the central compartment. The *i*th-compartment is considered open if it looses drug to the environment, $k_{0i}>0$, otherwise it is closed, $k_{0i}=0$. A multicompartmental model is considered mammillary if the secondary compartments are connected to the central compartment in a parallel arrangement, and is considered catenary if the secondary compartments are connected in a series alignment.

The mass balance equations for a multicompartmental system with *m* compartments are first-order differential equations that can take the vector-matrix form

$$\begin{aligned} \frac{d\vec{X}}{dt} &= -\mathbb{K}\vec{X} + \vec{R}\ , \\ \vec{C} &= \mathbb{V}^{-1}\vec{X} \end{aligned} \tag{1.9}$$

where $\vec{X}$ is a column vector of the *m* independent state variables (mass or concentration) of the system, $\mathbb{K}$ is a constant matrix composed of the first-order rate constants, $k_{i,j}$, such that, if the model is open (see Figure 1.3) then $\mathbb{K}$ is non singular and invertible ⟨2⟩, $\vec{R}$ is the column vector describing the sources, $\vec{C}$ is the vector of compartment concentrations, and $\mathbb{V}$ is the distribution volume matrix. Solutions to this differential system are realized by standard matrix methods to be sums of exponentials with the form for each compartment of

$$C_j[t] = \sum_{i=0}^{m} A_{ij}\, e^{a_{ij} t}, \tag{1.10}$$

where A_{ij} and a_{ij} are both functions of the first-order rate constants, $f[k_{i,j}]$, and m is the number of compartments in the model. The form of the solution is the key reason that multicompartmental modeling is so popular ⟨16⟩. The model parameters k_{ij} and V_j may be found directly from these solutions while the decaying exponential functions serve as a power basis set for describing the normally declining concentration time-course Pharmacokinetic data.

Classical mammillary multicompartmental models possess the properties of constant clearance, linearity, time invariance, and a terminal monoexponential phase. Linearity and time invariance of this model is due to the linearity and time invariance of the differential operator, d/dt, and the constant matrix $\mathbb{K}$. Similar to equation (1.7), the systemic clearance, CL_S, is the extraction rate (rate of elimination), dX_E/dt, divided by the plasma concentration of drug, such that for an i.v. bolus dose,

$$\mathrm{CL_S} = \frac{dX_E/dt}{C[t]} = \frac{\int_0^\infty dX_E}{\int_0^\infty C[t]\,dt} = \frac{X_E\big|_0^\infty}{\int_0^\infty C[t]\,dt} = \frac{0 - X_0}{\mathrm{AUC}} = -\frac{\mathrm{Dose}}{\mathrm{AUC}} = \mathrm{const.}$$

Finally, the terminal monoexponetial phase occurs, since beyond some time, t_z, all but one exponential term, say $i=m$, will be approximately zero, such that

$$C_j[t] \approx A_{mj}\, e^{a_{mj} t}\ \forall\ t > t_z .$$

Normally, a physical relevance while choosing the structure or form of the compartmentalization is attempted by the use of model state variables and parameters that have direct analogies in the biological model system. Due to experimental constraints and a limited physiological knowledge base, the required abstractions constrain the ultimate complexity and form of a compartmental model, such that, the actual correlation of pharmacokinetic compartments with real anatomical tissues or organs is rather complex and, at times, impossible.

It is often said in the recent pharmacokinetic literature, that the compartmental modelling view of the body as relatively few, kinetically homogeneous compartments is unrealistic and difficult to justify from physiological reality ⟨4, 17⟩. That the model structure and parameter values may have only an indirect relationship to real physiological structures and quantities. Yet despite efforts to purge this apparently hackneyed technique from Pharmacokinetics it remains in most modern books I have read on the subject ⟨5, 7, 14⟩ and some recent articles ⟨18, 19⟩. The multicompartmental model concept may have resilience because many of the same concerns, or other apprehensions of equivalent significance, are as applicable to alternative types of modeling in Pharmacokinetics.

A Synopsis of Physiologically Based PharmacoKinetic (PBPK) Models

> I have yet to see any problem, however complicated, which, when you looked at it the right way, did not become still more complicated.
>
> -Paul Anderson

Some Theoretical Context

PBPK models generally envisage the organism as a network of compartments representing individual organs or tissue groups interconnected by the arterial and venous blood (see Figure 1.4). They are motivated by the belief that physiologically based models have greater application and relevance, particularly those applied to hepatically eliminated drugs ⟨20⟩. A typical PBPK model can involve twenty or more physiological, physicochemical, and biochemical parameters, each of which is subject to some extent of error ⟨21⟩. Yet, the aim of a PBPK model is to accurately and realistically describe the Pharmacokinetics of a xenobiotic (a drug for our purposes) using an accurate and detailed biologically motivated internal structure ⟨22⟩. Uptake, distribution, metabolism, and excretion in a PBPK model are described in terms of quantitative interrelationships among certain physiological parameters such as tissue volumes and blood flow rates, physicochemical parameters such as partition coefficients, and biochemical parameters such as Michaelis-Menten constants.

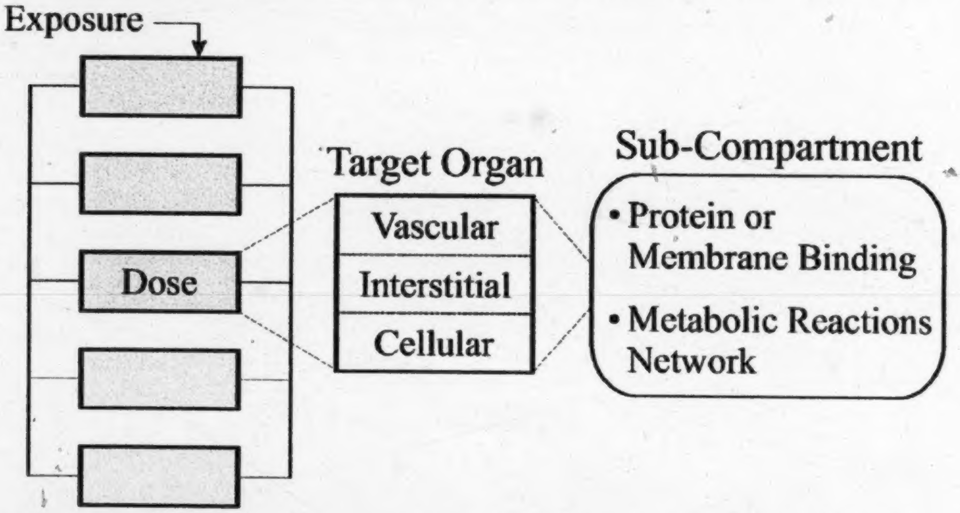

Figure 1.4: An abstract representation of a Physiologically-Based Pharmacokinetic (PBPK) Model indicating: a structural interrelationship between organs and tissue groupings, a possible internal arrangement within an organ, and an indication of some biochemical and physicochemical concerns within an organ or a part thereof.

It is clear that physiological and physicochemical parameters are subject to certain constraints. For example, the total volume of all body tissues must equal the total body volume, and the sum of the blood flow rates in different tissue groups must equal the rate of cardiac output. Most of the physiological quantities are estimated prior to modeling by in vitro experiments and are subject to a certain degree of uncertainty, depending on the precision and accuracy of the methods used for their determination. As the complexity of the PBPK model increases, the impact of the various assumptions, constraints, and parameter uncertainties on the predictions and results of the data becomes inscrutable without careful sensitivity analysis ⟨21, 23⟩.

Absorption of the drug from outside the model can occur via several routes of entry: ingestion, which involves the digestive system, inhalation, which involves the respiratory system, dermal absorption, which involves the cutaneous structure, or i.v. injection. Once absorbed, the drug is distributed throughout the body to various organs and tissues. A routine assumption regarding the transport of the drug between the various defined compartments, is that movement is constrained to be limited within the blood ⟨24⟩.

Absorption or transport into or out of a particular organ or group of tissues is described by a mass balance around that compartment (see Figure 1.5). Any tissue diffusion within the compartment could be illustrated by either a lumped-parameter or a distributed-parameter model. The lumped-parameter approach assumes that the concentration of drug within a compartment is homogeneous and that the physical variables describing the transport processes in the compartment are only time dependent. This approach would yield a system of ordinary differential equations (ODEs) with initial conditions required to describe the data. The distributed-parameter approach assumes that the physical processes change both spatially and temporally, thereby yielding a system of partial differential equations, such that both the boundary and initial conditions are needed to solve for the solution.

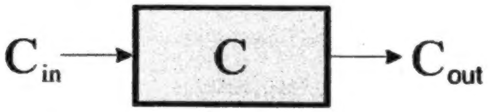

$$\frac{dC}{dt} = j_{in} - j_{out} - r[C]$$

$\frac{dC}{dt}$ = mass accumulating in organ per unit volume

j = drug flow density

r[C] = rate of drug elimination density in the tissue

$C_{in} \neq C_{out}$ generally

Figure 1.5: A general mass balance equation for a lumped-parameter compartment.

Most of the physiological based pharmacokinetic models published assume that all of the chemical delivered by the flow of blood rapidly equilibrates and is taken up by the various tissues under the control of a "partition coefficient" ($P_{ij} = C_j/C_i$ or $P = C/C_{out}$). This physicochemical parameter is an attempt to describe the different equilibrium concentrations of a drug within two compartments of a model that are in contact. Another issue is that of drug binding to the proteins in blood or in membranes, since it is often assumed that only the fraction of drug in the circulating blood which is free or unbound in the plasma is available for transport, metabolism, or excretion ⟨6⟩. When partition or binding occurs within any of the compartments, the mass balance ought to include the effects of the partition coefficient and any linear or non-linear binding constant, in the latter case, to account for both the free and bound fractions of drug.

Elimination of the drug can occur in various tissues via several processes, but the two most important are by enzymatic metabolism in the liver and by first order clearance in the kidney. Enzymatic mechanisms are often complex, resulting in nonlinear kinetic equations. Consequently, their incorporation into PBPK models is usually limited to the reduction of these equations into the Michaelis-Menten form, with apparent V_{max} and K_m usually fitted from in vitro empirical measurements ⟨24⟩.

Several levels of simplification of a PBPK model are possible and are often used depending on the availability of the data. To reduce the total number of compartments, tissues with similar characteristics, such as vascular perfusion, can be grouped together. Within a compartment, the interplay between blood flow, membrane transport, and binding describes the movement of the drug between the subcompartments. Assumptions regarding the rate limiting step in these processes lead to a simplification of the description of the organs and the resulting mass balance equations (see Figure 1.6). The resulting PBPK model is then the simplest possible one which would describe the physiological processes of interest.

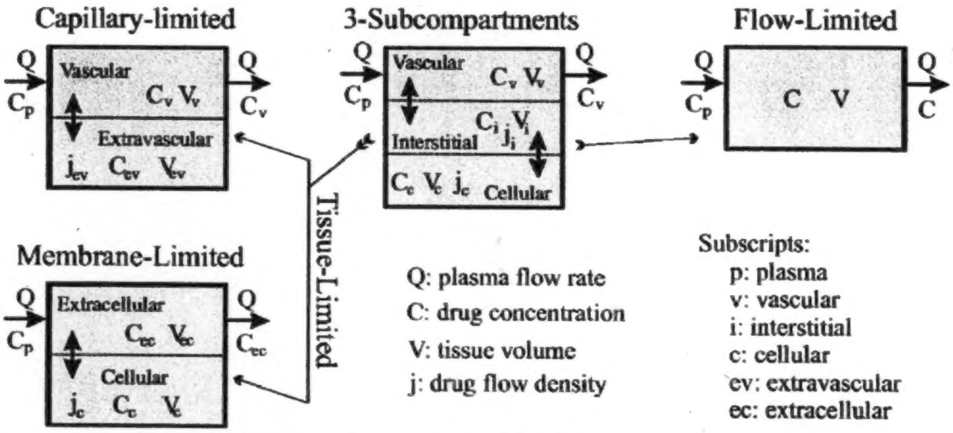
Capillary-limited
Q
C_p
Vascular
C_v V_v
Q
C_v
Extravascular
j_{ev} C_{ev} V_{ev}
3-Subcompartments
Q
C_p
Vascular
C_v V_v
Q
C_v
C_i V_i
Interstitial
j_i
C_c V_c j_c
Cellular
Flow-Limited
Q
C_p
C V
Q
C
Membrane-Limited
Q
C_p
Extracellular
C_{ec} V_{ec}
Q
C_{ec}
Cellular
j_c C_c V_c
Tissue-Limited
Q: plasma flow rate
C: drug concentration
V: tissue volume
j: drug flow density
Subscripts:
p: plasma
v: vascular
i: interstitial
c: cellular
ev: extravascular
ec: extracellular

Figure 1.6: An illustration of the possible internal structures of a compartment depending on the speculated rate limiting transport process in the subcompartments.

The Mathematical Framework for a Flow-Limited Lumped-Parameter PBPK Model

PBPK models are typically expressed mathematically with a system of first order differential equations ⟨90⟩, as shown by the following heuristic example. Let C_i represent the concentration of chemical in the ith compartment. The rate of change of concentration of drug in each non-eliminating compartment is described mathematically as

$$\frac{d\,C_i}{d\,t} = \frac{Q_i}{V_i}\left(C_{in} - \frac{C_i}{P_i}\right), \tag{1.11}$$

for i representing the various tissues. Here Q_i, V_i, and P_i are blood flows, tissue volumes, and partition coefficients which indicate the relative solubility of a circulating drug in a specific tissue, for the ith compartment, respectively. C_{in} is the concentration of the blood entering the compartment. The rate of change in the concentration of the drug in an eliminating or metabolizing organ is

$$\frac{d\,C_j}{d\,t} = \frac{Q_j}{V_j}\left(C_{in} - \frac{C_j}{P_j}\right) - \frac{1}{V_j}\,\frac{d\,X_j}{d\,t}, \tag{1.12}$$

where X_j is the amount of drug eliminated or metabolized in the tissue. The rate of metabolism is typically given by the Michaelis-Menten equation governing enzymatic reactions

$$\frac{d\,X_j}{d\,t} = \frac{V_{\max j}\,C_j/P_j}{K_j + C_j/P_j}, \tag{1.13}$$

where $V_{\max j}$ and K_j are the maximum velocity and the Michaelis-Menten constant for the metabolizing organ.

The PBPK model should contain a minimum number of adjustable parameters, to reduce data requirements and facilitate the use of the model in a predictive fashion ⟨25⟩. But a difficulty concerning physiologic pharmacokinetic models, somewhat reducing their value, occurs because of the inordinate number of assumptions which usually must be built into the model ⟨4⟩. All the physiological parameters such as the blood flow rate, tissue volume, binding terms, and kinetic terms need to be determined from physiological or in vitro experiments or taken from the literature. Another major obstacle is that the model structure is most frequently must be inferred from input-output data that are predominantly functional in nature. Unfortunately, the functional behavior of biological systems generally bears no simple relationships to these structural elements ⟨26⟩. Nevertheless, it is an attempt of this thesis to improve the Pharmacokinetic analysis of Mibefradil based on physical arguments. Once the final form of the model is determined and all parameter values are specified, the coupled ordinary, and sometimes nonlinear first-order differential equations which describe the mass balance of the system (1.11), (1.12), and (1.13) need to be solved, usually numerically, to simulate the real data ⟨27⟩.

A Note on Noncompartmental Analysis

For the purposes of this thesis, the general term noncompartmental modelling is used to broadly encompass, what have been called in the pharmacokinetic literature, "model-independent methods", "system analysis", or "the system approach". These methods are characterized by the attempt to describe the pharmacokinetic system or some response of the system with fewer restrictive assumptions than classical compartmental or PBPK modelling. Specific properties of the system are then mathematically described, and the resulting mathematical structures are exploited to address specific applications ⟨17⟩. When theoretical physical interpretations are attempted from noncompartmental analysis a model with a compartmental nature, as shown in Figure 1.7, is necessarily implied ⟨15, 16, 4⟩.

Motivating factors for the development of noncompartmental methods include the common criticisms of PBPK models, such as intractable complexity and extensive inputs, and the criticisms of classical compartmental modeling, such as it is physiologically fanciful, as well as the desire for estimating basic pharmacokinetic parameters quickly and automatically ⟨17⟩. But as such, noncompartmental analysis says little about mechanism. Theoretically, noncompartmental modelling provides few alternatives to these other methods, but, the system approach may provide a more general and efficient method to answering most of the practical questions in clinical pharmacokinetics. The use of noncompartmental techniques seems to have increased as the theoretical background and mathematical principles became more familiar to most pharmacokineticists.

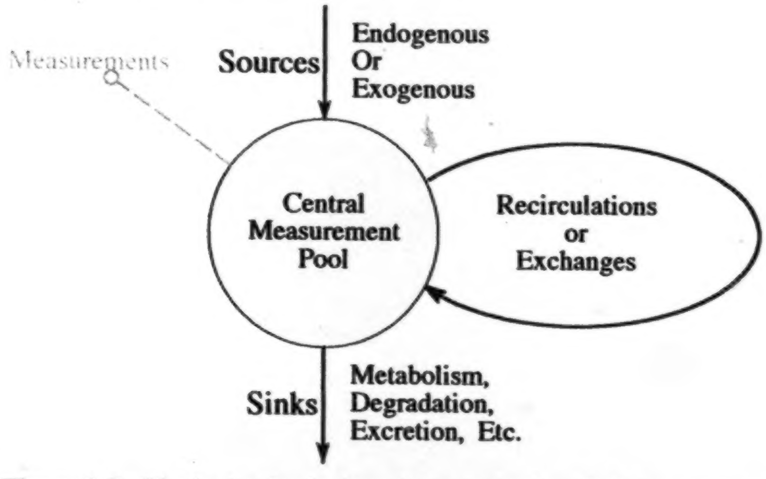
Measurements
Sources
Endogenous
Or
Exogenous
Central
Measurement
Pool
Recirculations
or
Exchanges
Sinks
Metabolism,
Degradation,
Excretion, Etc.

Figure 1.7: The basic physical model structure implied by noncompartmental analysis when a scientific physiological interpretation is made.

Three properties often used in the derivation of noncompartmental methods are as follows:

i. *Constant total clearance*: that is, the total elimination rate is proportional to the systemic drug concentration:

$$A'_{el} = \frac{d\,A_{el}[t]}{dt} = CL \bullet C[t]$$

where *CL* is the constant clearance with respect to time, and A_{el} is the cumulative amount of drug eliminated from the body. In the context of compartmental modelling, this is equivalent to first-order elimination from the central sampling compartment.

ii. *Linear, time-invariant pharmacokinetics*: id est, the relationship between the input rate and the resulting systemic concentrations has the properties of superposition and time invariance - properties that are a generalization of dose dependence. Under this assumption, the relationship between the input rate and the resulting systemic drug concentration is described by the convolution integral equation:

$$C[t] = (R * C_\delta)[t] = \int_0^t R[\hat{t}]\, C_\delta[t - \hat{t}]\, d\hat{t}$$

where $R[t]$ is the rate of drug input reaching the systemic circulation and the function C_δ is the unit impulse response for the relationship, that is, the systemic drug concentration time-course resulting from the instantaneous input of a unit of drug.

iii. *Existence of a terminal monoexponential phase in the systemic drug concentration time course*: id est, there exists some time t_z such that for all $t > t_z$ the concentration time-course is well described by:

$$C[t] = C_z\, e^{-\lambda_z t}, \quad t > t_z$$

where λ_z is the terminal rate constant, and is especially used for extrapolating beyond given concentration time course data.

On the basis of the general properties described above, noncompartmental modeling can be applied to the estimation of the pharmacokinetically descriptive summary parameters, such as clearances, volumes of distribution, and mean residence times. With estimates of the unit impulse response C_δ, predictions and simulations for the systemic drug concentration, resulting from any specified input rate time-course $R[t]$, can be made for all systems that satisfy the other assumptions of the noncompartmental modeling. Finally, it is also worth mentioning that accurate simulations through noncompartmental, multicompartmental, and PBPK modeling have the laudable potential to reduce the number of experimental animal model systems. A few other noncompartmental concepts and resulting formulas are located in Appendix 4.

Chapter Two

Certain Remarks on Scientific Modeling

Some Comments on the Philosophy of Modeling

The main problem we face as self aware subjects is how to obtain valid knowledge of the phenomena of reality.

-William S. Hatcher

Before considering any deeper or more complex questions addressing the Pharmacokinetics of Mibefradil, a delineation of the philosophical context of this thesis is introduced. Most generally it is recognized that no meaningful part of the universe is sufficiently simple that it can be grasped without abstraction, and, that almost all of our thoughts implicitly utilize abstraction to selectively focus on certain aspects of a situation and consider it in terms of one's personal aims. Let an abstraction or combination of abstractions attaining a certain level of refinement in structure and behavior be called a model. For the remainder of this thesis a model will be assumed to be a collection of specialized mathematical techniques for selection and analyzing data, as well as optimizing hypothesized system variables and parameters ⟨26⟩. Moreover, the author will endeavor to be conscious not to delude himself or others into believing that any resulting theory or model closely mimics the reality in which the model is anchored in, rather that the model in some small way contributes to our interpretation of said reality.

The paradigm of scientific method is that we start with experience on some level, primarily based on the research strategy of explanatory reductionism, and that we formulate a certain number of observational statements which we consider as facts. Inevitability there comes a point in this process when we seek a hypothesis capable of relating the separate facts and welding them into a coherent whole - here the mental processes are reversed. While collecting observations, we have been interested in exploring how things, in fact, are. We now need to use our creative imagination in order to conceive how things might, in fact, be. But it is now known, there are no rules for finding a fruitful hypothesis ⟨28⟩ - we must use our intuition and guided imagination. This seems to be true because there are generally a potentially infinite number of theories consistent with any given (necessarily finite) set of facts. In short, theory is underdetermined by fact, yet, as personally discovered, conceiving of even one plausible theory can be difficult.

Now, it seems that biological systems are amongst the most complicated physical systems known ⟨29⟩, and given the depth of understanding that Physicists assume in other, more traditional, fields of research, the steps forward that may be expected to be taken within the context of a Masters thesis in this field are modest by comparison. The inherent complexity of the biological system must be circumvented by the employment of an abstracting model, not by choice, but out of necessity. It is hoped that, by use of a homomorphic model and with the assumption that some less important information will be lost, more relevant information can be gained and isolated from the data. With this approach it can be made apparent that any model created does not capture any reality within, but may only serve as a human construct, as a tool, to help one understand the unobservable reality of the physical system on our own terms.

First one must decide what aspects of the physical system are important, and then create and manipulate models to reflect the system sufficiently well so as to answer those questions that were previously selected for study ⟨30⟩. It is at this point, during the formative stage at which the very questions that are asked that will determine the character of all following research, where the differences between those from Pharmacology and Physics, the two scientific disciplines that this thesis attempts to bridge, first appear. The individual scientist has ambitions, either held personally or imposed by his or her working environment, that require satisfying from any model developed. Now, two characteristics that models can offer in varying degrees are truthfulness and usefulness ⟨28⟩. A model that accurately interprets a broad array of data of some, hopefully large, portion of reality can be said to reflect some truth of that reality. We can say that a model is useful if it describes a state of affairs which would satisfy some important need by its application. Thus, the truth and usefulness of a model, as defined for this thesis are logically independent. Of course, everyone is allured to an seemingly truthful and useful model, but I suggest that the motivations of Pharmacokineticists are more immediately practical and yearn for application to clinical situations, so they would tend to be most attracted to an apparently useful model. On the other hand, the Physicist's motivations are more theoretical and focused on foundational knowledge, and he or she would be inclined to an apparently truthful model. Aforesaid differences are not revealed as an excuse for the author, studying within the Theoretical Physics Institute, to pursue an irrelevant or arcane area of Pharmacokinetics, but as an admonishment to any non-physicist reading this of the perspective from which further investigation respectfully proceeds.

A Concrete Proem to Modeling in Pharmacokinetics

> It is, after all, much easier for me to know what I need or want to know to be true, than to know what *is* true.
>
> William S. Hatcher

The value of a model usually derives from the supposition that the system undergoing analysis is a prototype or in some other manner typifies a class of similar systems. Although, the ultimate functions of models are usually to characterize and explain phenomena, they may be designed with a variety of emphases. Within this report, a mathematical model will be used: to permit some simulation, for the understanding of possible physical causative factors influencing the pharmacokinetics of Mibefradil, to establish the adequacy of a point of view, and even to estimate system parameters not directly accessible.

Models can be divided into two broad categories - "models of data" and "models of systems" ⟨16⟩. Models of data tend to be descriptive, phenomenological, and empirical; widely used examples in Pharmacokinetics include those based upon noncompartmental analysis, often called "model independent". The advantages of these, henceforth described, phenomenological models are: they require few assumptions about the system studied, they allow for predictions and simulations, they require few resources in their development relatively speaking, and they are simple and accurate. The disadvantages of phenomenological models are that they are superficial, so provide little theoretical insight, and they are not easily falsified, so they lack credibility ⟨15⟩.

Models of systems incline to be theoretical, structural, and mechanistic; a typical example in Pharmacokinetics is a PBPK model. Models of systems, henceforth termed representational models, link input to output by positing a mechanism, usually involving physical constructs (such as enzymes, organs, or blood), laws regulating model behavior (such as the law of mass balance), and a temporal vector of events - all to provide an interpretation of the data. The advantages of representational models are: they are lucid, providing insights into how we a least believe things work, they are easily falsified, thus providing a high degree of credibility, and finally, they fulfill our emotional need ⟨28⟩ to find cause and effect as well as meaning in nearly all events. Unfortunately, the development of representational models is often costly and time consuming, and as these models approach the full complexity of the system, the more unwieldy they become and the less intellectual leverage they provide.

The classification of a classical compartmental model, as a phenomenological or a representational model seems to be less obvious. Clearly, a polyexponential function, or similarly a spline function, with no analogy to biological model system states attempted, fitted ad hoc to drug plasma concentration-time data following an i.v. bolus injection, is a phenomenological model of data. However, given a well-structured multicompartmental model with some degree of physical relevance in choosing the structure to answer a question posed in advance, despite these being presently out of fashion, a physical interpretation of the data through the resulting polyexponential equation is nonetheless a representational model ⟨26, 15⟩. It is the epistemological context the model is used within and not the mathematical structure of the model itself that determines whether or not an approach is phenomenological or representational in character.

In attempting to describe fundamental differences between phenomenological models (which they include compartmental models within) and representational models, Colburn et alia ⟨4⟩ state: "With the exception of physiologic models, these methods are deterministic; the data determines what model can be fit to the data." In doing so, the mentioned authors exhibit, what I believe to be, a common misconception about the essential validity of PBPK (physiologic) models compared to multicom partmental models (see also ⟨31⟩ for a comparable misjudgment). The observation, "the data determines what model can be fit to the data", applies as well to PBPK models as any other types of models. No model can fulfill strong objectives without some relation to data. In the process of relating to data, the design of a PBPK model undergoes the same recursive pattern of modification of structure and comparison to data as any other model. As well, noncompartmental and classical compartmental models should not be applied ad libitum without critical consideration of whether the underlying assumptions are valid in each specific case.

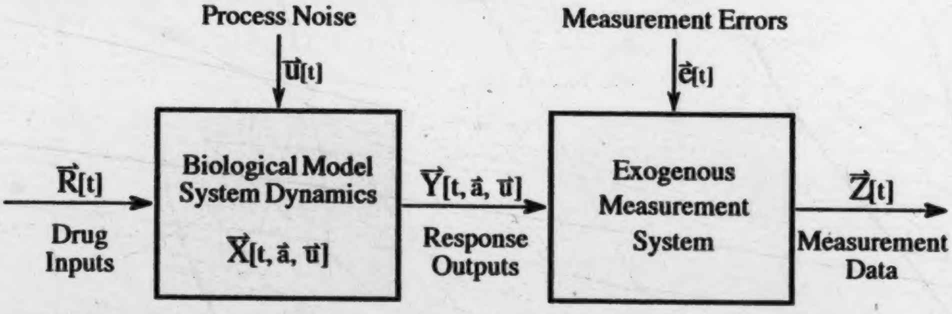
Process Noise
$\vec{u}[t]$
Measurement Errors
$\vec{e}[t]$
$\vec{R}[t]$
Drug Inputs
Biological Model System Dynamics
$\vec{X}[t, \vec{a}, \vec{u}]$
$\vec{Y}[t, \vec{a}, \vec{u}]$
Response Outputs
Exogenous Measurement System
$\vec{Z}[t]$
Measurement Data

Figure 2.1: An abstract block diagram indicating the distinction and relations between the biological model system, the measurement system, and the variables used to construct the mathematical model.

The elementary conceptual relation between the biological model system, experiment, data, and pharmacokinetic model is given in Figure 2.1. Usually, sets of differential equations believed to represent system dynamics or kinetics are written in concise vector notation,

$$\frac{d\vec{X}}{dt} = f\left[\vec{X}[t, \vec{a}, \vec{u}],\ \vec{R}[t];\ \vec{a}\right] \quad \bigwedge \quad \vec{h}\left[\vec{X}[t, \vec{a}, \vec{u}],\ \vec{R}[t];\ \vec{a}\right] \geq 0\,,$$

where $\vec{X}$ is a column vector of the m dependent state variables of the system, exempli gratia, amount of drug, $\vec{R}$ is a vector describing the drug inputs to the biological model system, $\vec{a}$ is a vector of the M model parameters, $\vec{u}$ is a vector describing any "noise", caused by random or chaotic unaccounted inputs, that impinges on the deterministic description of the biological model system, f is a vector function that embodies the model structure including topology, and $\vec{h}$ is a vector describing the initial and/or boundary conditions. The biological model system responses are described by

$$\vec{Y}[t, \vec{a}, \vec{u}] = g\left[\vec{X}[t, \vec{a}, \vec{u}]\right], \tag{2.1}$$

where $\vec{Y}$ is a vector of m model observable outputs, and g is a vector function that characterizes the structure of the measurement system ⟨16⟩. To account for measurement errors, an uncertainty term, $\vec{e}$, is usually added to $\vec{Y}$ in (2.1), such that the sum, $\vec{Z}$, is the actual measured data vector

$$\vec{Z}[t] = \vec{Y}[t, \vec{a}, \vec{u}] + \vec{e}[t]\,. \tag{2.2}$$

From the measured data, the sought after pharmacokinetic parameters are estimated.

It may be the case that classical multicompartmental models sacrifice more realism for precision, and that PBPK models sacrifice precision for realism. But all models, especially representational models, are at least partially based on presuppositions that are either false (e.g., instantaneous and homogeneous mixing of a drug in the compartments of a lumped-parameter PBPK model) or not known whether they are true or false (assumptions of classical kinetics). As well, the validity of a model is goal dependent, and any model can be judged successful if it fulfills the objectives of the investigator. Accordingly, the specific choice of pharmacokinetic model must be determined by the questions asked and the type of answers sought by the investigator with the legitimacy of the model being appraised on those terms. Therefore, despite the significance of many types of noncompartmental analysis techniques currently used in Pharmacokinetics, due to the limited role it plays in the revelation of underlying physical mechanism with which a thesis in Physics is generally concerned, noncompartmental analysis in Pharmacokinetics will not be considered in detail for the remainder of the thesis.

The Practicalities of Modeling in Pharmacokinetics

> You have erred perhaps in attempting to put colour and life into each of your statements instead of confining yourself to the task of placing upon record that severe reasoning from cause to effect which is really the only notable feature about the thing. You have degraded what should have been a course of lectures into a series of tales.
>
> -Sherlock Holmes, *The Adventure of the Copper Beeches*
> Sir Arthur Conan Doyle

Pharmacokinetic data do not speak to us directly, but require interpretation and context. Once the general intentions and emphases of the inquiry are determined by the investigator, the specific description, testing, and verification of any pharmacokinetic model are achieved by the tools of mathematics and statistics. The basic mathematical structures of the pharmacokinetic models considered in this thesis have already been described, while a broad description of the statistics to help evaluate the models follows.

To start, a figure-of-merit function, that measures the agreement between the data and the model, must be chosen or designed. The merit function is conventionally arranged so that small values represent close agreement between the data and the model with a particular choice of parameters. These parameters of the model are then adjusted to achieve a minimum in the merit function; thus, the attunement process is a problem of minimization in many dimensions yielding the best-fit parameters ⟨32⟩. Also, once calculated, the precision of the parameters as determined by the data set must be estimated for meaningful reporting of results.

In general, the data never exactly fit the model that is being employed, even when that model is veracious. This is a consequence of the pharmacokinetic data not typically being exact since each datum is subject to various measurement and systematic errors. Therefore, a test for the goodness-of-fit against some useful statistical standard is required to assess whether or not the model is appropriate. Unambiguous identification of the most correct model is often impossible because more than one model of comparable complexity is consistent with available data ⟨17⟩. But, the probability that the data observed was generated by a system faithfully described by the model can be calculated with the appropriate statistical tools. Whereas, it is not meaningful to ask or try to calculate what the probability that a particular set of fitted parameters within a model is correct for the data, since that is actually a question of truth and not probability, it is possible to consider, given the assumption of a particular set of parameters and a model, the probability that the data set could occur. This second approach is statistical in nature and so can never establish the essential truth of a model, that identification being left to the intuition, but if the probability of obtaining the data set is very small, then it can be concluded that the parameters and model under consideration are unlikely to be correct ⟨32⟩.

Consider a fit to N datum points (t_i, C_i), $i = 1, \ldots, N$, to a model that has M adjustable parameters a_j, $j = 1, \ldots, M$. Let the model predict a functional relationship between the measured dependent and independent variables,

$$C[t] = C[t; a_1, \dots, a_M]$$

where the dependence on the parameters is indicated explicitly on the right-hand side. A common assumption in pharmacokinetics, often taken so casually for granted that it's rarely specifically addressed, is that each datum point C_i has a measurement uncertainty that is independently random and distributed as a Gaussian distribution (see Appendix 3) with standard deviation σ_i about the true model $C[t]$ as observed by the data. Given that presupposition, the probability $\mathcal{P}$ of the data set occurring is the product of the probabilities of each point happening ⟨33⟩, such that

$$\mathcal{P} \propto \prod_{i=1}^{N} e^{-\frac{1}{2}\left(\frac{C_i - C[t_i]}{\sigma_i}\right)^2} .$$

Since the natural logarithm is a monotonic nondecreasing function, maximizing $\mathcal{P}$ is equivalent to maximizing the natural logarithm of $\mathcal{P}$, $\mathrm{Max}[\mathcal{P}] = \mathrm{Max}[\ln\mathcal{P}]$, such that

$$\ln\mathcal{P} \propto \ln\left[\prod_{i=1}^{N} e^{-\frac{1}{2}\left(\frac{C_i - C[t_i]}{\sigma_i}\right)^2}\right], \quad \ln[ab] = \ln[a] + \ln[b]$$

$$\Rightarrow \ln\mathcal{P} \propto \sum_{i=1}^{N} \ln\left[e^{-\frac{1}{2}\left(\frac{C_i - C[t_i]}{\sigma_i}\right)^2}\right] = \sum_{i=1}^{N} -\frac{1}{2}\left(\frac{C_i - C[t_i]}{\sigma_i}\right)^2 .$$

Therefore, because this is a negative function that is to be maximized, the maximum likelihood estimate for the model parameters is obtained by minimizing the quantity

$$\chi^2 \equiv \sum_{i=1}^{N}\left(\frac{C_i - C[t_i; a_1, \dots, a_M]}{\sigma_i}\right)^2 = \sum_{i=1}^{N} w_i\, \rho_i^2 = \sum_{i=1}^{N} \chi_i^2$$

called the "chi-square", where $\rho_i = C_i - C[t_i]$ are called the residuals and $w_i = 1/\sigma_i^2$ can be considered the statistical weight of each datum point.

There are a variety of mathematical techniques to minimize the usually large and complicated chi-square figure-of-merit functions that arise from often involved pharmacokinetic models ⟨34, 35⟩. If the model is linear with respect to the parameters $a_1, \ldots, a_M$ of the form

$$C[t] = \sum_{j=1}^{M} a_j \, \phi_j[t] \tag{2.3}$$

where $\phi_1[t], \ldots, \phi_M[t]$ are arbitrary, even nonlinear, basis functions of t, then a solution may be found by use of the normal-equation method or, even better, by use of singular value decomposition method. These approaches also provide parameter uncertainty estimates. When the model is nonlinear on the set of M unknown parameters a_j, $j = 1, \ldots, M$, iterative mathematical minimization procedures are utilized, exempli gratia Levenberg-Marqardt or Gauss-Newton methods. Starting from given trial values for the parameters, these procedures improve on the trial solution until some indifference criterion is satisfied and the effective minimum of χ^2 is established ⟨34, 36⟩, but no error estimates for the parameters are yielded immediately. Also, said procedures are of a general nature and can be applied to linear models as well.

Once the difficult task of calculating the parameters of the pharmacokinetic model is complete a reckoning of the goodness-of-fit must be ascertained. For absent this estimate, the parameter values lack objective statistical significance and physical meaning. If the model is linear, as defined in equation (2.3) then the probability $\mathcal{P}_\gamma$ that the calculated χ^2 value could be as large as it is or less by chance, is given by

$$\mathcal{P}_\gamma = \mathrm{P}\left[\frac{\nu}{2}, \frac{\chi^2}{2}\right] = \frac{1}{\Gamma[\frac{\nu}{2}]} \int_0^{\frac{\chi^2}{2}} e^{-u} \, u^{\frac{\nu}{2}-1} \, du,$$

where $\mathrm{P} \in [0,1)$ is the incomplete gamma function ⟨37⟩, $\nu = N - M$ is the number of degrees of freedom, and Γ is the gamma function. Alternatively, $Q \equiv 1 - \mathcal{P}$, the complement of $\mathcal{P}$, can considered and interpreted as the probability that the calculated χ^2 value could be as large as it is or greater by chance, to serve as a quantitative measure of the goodness-of-fit of the model. If Q is a very small probability, then the apparent discrepancies between the pharmacokinetic model and the particular data set are unlikely to be chance fluctuations. It would seem that more plausible explanations are: (i) the model interprets reality poorly and can be statistically rejected as useless, (ii) the measurement uncertainties σ_i are actually larger than stated, or (iii) the measurement uncertainties are not Gaussianly distributed. As always with statistical tests, the choice on the boundary between what is reasonably probable, and thus supportive of the model, and what is incredible, is a subjective decision made by the investigator and the scientific community.

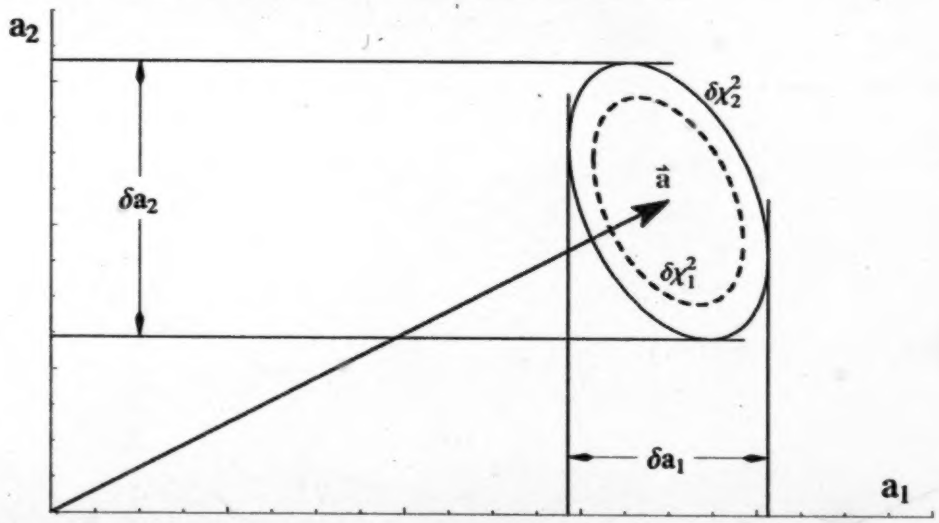

Figure 2.2: A hypothetical two-dimensional confidence region ellipse centered at $\vec{a}$ corresponding to values of chi-square larger than the fitted minimum. The one-dimensional confidence intervals for the parameters are indicated by the appropriate projections of the region onto the axes.

When the pharmacokinetic model depends nonlinearly on the set of M unknown parameters a_j, $j = 1, \ldots, M$, a straightforward analytical estimate of the goodness-of-fit of the model and the variances of the fitted parameters are generally not possible to derive. Instead, confidence limits on the fitted parameters are implied by analyzing the behavior of the χ^2 function near it's minimal value (see Figure 2.2). Let $\vec{a}$ be a vector of the M fitted parameters when the value of the chi-square function is a minimum, χ^2_{min}. A "confidence region" in the M-dimensional parameter space, centered at $\vec{a}$, is bounded by the constraint that $\chi^2 \leq \chi^2_{min} + \delta\chi^2$, where $\delta\chi^2$ is set by statistical analysis via Monte Carlo simulations. These M-dimensional surface contours of constant $\delta\chi^2$ are often ellipsoids and their projections onto the various M-axes indicate the confidence limits for the corresponding parameter ⟨38⟩.

Monte Carlo analysis rests on the premise that there exists some underlying true set of parameters, ${}^{true}\vec{a}$, that are essential to the nature of the pharmacokinetic model system, but hidden from the experimenter. These fundamental parameters are statistically realized via the response outputs, $\vec{Y}$, by the measured data, $\vec{Z}$ or ${}^{0}\vec{Z}$, to which the experimenter is privy (see Figure 2.1). By fitting the data to a model by χ^2 minimization, values for the parameters, $\vec{a}$ or ${}^{0}\vec{a}$, are calculated, but because process noise and measurement errors have a random component, ${}^{0}\vec{a}$ is not a unique realization of the true parameters of the pharmacokinetic model system, ${}^{true}\vec{a}$. Instead, Monte Carlo analysis assumes there could exist infinitely many other realizations of the true parameters potentially measured as the hypothetical data sets, ${}^{1}\vec{Z}$, ${}^{2}\vec{Z}$, ${}^{3}\vec{Z}$, ..., each one yielding a slightly different set of fitted parameters, ${}^{1}\vec{a}$, ${}^{2}\vec{a}$, ${}^{3}\vec{a}$, ..., respectively (see Figure 2.3) ⟨32⟩. Only from knowledge of the distribution of these hypothetical parameters and their corresponding chi-squared values can confidence intervals be constructed for the fitted parameters, $\delta\vec{a}$ or $\delta^{0}\vec{a}$.

Though direct observation of the true parameters of the pharmacokinetic model system, ${}^{true}\vec{a}$, or even the hypothetical parameters, ${}^{i}\vec{a}$, $i = 1, \ldots, \infty$, which could be discovered by repeated experiments is not possible, a precept of the Monte Carlo approach, that within the context of this thesis is unctuously accepted, is that the fitted parameters, ${}^{0}\vec{a}$, may serve as a reasonable surrogate for the true parameters, ${}^{\text{true}}\vec{a}$, for further statistical methods. A supplementary supposition is that the probability distribution of the hypothetical parameters around the true parameters, ${}^{i}\vec{a} - {}^{\text{true}}\vec{a}$, $i = 1, \ldots, \infty$, is comparable to the probability distribution of the synthetic Monte Carlo parameters around the fitted parameters, ${}^{i}_{S}\vec{a} - {}^{0}\vec{a}$, $i = 1, \ldots, N$. So, from the fitted parameters, ${}^{0}\vec{a}$, or from the actual data set, ${}^{0}\vec{Z}$ (when using the bootstrap method), a statistically significant number, N, of synthetic data sets, ${}^{i}_{S}\vec{Z}$, $i = 1, \ldots, N$ are randomly generated by computer to mimic the best understanding of the probability distribution, ${}^{i}\vec{a} - {}^{\text{true}}\vec{a}$, $i = 1, \ldots, \infty$, or the underlying the process noise, $\vec{n}$, and measurement errors, $\vec{e}$ (see Figure 2.1 and equations (2.1) and (2.2)). These synthetic pharmacokinetic data sets provide an accordant distribution of chi-squared values and best fit parameter vectors about, $\vec{a}$ or ${}^{0}\vec{a}$, from which a subjectively defined confidence region may be chosen (see Figure 2.2).

Lastly, and to me most incredibly, a statistical appraisal of the model adequacy can be ascertained. Following the above described tenets of the Monte Carlo approach, the fitted pharmacokinetic parameters, ${}^{0}\vec{a}$, may serve as a proxy for the true parameters of the biological model system, ${}^{\text{true}}\vec{a}$. At the appropriate set of times, t_i, $i = 1, \ldots N$, concurrent with the actual data set, ${}^{0}\vec{Z}$, a second series of synthetic data sets are begat. From the subsequently calculated chi-squared values, a tailored chi-square probability function can be approximated specific to the perhaps nonlinear pharmacokinetic model, taking into account the process noise of the biological model system and the measurement errors of the experiments ⟨Dr. Lele, Associate Professor of Statistics, University of Alberta, personal communication, 20 August, 2001⟩. To this probability function, may the chi-squared value of the actual data set, ${}^{0}\chi^{2}_{\text{min}}$, be compared, thus providing an objective account of the probability

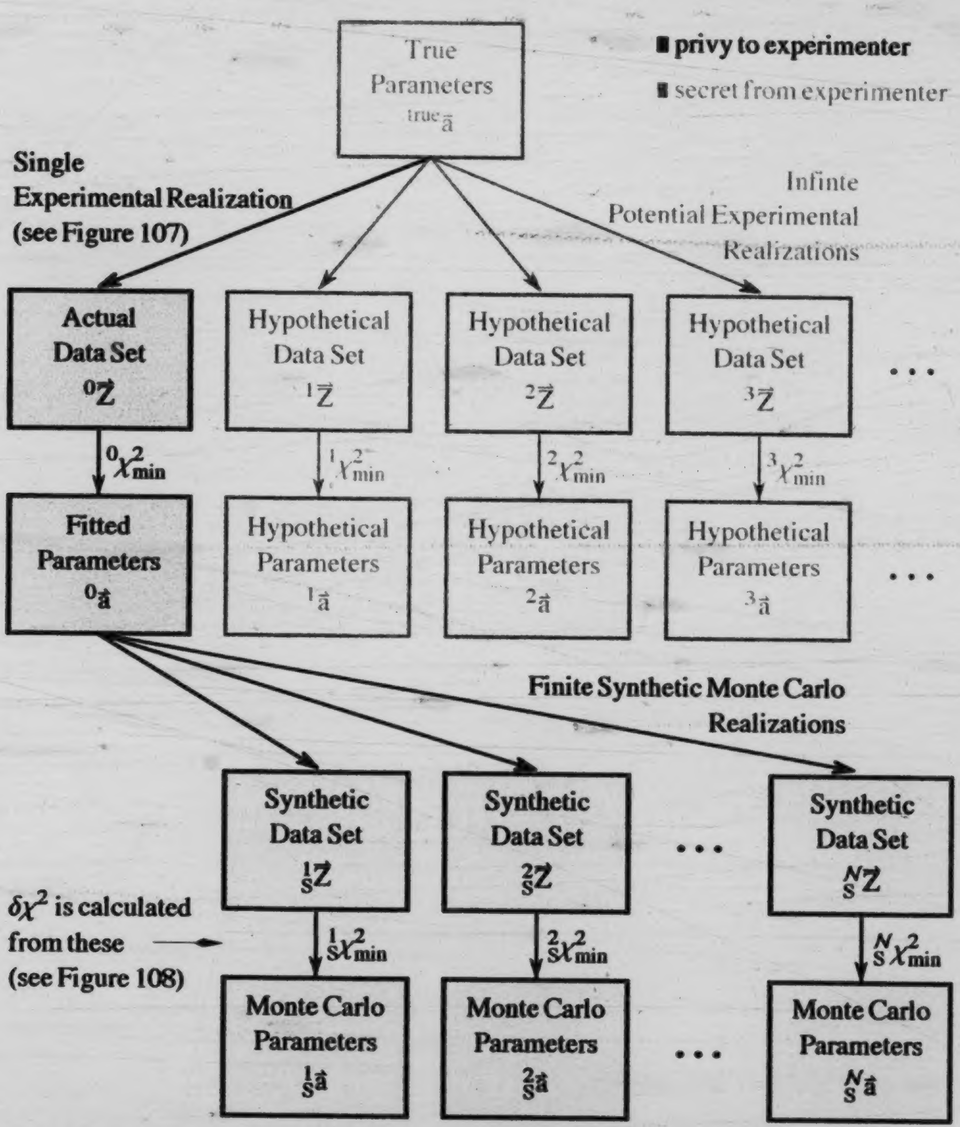
True Parameters ${}^{\text{true}}\vec{a}$
privy to experimenter
secret from experimenter
Single Experimental Realization (see Figure 107)
Infinte Potential Experimental Realizations
Actual Data Set ${}^{0}\vec{Z}$
Hypothetical Data Set ${}^{1}\vec{Z}$
Hypothetical Data Set ${}^{2}\vec{Z}$
Hypothetical Data Set ${}^{3}\vec{Z}$
. . .
${}^{0}\chi^2_{\min}$
${}^{1}\chi^2_{\min}$
${}^{2}\chi^2_{\min}$
${}^{3}\chi^2_{\min}$
Fitted Parameters ${}^{0}\vec{a}$
Hypothetical Parameters ${}^{1}\vec{a}$
Hypothetical Parameters ${}^{2}\vec{a}$
Hypothetical Parameters ${}^{3}\vec{a}$
. . .
Finite Synthetic Monte Carlo Realizations
Synthetic Data Set ${}^{1}_{S}\vec{Z}$
Synthetic Data Set ${}^{2}_{S}\vec{Z}$
. . .
Synthetic Data Set ${}^{N}_{S}\vec{Z}$
$\delta\chi^2$ is calculated from these (see Figure 108)
${}^{1}_{S}\chi^2_{\min}$
${}^{2}_{S}\chi^2_{\min}$
${}^{N}_{S}\chi^2_{\min}$
Monte Carlo Parameters ${}^{1}_{S}\vec{a}$
Monte Carlo Parameters ${}^{2}_{S}\vec{a}$
. . .
Monte Carlo Parameters ${}^{N}_{S}\vec{a}$

Figure 2.3: An abstract block diagram sketching the Monte Carlo simulation of an experiment. Computer generated random numbers are used to synthesize many simulated data sets from the single experimental realization. It is assumed that the statistical distribution of synthetic Monte Carlo parameters, ${}^{i}_{S}\vec{a}$, $i = 1, \ldots, N$, around the fitted parameters, ${}^{0}\vec{a}$, is similar to the distribution of hypothetical parameters, ${}^{i}\vec{a}$, $i = 1, \ldots, \infty$, around the true parameters, ${}^{\text{true}}\vec{a}$.

that the actual data set could occur and motivating subsequent subjective interpretations of model adequacy. Briefly summarizing, to be genuinely useful a fitting procedure should provide (i) values for the unknown parameters, (ii) error estimates on the parameters, and (iii) a statistical measure of goodness-of-fit.

Chapter Three

An Initial Consideration of the Biological Model System

A Summary of Relevant Knowledge on Mibefradil

Pharmacokinetic inquiries introduced to me by Dr. Tuszynski performed under the aegis of Dr. Yun K. Tam's laboratory in the mid-1990s at the University of Alberta on the drug mibefradil provided results that provoked the hitherto unstated thesis of this report. Now mibefradil is a calcium antagonist designed for the treatment of hypertension and angina since it has the useful effects of being able to relax blood vessels allowing more blood and oxygen to reach the heart but at the same time not reducing the performance of the heart ⟨39,40,91⟩. Most relevant for this report, was that experiments on chronically instrumented dog model systems evinced nonlinear pharmacokinetics for mibefradil as dosage was increased and that the liver was identified as the major organ for elimination of the drug ⟨41⟩. The resulting experimental facts were many plasma concentration time-course data sets for different dogs at different oral and i.v. dosages upon which the remainder of this report is based (see Figure 3.1).

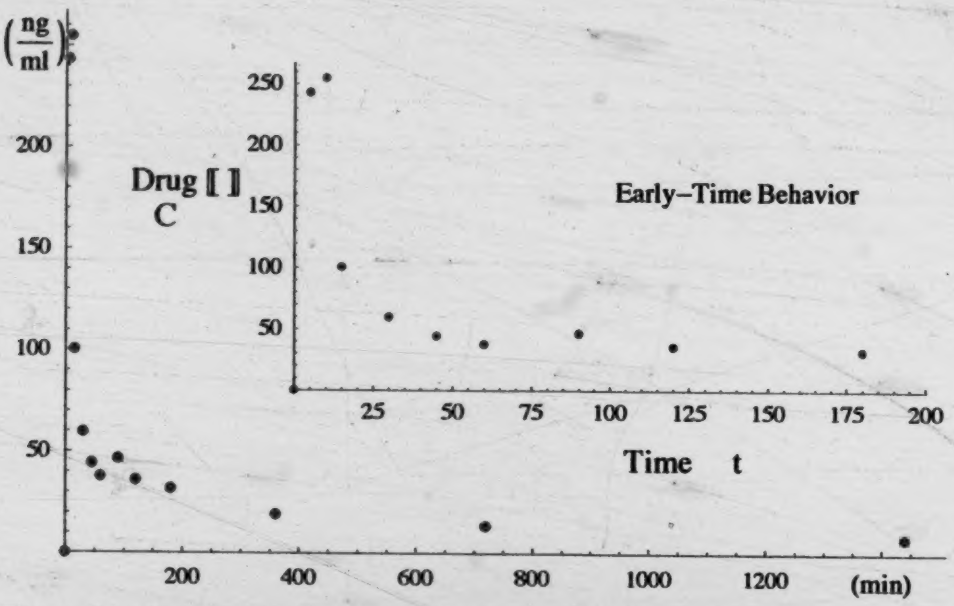

Figure 3.1: A representative concentration verses time data set from the dog model system studied with a characteristic sharp peak and elongated tail. The measured concentrations are of Mibefradil in the plasma of the number two dog taken at various times from the portal vein after an intravenous dose (IV-PV-D2). The uncertainty of the concentration measurements was calculated to be 9%.

Because the uncertainties of the concentration measurements were never explicitly stated and perhaps never calculated in either ⟨42⟩ or ⟨41⟩, this value was directly calculated from the documented concentration calibration chromatograms of HPLC assays of mibefradil in the dog plasma from ⟨41⟩. The percentage errors of measured concentration values of the known test standards were assumed to be Gaussianly distributed, such that the standard deviation of the distribution, to randomly account for the discrepancies 90% of the time, was 9%. The uncertainty in the documented measurements of the independent time variable likewise was not stated in ⟨42⟩ or ⟨41⟩, but is assumed to be small for the purposes of this report.

Since the declared nonlinear behavior of mibefradil after higher oral doses is at least partially attributed to a possible increase in gut absorption ⟨42⟩, and rather than challenge or confirm these results, or complicate this report with concerns of drug absorption via the gut or first-pass effect of the liver, only the data of the i.v. trials from the rather comprehensive study of Skerjanec in ⟨41⟩ was considered for renewed investigation and interpretation within this report. It was additionally concluded in ⟨41⟩ that the observed nonlinear kinetics of mibefradil in dogs was mainly due to dose- and/or time-dependent reductions of hepatic clearance, though the mechanisms remained unknown. Naturally, aside from the potential pharmacokinetic causes for the observed nonlinear behavior of mibefradil, such as alterations to: plasma protein binding, hepatic tissue binding, and enzyme activities ⟨43⟩ following drug administration, given the author's background, a physical explanation was pondered. Therefore, the major objective of this report is to offer a novel physical mechanism that at least contributes towards the explanation of the observed nonlinear pharmacokinetics of mibefradil.

A Scrutiny of the Data by Empirical Curve Fitting

> The triumphant vindication of bold theories—are these not the pride and justification of our life's work?
>
> -Sherlock Holmes, *The Valley of Fear*
> Sir Arthur Conan Doyle

A Brief Rationale

There are practical reasons for a pharmacokinetic researcher, regardless of motivations, to invest at least a modest amount of time to complete some empirical curve fits to the data of interest. Clinical researches can condense the real pharmacokinetic data to a comparatively small set of mathematical terms for efficient use in applied analysis, while theoretical researchers may glean some insights into the underlying processes of the situation - a low level empirical generalization may be constructed. Results obtained for the mathematical relationships describing the data should be distinguished from model parameters that may be deduced from the results. Nevertheless, initial observations of patterns by empirical curve fitting impel explanations and seed hypotheses.

Yet, it seems that empirical curve fitting can constrain conjectures somewhat, since simple observations have the asymmetric puissance to prove that a theory is wrong though not right. That is, the future model can in some sense be constrained without appealing to a priori knowledge. Misguided models may never be explored if the researcher understands, by curve fitting, the properties of the data then realizes that the model in question is unable to reproduce similar behavior. Of course, with enough parameters, many types of functions form a strong enough basis set to fit a wide variety of data. Therefore, parameter parsimony will assist in the interpretation of the data ⟨44⟩ based on the relevance of simplicity to physics. Yet, it remains a philosophically vexing problem how to justify the initial choices regarding the form of the phenomenological model and the trade off between the unification of the data by a paucity of parameters with the total degree of fit.

The Debut of a Modified Prony's Method to Include Weighted Datum Points for Curve Fitting in Pharmacokinetics

> What ineffable twaddle! I never read such rubbish in my life.
> -Dr. Watson, *A Study in Scarlet*
> Sir Arthur Conan Doyle

The equations generated by classical compartmental models, and sometimes used by noncompartmental techniques, are sums of exponentials. Prony's method is a mathematical routine to fit said equations to data and was studied for its merits in pharmacokinetic applications. Broadly described, the approach of Prony's method is to convert exponential expressions to nonlinear algebraic equations and then transform those to a larger number of linear algebraic equations that can be easily solved by the method of least squares. So, presuming that drug concentration time-course data is to be fit to an approximation with 2M unknowns of the form

$$C[t] \approx A_1 e^{a_1 t} + A_2 e^{a_2 t} + \cdots + A_M e^{a_M t} \tag{3.1}$$

let $\mu_k = e^{a_k}$, to put the exponential relation into the more convenient configuration of

$$C[t] \approx A_1 \mu_1^t + A_2 \mu_2^t + \cdots + A_M \mu_M^t \,. \tag{3.2}$$

Now Prony's method demands that ordinate values of $C[t]$ are specified on a set of $N \geq 2M$ equally spaced points, and that a linear change of variables has been introduced in advance in such a way that the abscissa datum points are at $t \rightarrow k = 0$, 1, 2, ..., N-1. Therefore, the real data must be translated in time so the first meaningful datum is at time $t = 0$, and then scaled by a lowest common denominator and mapped onto the natural numbers. If the data set is incomplete at this point, then the only known option is to complete the data set by interpolation between the actual datum points. By successive substitution of each transformed datum (k, C_k) into (3.2), each relation of the following group

$$\begin{aligned}
C_0 &\approx A_1 \mu_1^0 + A_2 \mu_2^0 + \cdots + A_M \mu_M^0, \quad \mu_k^0 = 1 \\
C_1 &\approx A_1 \mu_1^1 + A_2 \mu_2^1 + \cdots + A_M \mu_M^1 \\
C_2 &\approx A_1 \mu_1^2 + A_2 \mu_2^2 + \cdots + A_M \mu_M^2 \\
&\vdots \\
C_{N-1} &\approx A_1 \mu_1^{N-1} + A_2 \mu_2^{N-1} + \cdots + A_M \mu_M^{N-1}
\end{aligned} \tag{3.3}$$

necessarily would be met, such that, the exponential approximation may be based on the result of satisfying these *N* algebraic expressions as nearly as possible.

To help solve this group of mostly nonlinear *algebraic* relations, introduce a temporary variable μ and construct the equation

$$(\mu - \mu_1)(\mu - \mu_2)\cdots(\mu - \mu_M) = 0$$

where $\mu_1, \mu_2, \ldots, \mu_M$ are the roots of the expanded algebraic equation

$$\alpha_0 \mu^M + \alpha_1 \mu^{M-1} + \alpha_2 \mu^{M-2} + \cdots + \alpha_{M-1} \mu^1 + \alpha_M \mu^0 = 0 \tag{3.4}$$

where $\alpha_i = f[\mu_1, \mu_2, \ldots, \mu_M]$ and $\alpha_0 = 1$ without loss of generality ⟨45⟩. The strategy is to temporarily isolate the nonlinearity of the system within the single polynomial (3.4) and transform (3.3) into a set of linear algebraic equations. In order to determine the coefficients $\alpha_1, \alpha_2, \ldots, \alpha_M$, the first equation in (3.3) is multiplied by α_M, the second equation by α_{M-1}, …, the *M*th equation by α_1, and the $(M+1)$th equation by α_0, and add the results, as follows

$$\begin{aligned}
\mathrm{C}_0 &\approx \mathrm{A}_1\,\mu_1^0 + \mathrm{A}_2\,\mu_2^0 + \cdots + \mathrm{A}_\mathrm{M}\,\mu_\mathrm{M}^0 && \times\,\alpha_\mathrm{M}\\
\mathrm{C}_1 &\approx \mathrm{A}_1\,\mu_1^1 + \mathrm{A}_2\,\mu_2^1 + \cdots + \mathrm{A}_\mathrm{M}\,\mu_\mathrm{M}^1 && \times\,\alpha_\mathrm{M-1}\\
\mathrm{C}_2 &\approx \mathrm{A}_1\,\mu_1^2 + \mathrm{A}_2\,\mu_2^2 + \cdots + \mathrm{A}_\mathrm{M}\,\mu_\mathrm{M}^2 && \times\,\alpha_\mathrm{M-2}\\
&\ \vdots && \ \vdots\\
\mathrm{C}_\mathrm{M} &\approx \mathrm{A}_1\,\mu_1^\mathrm{M} + \mathrm{A}_2\,\mu_2^\mathrm{M} + \cdots + \mathrm{A}_\mathrm{M}\,\mu_\mathrm{M}^\mathrm{M} && \times\,\alpha_0
\end{aligned}$$

$$\begin{aligned}
\Rightarrow\ &\mathrm{C}_0\,\alpha_\mathrm{M} + \mathrm{C}_1\,\alpha_\mathrm{M-1} + \mathrm{C}_2\,\alpha_\mathrm{M-1} + \cdots + \mathrm{C}_\mathrm{M}\,\alpha_0\\
&\approx 0 = (\alpha_0\,\mu^\mathrm{M} + \alpha_1\,\mu^\mathrm{M-1} + \cdots + \alpha_\mathrm{M-1}\,\mu^1 + \alpha_\mathrm{M}\,\mu^0)(\mathrm{A}_1 + \cdots + \mathrm{A}_\mathrm{M}).
\end{aligned} \tag{3.5}$$

Notice, since $N \geq 2M$, the above demarche does not include all of the N equations in (3.3). But, with the same approach, by starting instead successively with the second, third, ⋯, $(N-M)$th equation, all of the equations of (3.3) are used, and $N-M-1$ additional equations of similar form to (3.5) are obtained. Together, the above treatment implies the set of $N-M$ linear algebraic equations

$$\begin{aligned}
&\mathrm{C}_\mathrm{M}\,\alpha_0 + \mathrm{C}_\mathrm{M-1}\,\alpha_1 + \mathrm{C}_\mathrm{M-2}\,\alpha_2 + \cdots + \mathrm{C}_0\,\alpha_\mathrm{M} \approx 0\\
&\mathrm{C}_\mathrm{M+1}\,\alpha_0 + \mathrm{C}_\mathrm{M}\,\alpha_1 + \mathrm{C}_\mathrm{M-1}\,\alpha_2 + \cdots + \mathrm{C}_1\,\alpha_\mathrm{M} \approx 0\\
&\quad\vdots\\
&\mathrm{C}_\mathrm{N-1}\,\alpha_0 + \mathrm{C}_\mathrm{N-2}\,\alpha_1 + \mathrm{C}_\mathrm{N-3}\,\alpha_2 + \cdots + \mathrm{C}_\mathrm{N-M-1}\,\alpha_\mathrm{M} \approx 0.
\end{aligned} \tag{3.6}$$

Since the ordinates C_k are determined from the real data, the above set generally can be solved using the method of least-squares.

From this course of actions, after the α's are determined, the M μ's, and subsequently the unknown parameters $a_1, \cdots, a_M$, are found as the roots of the single polynomial equation (3.4). After substitutions, the equations (3.3) then become linear equations in the M A's with known coefficients μ_k. Finally, the unknown parameters $A_1, \cdots, A_M$ are determined again by applying the least squares technique to this set of equations to complete the process of obtaining values for all of the sought after pharmacokinetic parameters.

A typical example of the adeptness of Prony's method in fitting the Mibefradil data set by a sum of exponentials of the form of equation (3.1) can be appreciated in

Figure 3.2. Because the real data from Dr. Tam's dog experiments was not complete in the sense, as previously described, that Prony's method demands, additional adscititious datum points were synthesized by linearly interpolating between the real datum points. Once combined, the resulting new set of data could be mapped to the natural numbers by division by the lowest common denominator: 5 minutes.

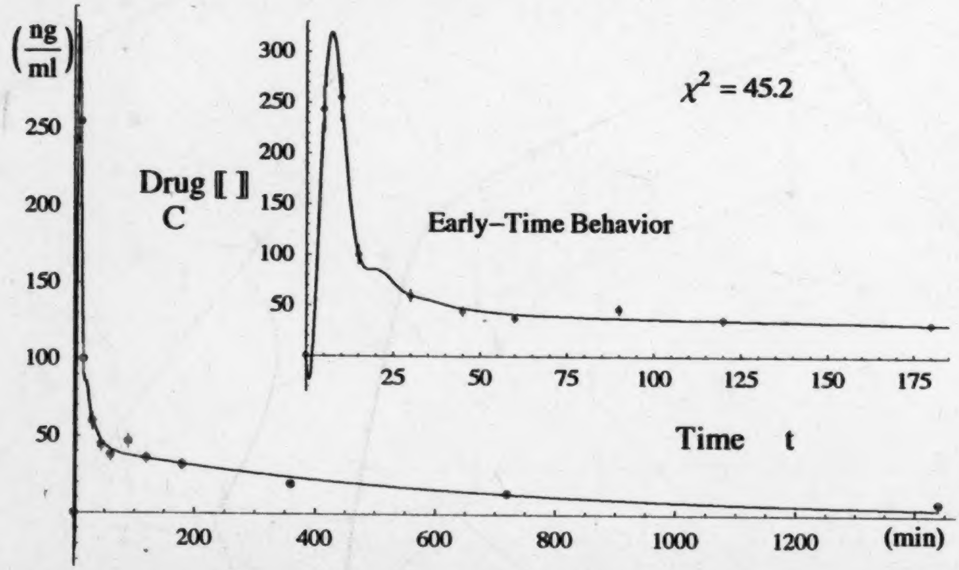

Figure 3.2: A curve generated using a sum of six exponential terms fit by the standard Prony's method compared to the concentration time-course data taken after an intravenous dose from the portal vein of dog number two (IV-PV-D2).

The first seven datum points of the concentration peak were matched remarkably well considering the rapidly changing, and broad range of, drug concentration values over a narrow domain of time. The global fit of the data was generally not as successful as indicated by a rather large figure-of-merit chi-square function value. A view of the statistical residuals, $R_i = |C_i - C[t_i]|$, of the data indicated that most of the discrepancy as measured by the figure-of-merit function between the curve fit and the data was due to the datum points in the long shallow sloped tail (see Figure

3.3). This was not surprising since the standard Prony's method must perform with all the data, real and synthesized, without discrimination, while the chi-square figure-of-merit function is only concerned with the agreement between the fitted curve and the real experimental data. Whereas the chi-square function weights all absolute deviations between the fitted curve and the real datum points inversely proportional to the uncertainty (previously shown to be 9%) of the measured concentration at that point ($w_i = 1/\sigma_i^2$), thus demanding greater absolute accuracy at the low concentrations of the tail, the standard Prony's method has no abilities to take into account weighted datum points and considers the absolute deviation of all datum points equally. An amelioration of Prony's method appeared necessary for the statistical technique to be influenced by the real datum points to a larger extent than the interpolated datum points and, since the range of the ordinate data spans 4.3 orders of magnitude (relative to base ***e***), to consider absolute residuals differently for each datum point.

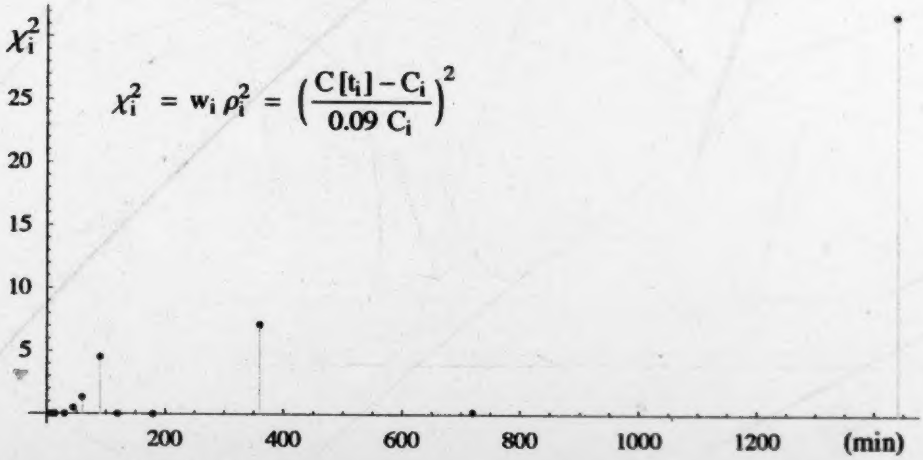

Figure 3.3: A plot of the weighted residual squared for each of the real datum points separated in time to indicate their relative contribution to the disparity with the curve produced by Prony's method as measured by the chi-squared figure-of-merit function for the trial IV-PV-D2.

From the theory of approximation by the method of least-squares for discrete data (see Appendix 2), a system of equations of the form (3.6) can be used to manufacture a set of *M* normal equations with which the *M* unknowns $\alpha_1, \alpha_2, \ldots, \alpha_M$, can be exactly solved for using matrix methods. Establishing the *r*th normal equation entails multiplying each relation of (3.6) by the coefficient of α_r in that equation, and by the weight associated with that equation, and summing the results, as follows

$$\begin{array}{lll} -C_M & \approx C_{M-1}\,\alpha_1 + C_{M-2}\,\alpha_2 + \cdots + C_0\,\alpha_M & \times C_{M-r} \quad \times w \\ -C_{M+1} & \approx C_M\,\alpha_1 + C_{M-1}\,\alpha_2 + \cdots + C_1\,\alpha_M & \times C_{M+1-r} \quad \times w \\ \quad\vdots & & \quad\vdots \\ -C_{N-1} & \approx C_{N-2}\,\alpha_1 + C_{N-3}\,\alpha_2 + \cdots + C_{N-M-1}\,\alpha_M & \times C_{N-1-r} \quad \times w \end{array} \tag{3.7}$$

where $r = 1, 2, \ldots, M$, $\alpha_0 = 1$, and w_i are the unknown weights. Besides possessing the appropriate form to be susceptible to solution by the method of least-squares through the use of normal equations, the above group of relations possesses the critical difference, compared to groups of relations formed by an approximation to data with a linear model, of each of the relations not being dependent on a single discrete datum value (see Appendix 2, equation (a.2)). Usually, each of the relations, analogous to those of (3.7), have coefficients that are dependent on one abscissal datum value and constants that are dependent on the corresponding ordinate datum value. An examination of the individual relations of (3.7) evinces that the coefficients and constants are dependent on a train of $M+1$ ordered ordinate datum values.

Since weights are normally applied to a single relation, such as those of (3.7), as functions based on the one corresponding datum point determining the coefficients and constants of the single relation, the same weighting scheme for Prony's method is unworkable. An altered weighting scheme based on the entire ordered series of ordinate concentration values of an individual equation was devised ad hoc.

Because any ordered sequence of ordinate data implies an ordered sequence of abscissal data, the weight assigned to each equation was considered to be the average weight attributed to each datum point as a function of time. For example, the first equation in (3.7) was given the weight

$$\begin{aligned} w_? &= w_?[C_M[t_M],\ C_{M-1}[t_{M-1}],\ C_{M-2}[t_{M-2}],\ \ldots,\ C_0[t_0]] \\ &= \mathrm{Mean}[w[t_M],\ w[t_{M-1}],\ w[t_{M-2}],\ \ldots,\ w[t_0]], \end{aligned}$$

where $w[t_k],\ k=0,\ldots,N-1$ are the values of the weight function at the discrete datum points.

Using aggregate weights as define above, effectively smears in time the influence of the weight function, *w*, around each abscissal datum value, t_k, over a domain $t \in [t_{k-M-1}, t_{k+M+1}]$. This occurs because each equation in (3.7) that is used to calculate the aggregate weight is a train in time, $M+1$ cars long, that requires $2M+1$ units of time to pass. Therefore, this weighting scheme performs most like a regular linear least-squares weighting procedure when the number of parameters, *M*, is small and the short train is more like a point along the abscissa than a long line. Illustrative results of the process can be discerned from Figure 3.4.

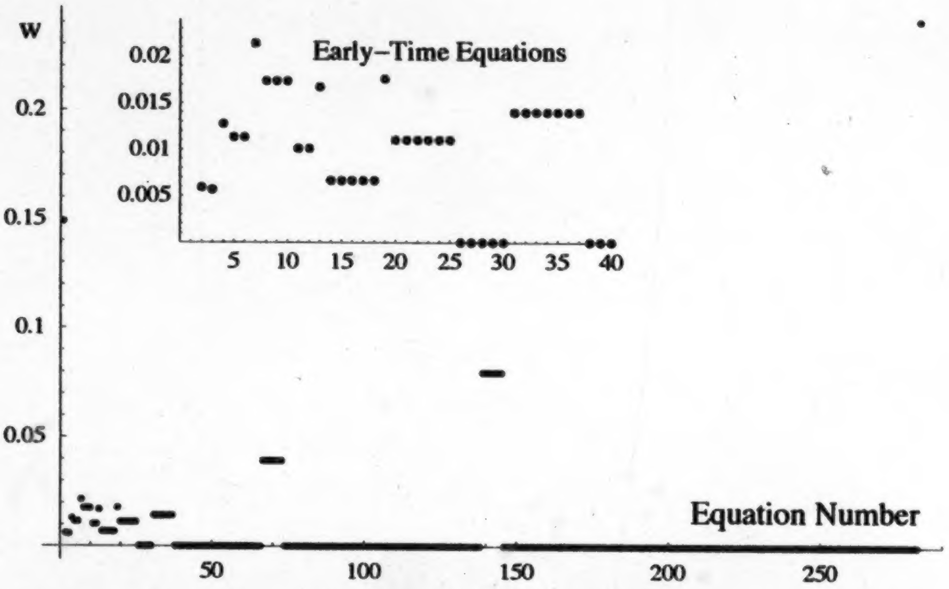

Figure 3.4: A plot of the calculated aggregate weight values assigned to each of the *N*-*M* equations of (3.7) for the IV-PV-D2 data. Large values cluster around real datum assigned large weights whereas zero values indicate equations constituted entirely of interpolated data given no weight.

An advantage of the described weighting system for Prony's method for fitting pharmacokinetic data, is that much of the influence of the interpolated datum points, introduced because of an incomplete data set as a necessity of the procedure, can be removed by setting the weight function to be zero for all interpolated data, such that $w[t_k] = 0 \;\forall\; (k, C_k) \in$ {interpolated data}. This results in the interpolated data mostly being diminished to valueless placeholders that the method requires, but that affect the final fit diminutively. The nonzero weights assigned to real datum points were the same as those for the normal linear least-squares method: $w[t_k] = 1/\sigma_k^2 \;\forall\; (k, C_k) \in$ {real data}, where $\sigma_k = 9\% \, C_k$. Because Prony's method uses a least-squares fit a second time, in a more conventional format of (3.3), the weights of the individual datum points are used again to calculate for the *A*'s.

Finally, to calculate the *r*th normal equation contributing to a direct solution as described above, as a first step in Prony's method, for the unknowns $\alpha_1, \alpha_2, \ldots, \alpha_M$, the aggregate weights were implemented explicitly as follows

$$\begin{array}{lll}
-C_M & \approx C_{M-1}\,\alpha_1 + C_{M-2}\,\alpha_2 + \cdots + C_0\,\alpha_M & \times C_{M-r} \times w[t_M, \ldots, t_0] \\
-C_{M+1} & \approx C_M\,\alpha_1 + C_{M-1}\,\alpha_2 + \cdots + C_1\,\alpha_M & \times C_{M+1-r} \times w[t_{M+1}, \ldots, t_1] \\
\vdots & & \vdots \\
-C_{N-1} & \approx C_{N-2}\,\alpha_1 + C_{N-3}\,\alpha_2 + \cdots + C_{N-M-1}\,\alpha_M & \times C_{N-1-r} \times w[t_{N-1}, \ldots, t_{N-M-1}] \\
+ & \overline{\qquad\qquad\qquad\qquad\qquad\qquad\qquad\qquad} & \\
 & \varsigma_{r,1}\,\alpha_1 + \varsigma_{r,2}\,\alpha_2 + \cdots + \varsigma_{r,M}\,\alpha_M = \xi_r & (r\text{th normal equation}),
\end{array}$$

where $\varsigma_{r,j}$ are the constant coefficients of the unknown parameter variables α_j described by

$$\varsigma_{r,j} = \sum_{i=M}^{N-1} w[t_i, t_{i-1}, \ldots, t_{i-M}]\, C_{i-r}\, C_{i-j}$$

and ξ_r are constants described in terms of known values by

$$\xi_r = -\sum_{i=M}^{N-1} w[t_i, t_{i-1}, \ldots, t_{i-M}]\, C_{i-r}\, C_i\,.$$

The consequences of the utilization of the weights can be appreciated in Figure 3.5.

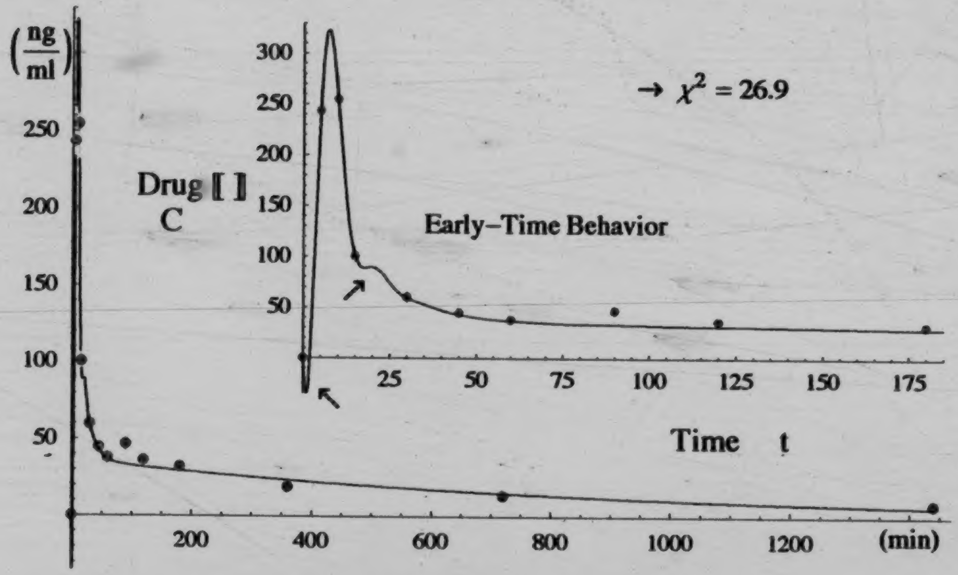

Figure 3.5: A curve generated using a sum of six exponential terms determined by the weighted Prony's method to the IV-PV-D2 concentration time-course data exhibiting an improved fit, but where arrows indicate anomalous behavior.

The improvement of the curve fit to the Pharmacokinetic data was most clear by the observed reduction in the calculated chi-square merit function value from 45.2 to 26.9. But, I expect the regular Prony's method was fortunate to fit the real data so well in the first place. Since, although it did not weigh the calculated residual values from the tail any more than the residual values from the peak, as it should have because of the smaller variances there ($w \propto 1/\sigma^2$), the nature of the incomplete data set conspired to provide hundreds of interpolated datum points along the shallow extended tail that compensated for this neglect. I predict that the improvements of the weighted Prony's method would be even greater if the original data contained gaps more evenly spread or contained no interruptions at all.

Regardless of the improved accuracy of a weighted Prony's method for fitting pharmacokinetic concentration-time course data, apparently the method can not be used to assist in any kind of standard interpretation of results in connection with classical compartmental models. The actual expression, in the form of (3.1), for the curve of Figure 3.5 was

$$\begin{aligned} C[t] \approx{} & 37\,e^{-0.001\,t} + 250\,e^{-0.08\,t} + (9 - 132\,i)\,e^{(-0.2+0.2\,i)\,t} \\ & +(9+132i)e^{(-0.2-0.2i)\,t} - (152-181\,i)e^{(-0.2+0.4i)\,t} - (152+181i)e^{(-0.2-0.4i)\,t} \end{aligned}$$

The complex exponential coefficients arise naturally, and without possible restriction, from equation (3.4) when the μ's are solved for as the roots of a polynomial. Since the exponential coefficients are a function of the μ's, $\mu_k = e^{a_k}$ from (3.2), the a's, and the A's from subsequent calculations, have imaginary components generally. The result is a concentration curve that is oscillatory and that possesses physically impossible negative concentration values at very early times. Obviously, until complex disposition rate constants, as those produced in the equation above, are considered, Prony's method will never find significant use in pharmacokinetics.

Yet if classical multicompartmental models are generalized somewhat to similarly include linear interactions, based on the amount of drug in a compartment with other compartments, that do not imply a direct transfer of material, then control systems based on positive or negative feedback signals can be represented by compartmental analysis ⟨46⟩. Allowing this paradigm, the influence of one compartment upon the other can be represented by a constant of a meaning that is no longer restricted to the fraction of the material in a given compartment entering another in one unit of time as for a first-order transfer constant (exempli gratia, k_{21} and k_{12} in Figure 1.3), but corresponds to a signal from one compartment acting upon the other. In this case the signal or coupling coefficient may be negative such that the level of drug in one compartment decreases the level of drug of another compartment. I speculate the means of this may be from the induction of metabolism in one compartment due to the presence of drug in another compartment via one of the signaling systems of the body. Prony's method could then serve a useful purpose when describing a system from this new perspective.

A Justification for Restriction of the Data

If the early time-course data, following an I.V. dose of Mibefradil given at a constant rate of ten minutes duration, for all four dogs are compared, such as in Figure 3.6, then it is observed that between the initial condition, $(t_0,C_0)=(0,0)$, and the peak concentration, there exists zero or one datum point. This condition of limited early sampling is considered as a "lack of sampling" by Tam et alia in ⟨47⟩. The I.V. infusion is a zero-order process, such that $dC/dt = +k_o$, resulting in a linear rise of concentration in a homogeneous system in the absence of elimination or a curve of decreasing slope in the presence of drug elimination. With one parameter remaining, k_o, after the initial condition is satisfied, and only one or two datum points to the peak concentration, the rise in the concentration data is trivially and superficially fit. Therefore, to focus on the more complicated pharmacokinetic process of the elimination of the drug, and to reduce the number of parameters utilized while only expending zero or one datum point and an initial condition, further analysis of the Mibefradil concentration time-course data was restricted to the time of the peak concentration onward. Further analysis proceeded as if the brief I.V. dose was actually a I.V. bolus dose (a reasonable assumption in itself given the short time duration of the dose compared to the entire domain of the data), with the assumption that the original initial condition and a first-order I.V. infusion approach could be accommodated later without significant changes to any conclusions made.

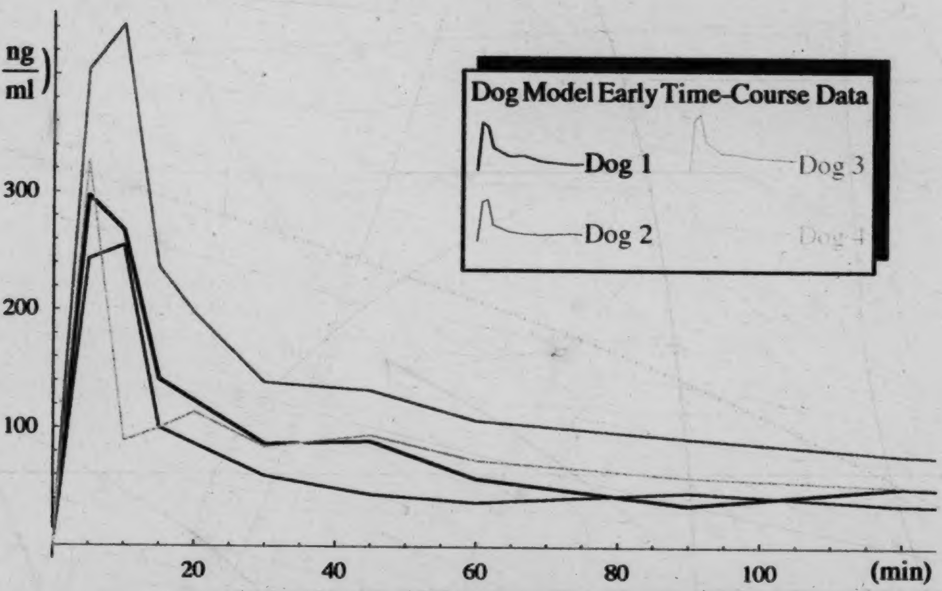

Figure 3.6: An inspection of the very early time behavior of the concentration time-course data for each dog model indicating the initial increase in drug concentration occurs over a shorter time than the resolution of the experiment.

A General Technique of Nonlinear Fits with a Global Optimization Method

Only a small portion of curves that can economically fit data are expressible as a linear combination of terms with respect to the adjustable parameters of the form (2.3). Generally, nonlinear functions, of free parameters that cannot be linearized, generate the most economical match to the data, and those curves must be fit by minimizing a figure-of-merit function as previously described. Locating the absolute minimum, and not some local minimum, of a function is a challenging undertaking and was pursued for the remainder of the thesis using global optimization techniques.

Given a real valued function $\chi^2[\vec{a}] \ni \mathbb{R}^M \to \mathbb{R}$ and a compact set $S \subseteq \mathbb{R}^M$, a point $\vec{a}^* \in S$ is a global minimizer ⟨48⟩ of $\chi^2[\vec{a}]$ if

$$\chi^2[\vec{a}^*] \le \chi^2[\vec{a}] \ \forall \ \vec{a} \in S.$$

With the challenge originating from the difficulties in winnowing the global minimizer from any local minimizers, such that a point $\vec{a}^* \in S$ is a local minimizer of $\chi^2[\vec{a}]$ if

$$\exists\ \varepsilon \in \mathbb{R} \wedge \varepsilon > 0 \ni \chi^2[\vec{a}^*] \leq \chi^2[\vec{a}]\ \forall\ \vec{a} \in B[\vec{a}^*, \varepsilon] \cap S,$$

where $B[\vec{a}^*, \varepsilon]$ is a neighborhood around $\vec{a}^*$. The largest open connected neighborhood of $\vec{a}^*$, $D[\vec{a}^*]$, for which

$$\chi^2[\vec{a}^*] \leq \chi^2[\vec{a}]\ \forall\ \vec{a} \in D[\vec{a}^*] \subseteq \mathbb{R}^M,$$

is called the region of descent to $\vec{a}^*$ ⟨23⟩. Specifically for this thesis, the real function just defined above to be minimized will be the chi-squared figure-of-merit function and the vector $\vec{a}$ will be a $M \times 1$ matrix of the adjustable parameters for the curve $C[t; a_1, \ldots, a_M]$. Therefore, the problem of realizing a curve that best fits the pharmacokinetic data (t_i, C_n), $i = 1, \ldots, N$ becomes a problem of finding a vector $\vec{a}[a_1, \ldots, a_M]$ in M-dimensional parameter-space that globally minimizes χ^2.

Traditional iterative gradient (local) approaches briefly mentioned previously, such as Levenberg-Marqardt or Gauss-Newton methods have the following disadvantages: they generally require a reasonably accurate initial trial solution, they require that the function be continuous, they often have difficulty converging to a solution when the optimum is within a very flat neighborhood, $B[\vec{a}^*, \varepsilon]$, or when there is non-unique global minima, and they are susceptible to converging to local minima, $\vec{a}_k^*$, with substantial regions of descent, $D[\vec{a}^*]$. Adaptive Grid Refinement (AGR) is a simple though robust alternative global algorithm for minimizing functions. It generally requires less presupposed comprehension of the nature of the function to be minimized, and no trial solution to begin ⟨38⟩. The function even may be discontinuous since no derivatives are made and no search vectors are used. The drawback of this convenience and capability tends to come at an additional cost of computer time due to the large number of function calls (repeated evaluations of χ^2) within programs implementing AGR.

The adaptive grid refinement algorithm works as follows and is portrayed in Figure 3.7. A closed continuous set, $S \subseteq \mathbb{R}^M$, which may be large, is defined such that for each of the M parameters, a_i, the projection of S is a closed domain $[{}^{\text{start}}a_i, {}^{\text{end}}a_i]$ within which the minimizing value of that parameter, a_i^*, is hopefully a member. Over the defined domain, n grid points, where $n=7$ in Figure 3.7, are chosen to be separated by a distance $\Delta a_i = [{}^{\text{start}}a_i, {}^{\text{end}}a_i]/n$, and aside from the domain boundary at a distance of $\Delta a_i/2$. At each grid point, $a_{i,1}, a_{i,2}, \ldots, a_{i,n}$, the chi-squared function to be minimized, $\chi^2[a_i]$, is evaluated and the extrema, χ^2_{min} and χ^2_{max}, are identified. A selection criterion, χ^2_{cutoff}, calculated as a function of the difference between the extrema, then determines which grid points will be kept for further refinement in the forthcoming iteration.

$$\chi^2_{\text{cutoff}} = \chi^2_{\text{min}} + (\chi^2_{\text{max}} - \chi^2_{\text{min}})\varphi, \quad \varphi \in (0, 1).$$

All those grid points with function values less than χ^2_{cutoff} are retained, while the rest are discarded. For each grid point preserved beyond the selection process of the previous iteration, new daughter grid points are spawned on each side at one-third the distance between the previous grid points. This provides a new grid of higher resolution covering a generally smaller, sometimes piecewise, domain for the iterative AGR algorithm to repeat itself.

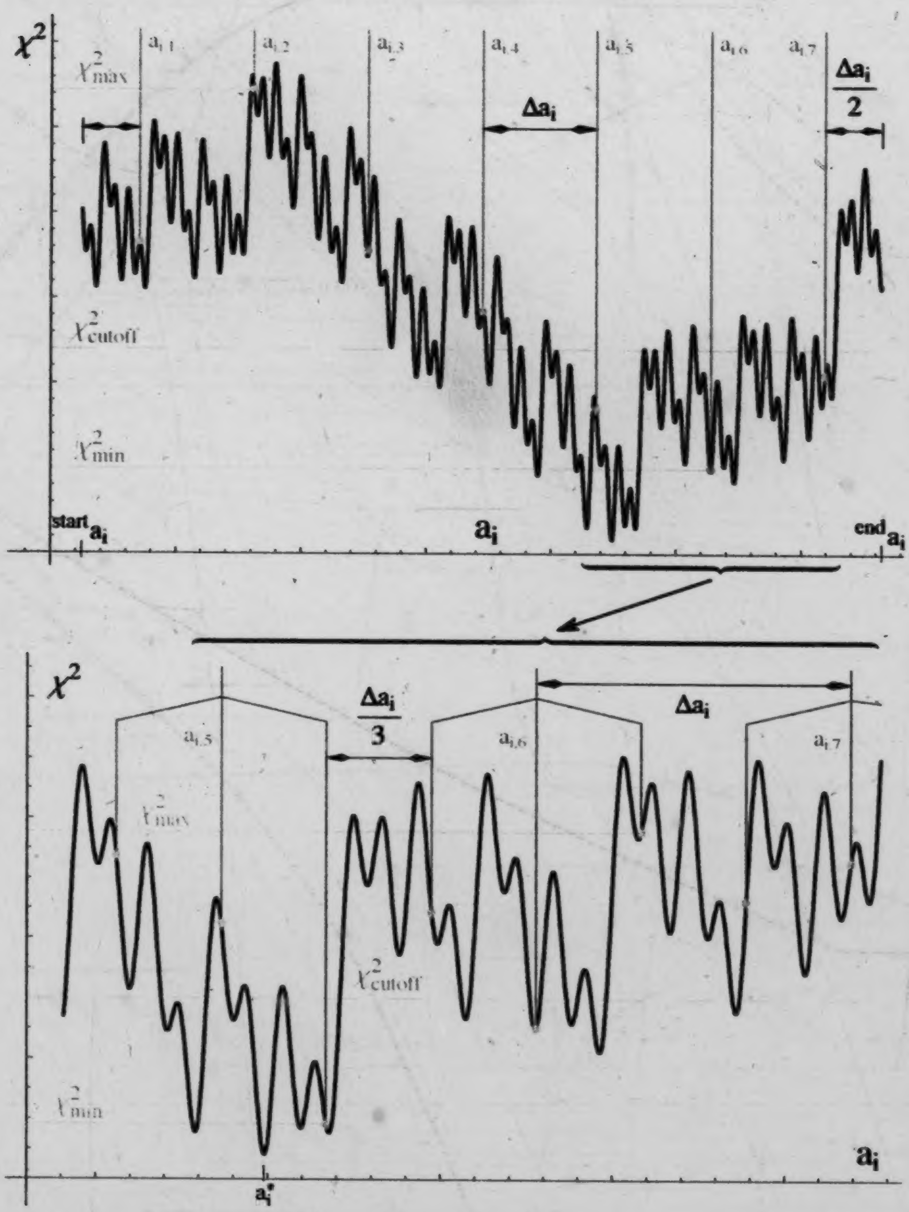
χ^2
χ^2_{max}
χ^2_{cutoff}
χ^2_{min}
$a_{i,1}$
$a_{i,2}$
$a_{i,3}$
$a_{i,4}$
$a_{i,5}$
$a_{i,6}$
$a_{i,7}$
Δa_i
$\frac{\Delta a_i}{2}$
${}^{start}a_i$
a_i
${}^{end}a_i$
χ^2
$\frac{\Delta a_i}{3}$
Δa_i
$a_{i,5}$
$a_{i,6}$
$a_{i,7}$
χ^2_{max}
χ^2_{cutoff}
χ^2_{min}
a_i
a_i^*

Figure 3.7: A heuristic illustration along one-dimension of the first two stages of the AGR procedure for minimization of a hypothetical merit function with many local minima starting with a grid size of seven over a defined domain.

The evolution of the grid refinement continues until an earlier chosen tolerance, T_{stop}, defining the minimal amount of absolute improvement (decrease) in the value of the chi-square function, is not achieved after the completion of an iteration, such that

$$\text{IF } T = \chi^2_{\min} - \chi^2_{\min,\,\text{previous}} \geq T_{\text{stop}} \text{ THEN STOP.}$$

The lastly identified minimal value of chi-square is assumed to be the global minimum, while the *i*th corresponding grid point is assumed to be a parameter of best fit and the *i*th component of the global minimizer, $\vec{a}^{*}$. The above described global minimization technique requires computing time in proportion with grid density to the power of the dimension of the problem in parameter space ⟨38⟩,

$$\text{computing time} \propto (\text{grid density})^{m}.$$

But since the law of parsimony was liberally administered to keep the number of unknown parameters from being large, this constraint on the applicability of the method was not a factor. With little further mention of any more practicalities of the implementation of AGR, the method was utilized in all further calculations involving the minimization of a chi-squared function.

A Second Study of the Sums of Exponentials

The initial estimates of the macroconstants, $A_i\,s$ and a_is of (1.10), was conducted by an exponential curve stripping process from the original program Model Maker to reduce the potential domains of the parameters, the corresponding computing times, and any resulting chances for bias (see Figure 3.8) ⟨19⟩. The equations were then fitted by minimizing weighted sum of squares within Model Maker for a one, two, and three term sum of exponentials to obtain the macroparameters, A_i and a_i, $i = 1, 2, \text{or } 3$.

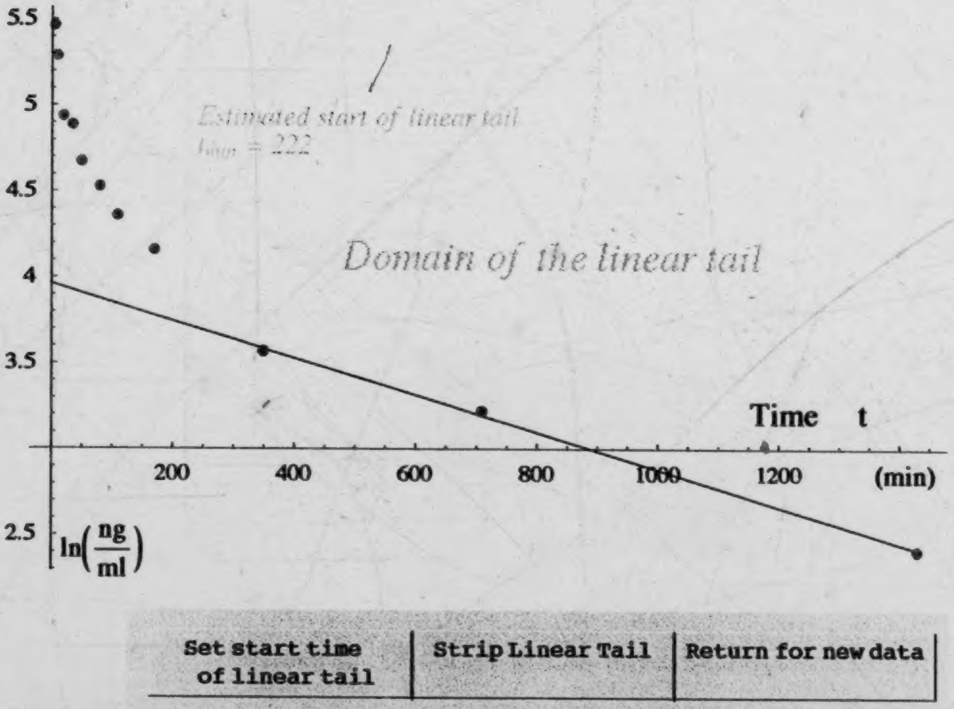

Figure 3.8: A Semi-Log plot of ⟦Mibefradil⟧ verses time shows an intuitive estimation of the domain of the linear elimination before curve stripping for the IV-PV-D2 data. The graph and associated buttons below are from an original curve stripping program designed to provide first estimates of parameter values for the original nonlinear fit program Model Maker.

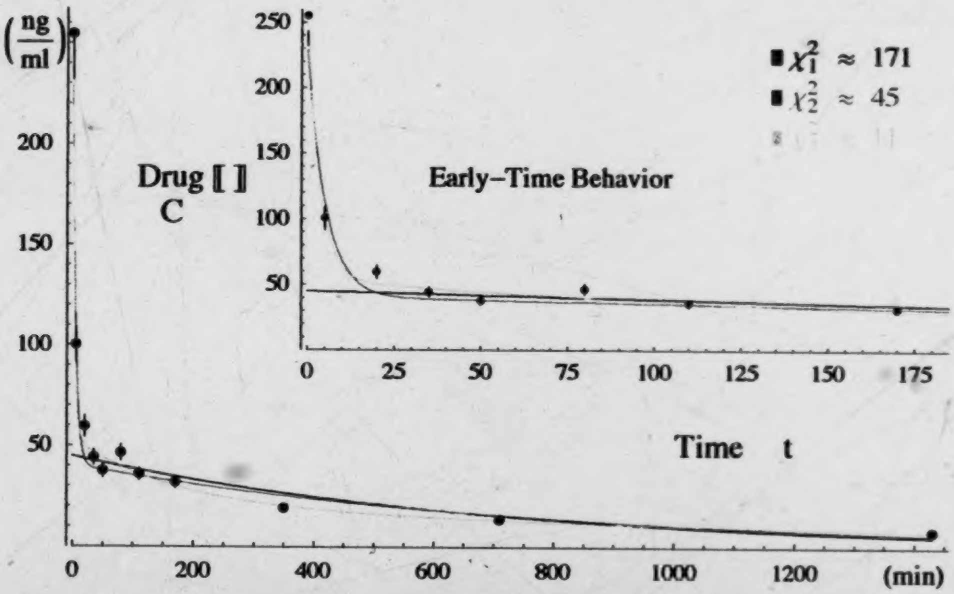

Figure 3.9: Mibefradil time course data fit with a single exponential term, ■, a sum of two, ■, and a sum of three exponential terms, ■, for trial IV-PV-D2.

As the number of terms in the sum of exponential functions was increased the deviation of the curve from the data decreased, as measured by the chi-squared merit function (see Figure 3.9). The data seemed to be closely fit with a three-term sum of exponentials requiring six free parameters, yet the domain where the slope of the graph subjectively changed from the early-time behavior of the peak to the late-time behavior of the tail, was estimated to be $[5,25)$ where few datum points reside. Observations of the residuals for those datum points in this domain for all of the dog trials, intuitively revealed a non-normal distribution indicating an unrealized pattern. The inability of the exponential functions to describe this transition was unsatisfying. This in turn implied that an interpretation of the pharmacokinetics of mibefradil based on a classical compartmental model would also be disappointing.

The Analytical Equations Implied by Michaelis-Menten Kinetics

A fit by analytical functions, never observed by the author in any Pharmacokinetic related material, implied by Michaelis-Menten kinetics was studied. Starting from the common statement describing a simple enzymatic reaction,

$$\frac{dC}{dt} = -\frac{V_{max}\,C}{K_M + C} \Rightarrow \left(\frac{K_M}{C} + 1\right) dC = -V_{max}\,dt$$

$$\Rightarrow K_M \int \frac{1}{C}\,dC + \int dC = -V_{max} \int dt$$

$$\Rightarrow K_M \ln[C] + C = -V_{max}\,t + C^{*},\;\; C \geq 0.$$

At $t = 0$, let $C[t] = C[0] = C_o$, so $C^{*} = K_M \ln[C_o] + C_o$, therefore

$$\ln[C] + \frac{C}{K_M} = \ln[C_o] + \frac{C_o - V_{max}\,t}{K_M} \qquad \times \frac{1}{K_M}\, e^{[\_]}$$

$$\Rightarrow \frac{1}{K_M}\, e^{(\ln[C] + \frac{C}{K_M})} = \frac{C}{K_M}\, e^{\frac{C}{K_M}} = \frac{C_o}{K_M}\, e^{(\frac{C_o - V_{max} t}{K_M})} \qquad \times W[\_]$$

$$\Rightarrow W\left[\frac{C}{K_M}\, e^{\frac{C}{K_M}}\right] = \frac{C}{K_M} = W\left[\frac{C_o}{K_M}\, e^{(\frac{C_o - V_{max} t}{K_M})}\right]$$

$$\Rightarrow C[t] = K_M\, W\left[\frac{C_o}{K_M}\, e^{(\frac{C_o - V_{max} t}{K_M})}\right], \tag{3.8}$$

where W (see Appendix 1) is called Lambert's W function ⟨49⟩ or the product log function ⟨50⟩, such that $W[z] = W[\omega e^{\omega}] = \omega$. Equation (3.8) satisfies the given initial conditions since

$$C[0] = K_M\, W\left[\frac{C_o}{K_M}\, e^{\frac{C_o}{K_M}}\right] = K_M\,\frac{C_o}{K_M} = C_o\,.$$

Using equation (3.8) a fit of the data was attempted with typical results illustrated in Figure 3.10.

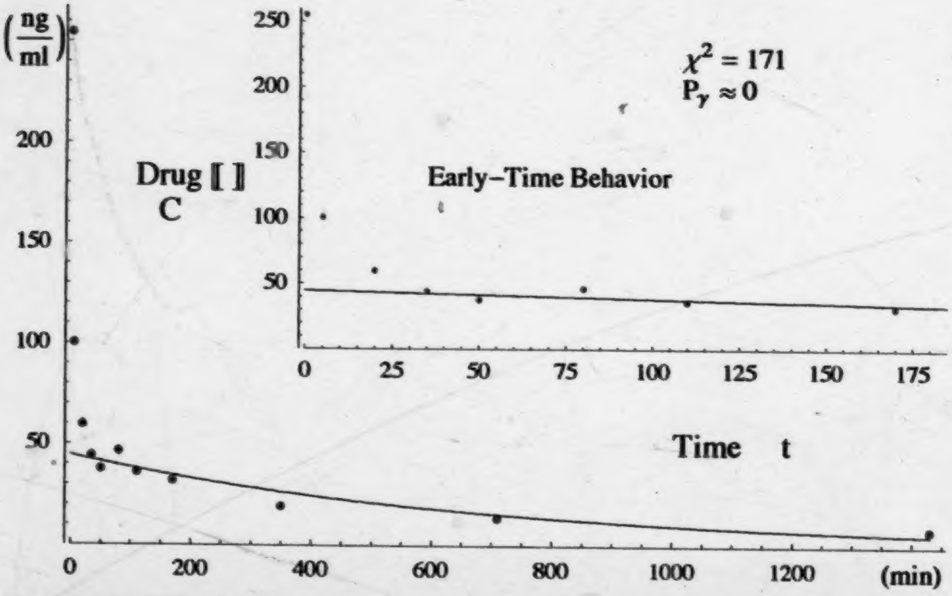

Figure 3.10: Mibefradil time course data fit with a single term analytical function implied by Michaelis-Menten enzyme kinetics for trial IV-PV-D2 using the original program Model Maker. The calculated value of the chi-square merit function is no better than that of a single exponential term.

It was observed that sums utilizing the product log function, empirically fit the data with no better accuracy, as measured by the chi-squared merit function, than sums of exponentials with the same number of terms and fewer parameters. This occurs when the Michaelis-Menten constant, K_M, often associated with the strength of binding of drug to enzyme, is large such that from (1.8)

$$\frac{d\mathrm{C}}{dt} = \frac{\mathrm{V_{max}\,C}}{\mathrm{K_M + C}} \approx \frac{\mathrm{V_{max}\,C}}{\mathrm{K_M}} = \text{constant} * \mathrm{C}.$$

The low concentration limit of the Michaelis-Menten equation is revealed as following first-order kinetics while the analytical functions implied by Michaelis-Menten kinetics fit the data no better than exponentials. Therefore, it is unlikely that significant aspects of the pharmacokinetics of Mibefradil in a dog model system are explained by the phenomenon of enzyme saturation. Consequently, the use of the otherwise common Michaelis-Menten equation in this thesis for further investigations is unjustified by the phenomenological observations.

A Fit by a Single Power Function

Empirical observations that the concentration time-course of several studied drugs metabolized in the liver were well approximated by a power function were reported by Norwich et alia ⟨51⟩. Later, a physiological interpretation for pharmacokinetic data described by the power function of the kind, $C = At^a e^{-bt}$, was proposed based on the assumption of gamma distributed disposition residence times of drugs for a random walk model of circulatory drug transport within a noncompartmental model (see Figure 1.7) ⟨52⟩. Here the parameter a determines the shape of the concentration time-course, while the parameter b defines the time scale of the kinetic process. After a trivial temporal translation of Tam's pharmacokinetic data, such that the initial condition was set to be $(t_0, C_0) = (1,0)$ rather than (0,0), matches to a humble power function of the variety, $C = At^a$, were completed (see Figure 3.11).

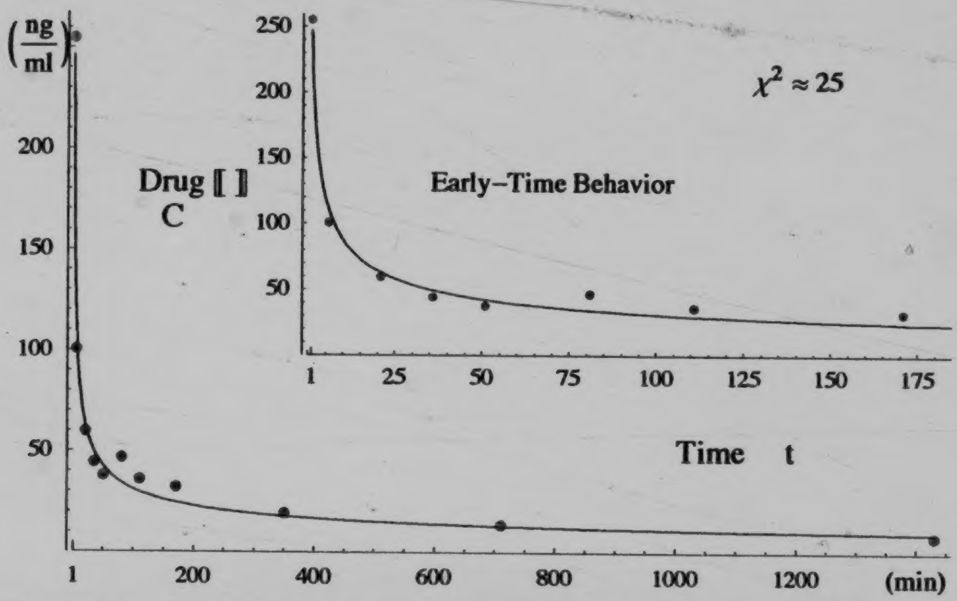

Figure 3.11: Mibefradil time course data fit with a single power term for the trial IV–PV–D2 using the original program Model Maker. The ostensibly apt way a function with so few parameters seems to deftly shift from early to late-time behavior to match the data was impressive.

Several Illations from Empirical Curve Fitting

Because the models are not linear with respect to their parameters, simple tests of goodness-of-fit cannot be enlisted to discriminate between the capabilities of the analytical functions employed for empirical curve fitting. Yet, direct comparison of quantitative chi-squared figure-of-merit function values can be used to compare the absolute accuracy of the curve fits ⟨Dr. Lele, Associate Professor of Statistics, University of Alberta, personal communication, 20, August, 2001⟩ as summarized in Table 3.1.

Type of Analytical Functions	# of Terms in Equation	# of Parameters Employed	χ^2
exponential	1, 2, 3	2, 4, 6	171, 45, 11
product log (Michaelis – Menten)	1	3	171
power	1	2	25

Table 3.1: A comparison of empirical fits to the pharmacokinetic data by equations utilizing three distinct types of functions as measured by the chi-squared figure-of-merit function.

The comparison of fits between product log and exponential functions indicated that the mibefradil concentrations in the experiments were not high enough to observe the effects of Michaelis-Menten kinetics beyond first-order kinetics. The comparison of fits between power and exponential functions indicated that the power function most efficiently summarized the data. Indeed, a single-term power function with two parameters captured the nature of the experimental data nearly as well as a three-term sum of exponentials with six parameters. These qualitative results compelled further investigations to establish a sound physical motivation for the at least partial description of the concentration time-course data as some function of powers of time and without consideration of Michaelis-Menten kinetics.

Chapter Four

A Furtherance of the Metabolic Context of Mibefradil

A Curt Overview of Liver Physiology

In an attempt to bring some aspects of physical analysis to bear on the study of the pharmacokinetics of Mibefradil, the physical structure of the liver, the main site of the drug's metabolism ⟨41⟩, is selectively considered. It appears that in humans the liver is the largest visceral organ and it possesses unusual microcirculatory pathways ⟨53⟩. It is supplied with blood by both the hepatic artery and the hepatic portal vein, thus firstly receiving all of the xenobiotically laden blood from the

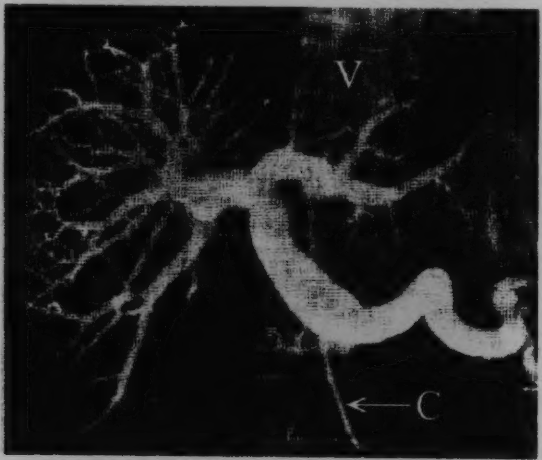

Figure 4.1: A picture of the macroscopic branching of the intrahepatic portal vein throughout the liver of a human. Additionally, there are vertebrae (V) visible in the background that offer scale and the catheter (C) that provided a contrast medium. A slightly altered photo taken from ⟨54⟩.

intestines. This macrocirculation spans the axes of the liver while branching into successively smaller vessels (see Figure 4.1). At the anatomical level, there exist small histological units, called lobules, made up of an interlacing channel network of sinusoids supplied with blood and drug by the terminal ends of the portal venules and hepatic arterioles (see Figure 4.2).

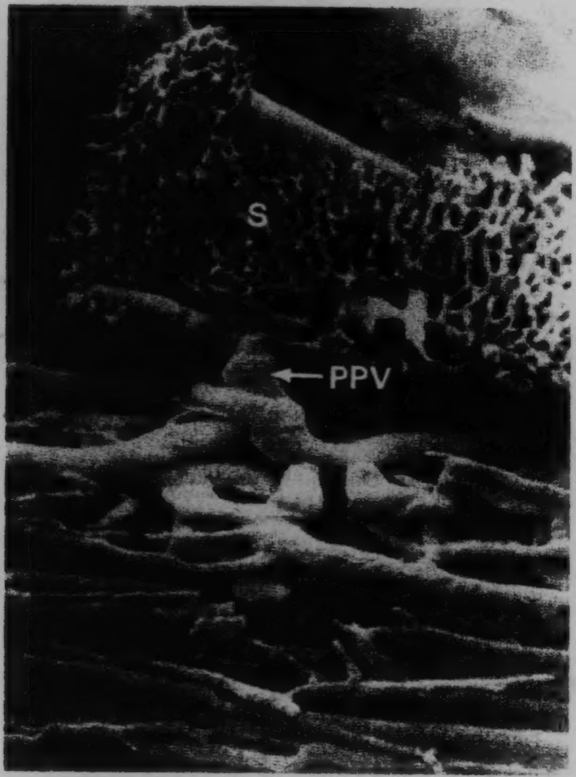

Figure 4.2: Two levels of microcirculatory structure within the monkey liver. A tiny near peribiliary portal vein (PPV, arrow) branches from the plexus below to supply blood to a small sinusoid region (S) of a lobule. Magnification ≈ ×500. Photo taken directly from ⟨53⟩.

Between the individual sinusoids of the interior of a lobule, one-cell-thick sheets of hepatocytes are interspersed ⟨55⟩. Facing the blood spaces, the convoluted uptake surface of the hepatocytes expands the blood-tissue interface by the presence of numerous microvilli, as shown in Figure 4.3. Separating the hepatocytes and the blood space, is a topologically complex enothelium lining that defines the minute passages of the sinusoids (see Figure 4.4). The fenestrae of the endothelium allow direct access of drug within the circulating plasma to the surface of the hepatocytes via the space of Disse. A very thin but functional and distinct extracellular space of the liver, comprising the space of Disse, exterior of the sinusoid, which contains both collagen fibers and ground substance, and wherein the microvilli of the hepatocytes extend, can also be seen in Figure 4.5. Summarily stated, observations

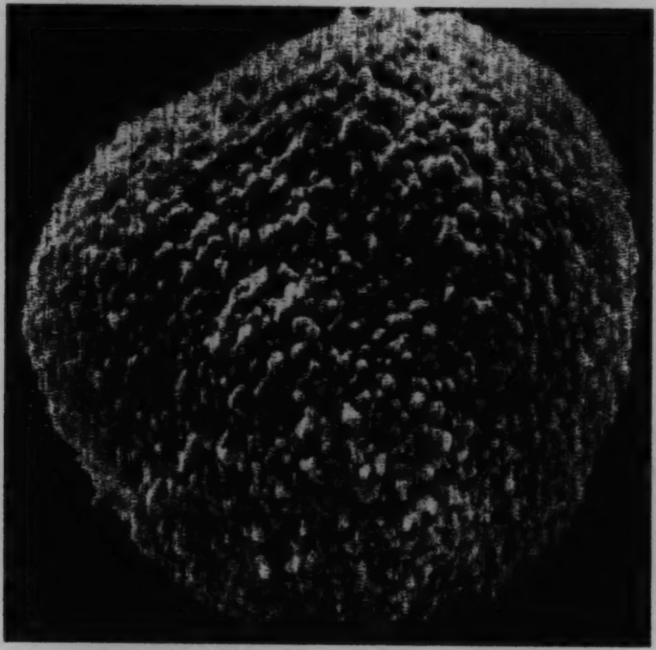

Figure 4.3: A picture of the decidedly structured microvillar surface of the sinusoidal face of and isolated liver cell. Magnification = ×6 000. Photo taken directly from ⟨53⟩.

of the liver reveal an anatomically unique and complicated structure over a range of length scales designating the space where mibefradil metabolism transpires.

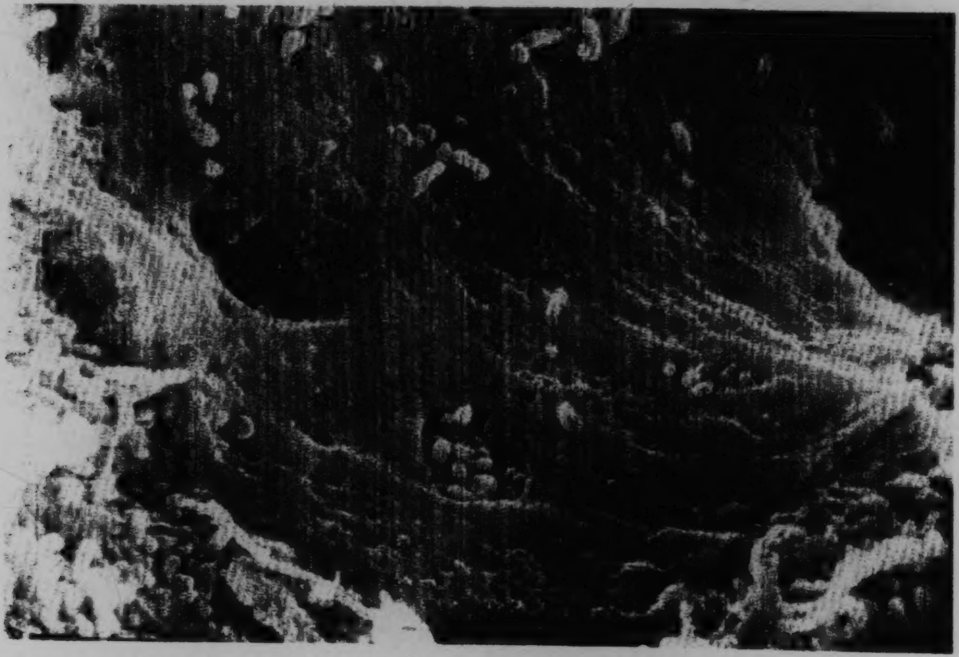

Figure 4.4:. The porous endothelial lining of a sinusoid containing fenestrae (pores or holes) on different scales of size (but all smaller than the diameter of an erythrocyte). The two faint black arrow heads point to hepatocyte microvilli (see Figure 4.3) protruding through the larger fenestrae into the sinusoid lumen (space). Magnification= ×10 000. Photo taken directly from ⟨53⟩.

The Liver as a Fractal

> I am obviously walking a tightrope between the law of parsimony on the one hand and the reductionist fallacy on the other.
>
> -William S. Hatcher

An important observation in sundry research fields is that many complex natural objects, over wide scale intervals, can be efficiently approximated to ideal fractal forms - a mathematical concept expounded in the next section. It is observed that complexity is encapsulated in comparatively simple hierarchical and iterative descriptions that lead to fractal sets. Fractal analysis consists in associating such a fractal set to an object under study and describing it through fractal geometry approximations, instead of using simpler Euclidian sets at the expense of realism or very complex calculations ⟨56⟩.

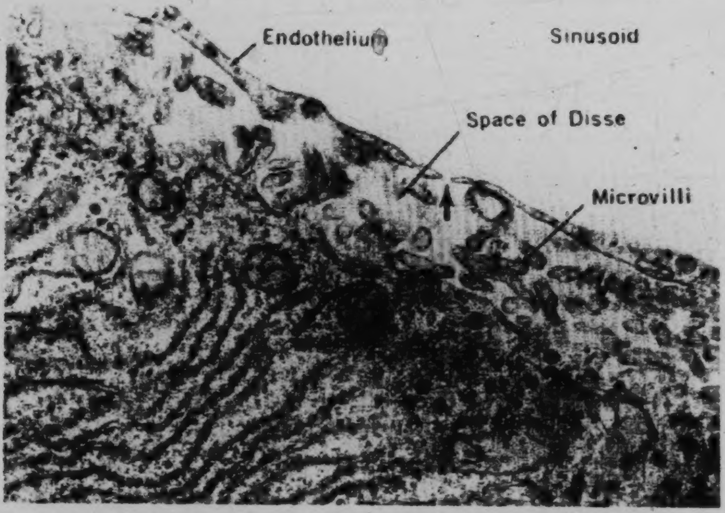

Figure 4.5: A cross-section of a liver cell bordering a sinusoid. Numerous irregularly oriented microvilli project into the narrow space of Disse between the hepatic cell and the endothelium lining the sinusoid. A black arrow indicates a small fenestra in the the sinusoid lining. Magnification = ×18 000. Photo taken directly from ⟨53⟩.

By the above observations that the liver has a hierarchic structure with complications at many length scales from the order of its macroscopic diameter to the order of the macromolecular make-up of the matrix within the space of Disse, it is hypothesized that the liver is fractal-like. That the structure of, and blood flow heterogeneity in, the liver and other visceral organs is fractal, has been suggested and at times experimentally tested before, especially in fields outside of pharmacology and pharmacokinetics ⟨57,58,59⟩. For example, by means of analysis of ultrasonic wave scattering from calf liver tissue, Javanaud measured the fractal dimension as approximately $d_f \approx 2$ over a wavelength domain of $(0.15, 1.5)$ mm ⟨60⟩. Correspondingly, the liver, as experienced by the drug mibefradil, will hereafter be assumed to at least have the possibility of being well approximated by a fractal between experimentally relevant length scales ⟨61⟩.

An Introduction to Fractals

> For any speculation which does not at first glance look crazy, there is no hope.
> -Freeman J. Dyson.

Scientific approaches to measure and model phenomena are characteristically simple in geometric terms. Yet, many objects in nature are so complicated and irregular that they cannot be modeled well using conic sections, polygons, spheres, cylinders, and the other familiar objects of classical geometry with the corresponding mathematical milieu. For example, circulatory systems, clouds, trees, mountains, and coastlines cannot easily be reduced to, or be approximated by, combinations of simple shapes from classical geometry. The term fractal was introduced by the mathematician Benoit Mandelbrot in response to the need for a more sophisticated explanation of numerous phenomena commonly encountered in nature ⟨62⟩. But even by the end of last century, mathematicians, such as Cantor and Koch, had studied the sets that are now known as fractals.

However, even the definition of fractals is far from being trivial, such that several articulations have been proposed over the years as mathematicians struggled with the complex properties of fractals; and, all notions of fractals first depend on a formal definition of dimension. That the topological dimension of a smooth curve is expectantly one and that of a surface of a sphere is two may seem very intuitive. Yet, the formal definition of dimension was only given in 1913 by the Dutch mathematician L. Brouwer (1881-1966). Importantly, the notion is not unique, moreover, given the continued development of the new study of fractal geometry - a discipline as yet without a strong foundation, it seems that fractal dimension is necessarily a multi-faceted concept ⟨63⟩.

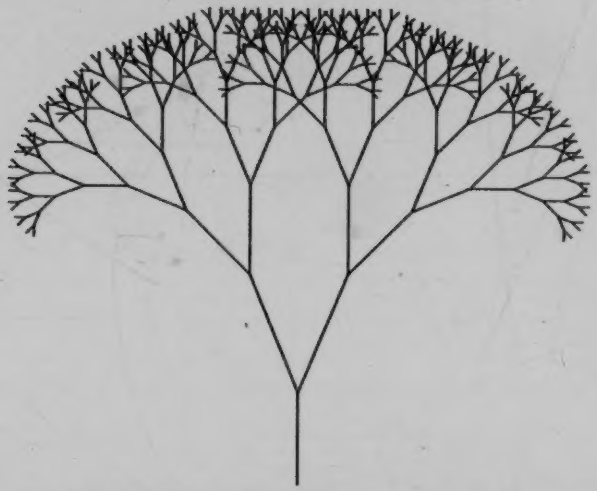

Figure 4.6: Levels 0-8 of a dichotomously branching "tree" in two dimensions generated by a trivial recursive rule: for each generation pairs of branches are added with a length and at an angle relative to the terminal segments of the previous generation. Qualitatively, compare to some aspects of the branching network of microcirculatory structure of Figure 4.2.

For this report a relaxed definition of a fractal will be adopted: a geometric figure or natural object that combines the following characteristics: a) the parts have a related form or structure as the whole, except that they are at a different scale and may be slightly deformed; b) the overall form is extremely irregular or fragmented, and remains so, over a broad scale of examination; and c) it contains distinct elements whose scales are very varied and cover a large range ⟨64⟩. From this nebulous concept, a few specific features of fractals are proffered:

self-similarity: a hallmark of an object with parts that are sculpturally or statistically resembling the whole object in a non-trivial manner (see Figure 4.6 and Figure 4.7), such that some property, *L[qr]*, measured on a piece of an object at a particular resolution is proportional to the same property, *L[r]*, measured over the object at a coarser or finer resolution. Hence,

$$L[qr] = \omega[q]\,L[r]\ , \tag{4.1}$$

where ω is a constant of proportionality and q determines the scale or resolution. In the analysis of experimental data, a scaling, qr, can only extend over a finite range, constrained by either the measurement technique or the limits of the physiologic object. For example, the average rate at which new vessels branch off from parent vessels in a physiological structure can be related for large and small vessels over a circumscribed range.

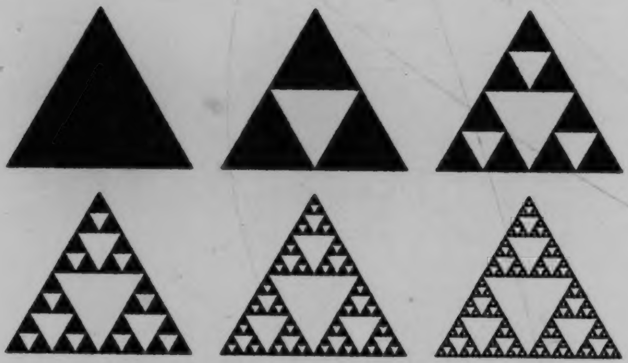

Figure 4.7. Levels 0-5 of the Sierpinski Gasket. Qualitatively, compare to some aspects of the porous endothelial lining of a sinusoid containing fenestrae on different scales of size in Figure 4.4.

scaling: attributed to an object with characteristics that depend on the measurement resolution, such that there is no one unique value for some measurements. How the estimated value depends on the measurement resolution is called the scaling relationship. It is often determined by the self-similarity of the object to be of the power law form

$$L[r] = A\,r^{a}\ , \tag{4.2}$$

where *A* and *a* are constant for any particular fractal object or process ⟨65,57⟩. Such power law scalings are revealed on a ln-ln graph of the measurement of a characteristic plotted against the measurement scale since

$$\ln[L] = a\ln[r] + \ln[A]$$

has the format of a straight line. The scaling relationship as a function of the resolution scale *q* is reveal by the substitution of (4.2) into (4.1) to find

$$L[q\,r] = L[r]\,q^{a}. \qquad (4.3)$$

Different scaling relationships produce different exponent values, *a*, each of which are identified as a dimension of the fractal; therefore, fractals differ from Euclidean objects by having more than one relevant dimension.

self similarity dimension: a simple and applicably limited but heuristically useful notion to grasp the concept of a fractal dimension, formed by considering geometrically self-similar objects at different resolutions. If the scale of resolution of an object, *F*, is changed by a factor *q*, and there are *N* pieces observed to be similar to the original, then let the self-similarity dimension, d_f be given by the scaling relationship

$$N = q^{d_f} \qquad \Rightarrow \qquad d_f = \frac{\ln[N]}{\ln[q]}.$$

Figure 4.8 illustrates how this fractal dimension is consistent with our usual sentiments of the properties of integer dimensional objects. Furthermore, the relatedly defined Hausdorff dimension, which is a measure of the number of bounded, non-overlapping, D-dimensional hyperspheres of Euclidean radius *r* that are required to cover the object *F*, is useful for grasping the dimension of a fractal that is not strictly a self-similar one, as the liver is likely to be ⟨66⟩.

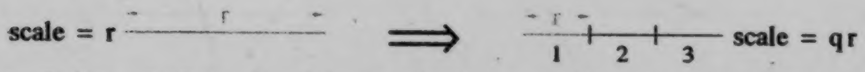

Line: 3 pieces similar to the original result when the resolution is increased 3 times $\ni$

$$N = 3 \;\wedge\; q = 3 \;\Rightarrow\; d_f = \frac{\ln 3}{\ln 3} = 1.$$

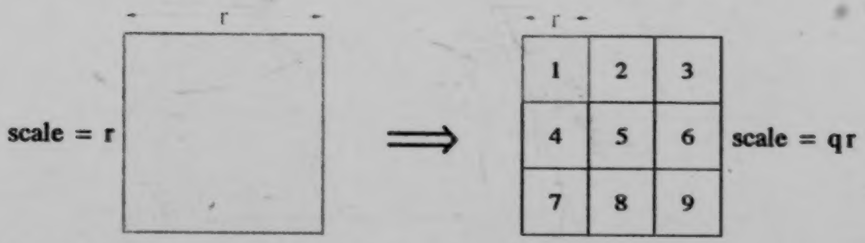

Square: 9 pieces similar to the original result when the resolution is increased 3 times $\ni$

$$N = 9 \;\wedge\; q = 3 \;\Rightarrow\; d_f = \frac{\ln 9}{\ln 3} = \frac{2\ln 3}{\ln 3} = 2.$$

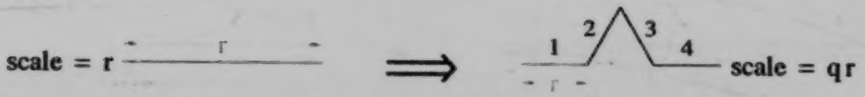

Koch: 4 pieces similar to the original result when the resolution is increased 3 times $\ni$

$$N = 4 \;\wedge\; q = 3 \;\Rightarrow\; d_f = \frac{\ln 4}{\ln 3} \approx 1.26.$$

Figure 4.8: Illustrated calculations of the fractal dimension based on self-similarity considerations for a line, square, and Koch curve. Calculated values for the more general Hausdorff dimension would be similar for the above examples. See Figure 6.1 to view an example of a further developed Koch curve (snowflake).

space filling properties: fractal objects may be considered to exist between the familiar Euclidean dimensions, such as between points and segments, segments and planes, or planes and solids. The fractal abides between the integer topological dimension, d_T, of the structures that compose it, and the integer Euclidean dimension, D, that the entire fractal object is embedded within. For example, the tree-like fractal shown in Figure 4.6 (or regard Figure 4.9) has a topological dimension of one since the basic units of its construction are lines, while the fractal itself is embedded in a two dimensional plane. Since the tree-like fractal fills space to a greater extent than a line yet does not completely cover the plane that it is embedded in, its fractal dimension, as defined above, has a value $d_f \in (1,2)$.

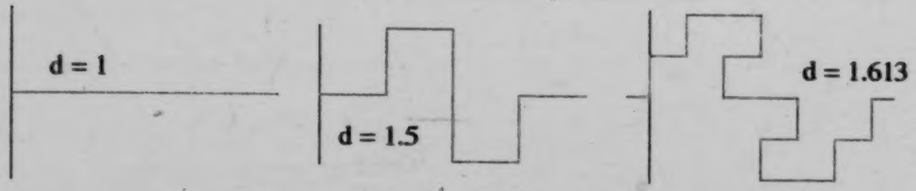

Figure 4.9. My own tentative attempts to construct a knobby fractal. The topological dimension is $d_T = 1$ and the Euclidean space in which the fractal structure is embedded in is $D=2$. Instead of alterations of a one-dimensional line, imagine similar protrusions of a two-dimensional surface and qualitatively, compare to aspects of the microvillar structure on the surface of a hepatocyte in Figure 4.3.

spectral dimension: first introduced in 1982 by Alexander and Orbach, especially relating to random walk properties confined to fractal structures, that is most useful in the study of dynamics and critical phenomena. It is generally not of the same value as d_f since it relates to different features of the fractal and it contains different information ⟨67⟩. While the fractal dimension, d_f, is intimately related to the extent an object pervades the space in which it is embedded, the spectral dimension, d_s, appertains to how many options a random walker will posses on average for each step made as it diffuses about due to the connectivity of the structure. At a particular resolution, let the connectivity of a structure be defined as the average number of traversable bonds connecting one site of the object to its neighbors (see Figure 4.10).

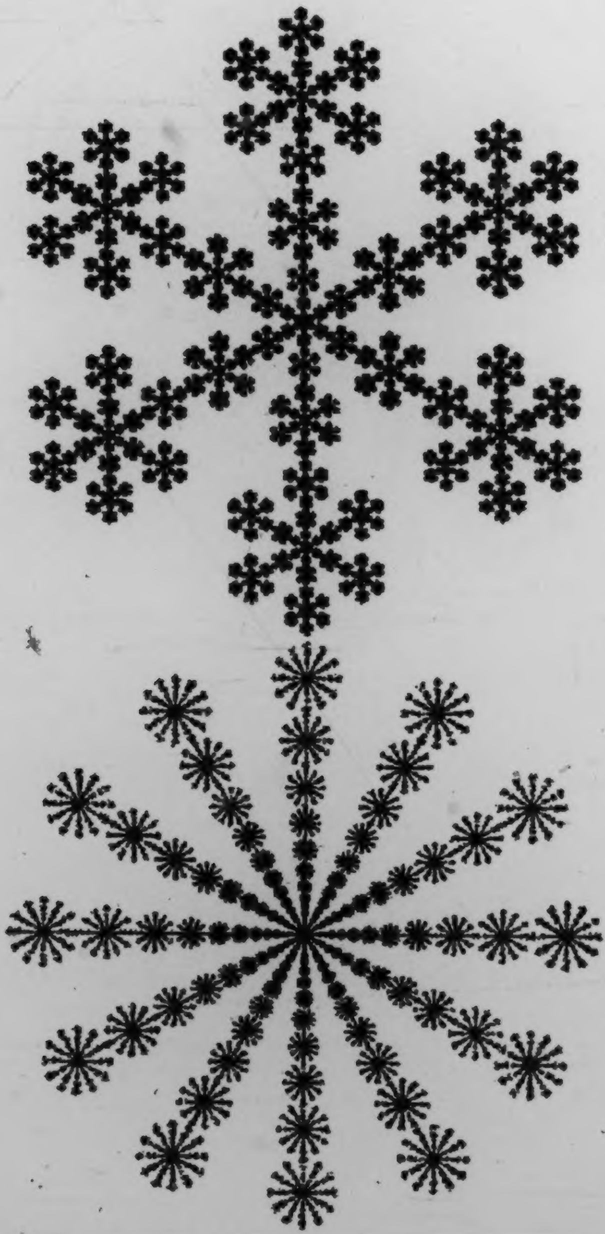

Figure 4.10: Geometric figures with equal fractal dimensions $d_f \approx 1.65$, but with different spectral dimensions arising from the differences in the connectivity of the geometric objects. The connectivity of the top fractal is equal to six, while for the lower fractal, the connectivity is twelve. Picture taken directly from ⟨68⟩.

The spectral dimension is defined as an exponent in a scaling relationship with the same form as (4.3) common to other fractal dimensions. Consider the diffusion of a particle in a fractal medium, such that the return probability, $\mathcal{P}_R[t]$, may be defined as the probability for the particle to be back at the initial position at some later time, *t*. The scaling exponent with time defines the spectral dimension ⟨68⟩:

$$\mathcal{P}_R[t] \propto t^{-d_s/2}, \quad t \gg 1. \tag{4.4}$$

Notice that for a limiting case when $d_s \to 0$, as for a fractal dust, the random walker diffuses away not at all, but remains sequestered. Now for a Euclidean structure, $\mathcal{P}_R[t]$, can be obtained from the normalized solution of the diffusion equation in a radially symmetric media corresponding to an initial Dirac delta profile, such that

$$\mathcal{P}_R[r, t] = A\, t^{-D/2}\, e^{-r^2/4\mathcal{D}t},$$

where *A* is a normalization constant, *D* is the Euclidean dimension, $\mathcal{D}$ is the diffusion constant of the particle, and *r* is the distance from the origin. So the return probability for the particle to be back at the initial position is offered when $r = 0$, such that

$$\mathcal{P}_R[t] \propto t^{-D/2},$$

has the same form as (4.4). Consequently, the spectral dimension, d_s, is revealed as equal to the Euclidean dimension, *D*, for Euclidean structures ⟨69⟩. In summary, for Euclidean spaces, $d_T \le d_s = d_f = D$, while, for fractal spaces, $d_T < d_s \le d_f \le D$ ⟨9⟩.

The aforementioned properties of fractals may have subtle or overt manifestations within natural phenomena. The relatively new analytical tool of fractal analysis as applied to pharmacokinetics, will be adopted and wielded with the intentions of offering a novel interpretation of the experimental pharmacokinetic data.

The Implications of Fractal Kinetics

> Early humans were faced with the task of explaining quite an extensive variety of phenomena, but based on relatively limited experience. It is therefore natural that this situation led to a veritable riot of speculative imagination.
>
> -William S. Hatcher

A deeper analysis of the metabolism of mibefradil in the liver requires a consideration of the theoretical description of transport phenomena with chemical reaction in complex media. This can be performed by means of fractal geometry, using two introduced basic exponents: the fractal and the spectral dimension. Yet, the definition of mean field approximation for reaction-diffusion phenomena in complex fractal media is still an open question, such that a comprehensive theory for reaction processes in fractal media is still to be elaborated ⟨68⟩. But, some enlightening and influential upshots are established.

Classical transport theories, and the resulting mass-action kinetics, applicable to Euclidean structures do not apply to transport phenomena in complex and disordered media. The geometrical constraints imposed by the heterogeneous fractal like structure of the liver strongly modify diffusional dynamics ⟨70⟩. Topological properties like connectivity, presence of loops or dead ends, etcetera, play an important role, hence, it is to be expected that media having different dimensions or even the same fractal dimensions, but different spectral dimensions, could exhibit deviating behavior in diffusional propagation ⟨68⟩. The resulting abnormal diffusion requires a significant change in the mathematical description of reactions in the liver and implies the introduction into transport theory of the results of fractal geometry. Secondly, the statistical probability accounting for the existence of adjacent reactive pairs must be considered. In the language of statistical mechanics this probability factor is the pair distribution function for the reactive molecules. These two related concerns are addressed in the microscopic concept of an exploration volume of a migrating random walker (drug particle) within the fractal (liver), or otherwise described as the mean number of distinct sites, *S*, visited on the fractal for some resolution. A second scaling relationship for the spectral dimension that includes *S* is

$$S[t] \propto t^{d_s/2}, \qquad (4.5)$$

where time *t* is proportional to the number of random walk steps ⟨71⟩, such that, the diffusion is monitored by the spectral dimension. Notice that for low spectral dimensions, the random walk will be compact. Subsequently the macroscopic reaction rate, which is given by the time derivative of *S*[*t*], sometimes described as the efficiency of the diffusing, reacting, random walker, will be

$$k[t] \propto \frac{d\,S[t]}{d\,t} \propto t^{d_s/2-1} = t^{-(1-d_s/2)}, \qquad (4.6)$$

for transient reactions. While strictly valid for low concentrations ($C \to 0$) as an asymptotic limit ($t \to \infty$), the above equation (4.6) is rapidly approximated for realistic concentrations ⟨72⟩. This time dependent rate constant, is the manifestation of the anomalous microscopic diffusion in a dimensionally restricted environment leading to a resulting anomalous macroscopic kinetics.

Phenomenological Issues

It is now well understood that chemical rate laws are a direct reflection of the spatial distribution of particles ⟨73⟩ (see Figure 4.11). In particular, the classical rate law reflects a random Hertzian distribution, that is one in which the probability that the nearest neighbor of a given particle, to be found at a distance r in a given direction, peaks at $r=0$. It is the continual supply of close pairs of particles, even as they react, as capacitated by diffusion characteristic to three dimensions, that is embodied in the usual bimolecular rate law - a law that assumes that changes in concentration with time do not affect chemical reactivity. Practically, classical kinetics is often justified since the fluid systems considered are usually three dimensional and habitually well-stirred mechanically or by convection ⟨74⟩, such that, the experimental canons fulfill the tenets of classical mass-action formalism. But heterogeneous reactions taking place at interfaces, membrane boundaries, or within a complex medium like a fractal when the reactants are spatially constrained on the microscopic level culminate in deviant reaction rate coefficients, as described by (4.6), that appear to have a sort of temporal memory. The compactness of the low dimensional random walk implies ineffective diffusion and an entailing aberrant macroscopic rate coefficient. In a fractal-like reaction system the distribution of reactants becomes less random on a mesoscopic scale due to the formation of depletion zones around the traps ⟨75⟩ resulting in a self-ordering or self-unmixing of the reactants around traps - a spontaneous segregation of the reactants occuring at both low and high concentrations ⟨76⟩.

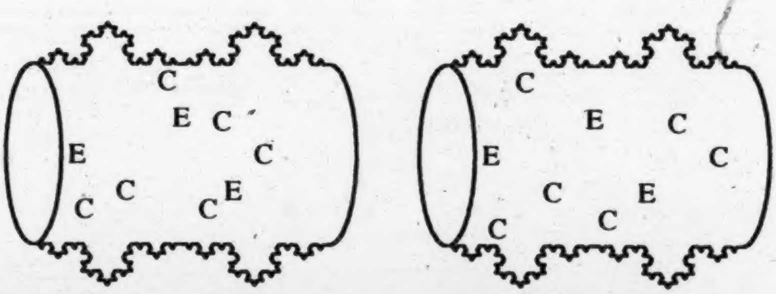

Figure 4.11: Two identical fractal containers, with identical macroscopic concentrations of reacting molecules, but with different instantaneous reaction rates. The probability for instantaneous reaction is obviously higher in the container on the left. In specifying a concentration, a uniformly random distribution in space of the reactants is implicitly assumed. Only under such an assumption can two containers with the same concentration have identical reaction rates - this seems not to be the case with fractal containers.

The case $d_s=2$ is found to be a critical dimensional value (critical point) of the phenomena of self organization of the reactants for the consequential atypical time-dependent reaction rate coefficients ⟨77,78⟩, where if $D<3$ then $d_s \leq 2$ ⟨72⟩. For $d_s>2$, the scale of the self organization of the reactants is microscopic and independent of time, such that, $S[t] \propto t^1$ (is linear) and $k=dS/dt$ is a constant so the reaction kinetics is classical ⟨74⟩. Below the critical dimension, mesoscopic density fluctuations of the drug become relevant and affective upon the reaction rate coefficient ⟨60⟩, whereby S is sublinear of the form (4.5). This can be further appreciated by attention to (4.4): if d_s is low (<2), then a random walker (drug) is likely to stay at its original vicinity and will eventually recross its starting point - microscopic behavior conducing to produce mesoscopic depletion zones around traps (enzymes), else, at higher spectral dimensions (>2), a random walker has a finite escape probability and tends not to return to its starting point - microscopic behavior conducing to rerandomize the distribution of reactants (ensemble) around a trap and replete a supply of reactive pairs and thus stable macroscopic reactivity as attested by the classical rate constant.

The Thesis

As exemplified by Ngo, there generally exists a tacit assumption, almost by definition, that time-dependent pharmacokinetic phenomenon necessarily "involves actual physiological or biochemical changes in body tissues which are associated with nonlinear drug disposition processes" as manifested by a time-dependency of the drug elimination rate during i.v. infusion trials ⟨43⟩. Yet fractal kinetics implies time-dependent pharmacokinetics will occur given only a static, time-independent fractal physiological environment, as in the liver, where resulting time-dependent metabolic reactions take place. The thesis of this report shall be that important aspects of the pharmacokinetic disposition of mibefradil in the dog model system are due to the fractal structure of the liver via the occurrence of non-classical, heterogenous kinetics within. A physiologically motivated model will be constructed with the dual goals of supporting this hypothesis by comparison to experimental data, and, providing an objective estimation for the spectral dimension of the liver.

Considering the implications of Chapter Three and Chapter Four above, the metabolism of mibefradil will be presupposed hereafter to follow the bimolecular annihilating trap reaction of equation (1.1) within a fractal liver. Furthermore, a constant concentration of a metabolizing enzyme, $E \leftrightarrow [\![E]\!]$, is presumed to be present in the liver such that the reaction is premised to be a psuedo-monomolecular equation where only C (the concentration of drug) varies in time. Using (4.6), the form of the pseudo-first-order rate coefficient for the metabolism of mibefradil is assumed to be of the power law form:

$$\mathrm{k}[\mathrm{t}] = \kappa \mathrm{t}^{-(1-\mathrm{d}_s/2)} = \kappa \mathrm{t}^{-\zeta}, \quad \mathrm{t} > 1, \quad \mathrm{d}_s \leq 2, \tag{4.7}$$

where $\kappa = \mathrm{f}[E]$ and is taken to be constant for the experimental data and $\zeta \in [0,1)$ is an unknown parameter to be fit by the experimental data ⟨83⟩.

Chapter Five

The Developement of a Theoretical Model

> **Indeed, we might say that the essential characteristic of human intelligence is its capacity to model phenomena.**
>
> **-William S. Hatcher**

As far as I can tell, there has not been a paper published explaining the mathematical methods for implementing fractal kinetics nor any other time-dependent kinetic coefficients for PBPK models or classical multicompartmental models. A simple approach for including, within a multicompartmental model, time dependence of the transfer coefficients that vary continuously with the age of human patients was described by Eckerman et alia ⟨79⟩, but time dependence was for over periods much greater than a single or small series of dosages. This simplified the mathematics such that there was no time dependence of coefficients for the time course of a single dose. Within a physiological model, over a very long time-scale of 98 days, Ferris et alia ⟨80⟩ introduce time-dependent compartment volume changes due to growth in the studied rat model system. Finally, Macheras in ⟨61⟩ introduces the explicit use of time-dependent drug disposition, motivated by the microvascular fractal networks of the body, within what is ostensibly a noncompartmental approach but is mathematically and conceptually equivalent to a one-compartment model. Presented below is a simple physiologically-based pharmacokinetic model containing an eliminating compartment with a time-dependent rate of elimination based on fractal kinetics (see Figure 5.1).

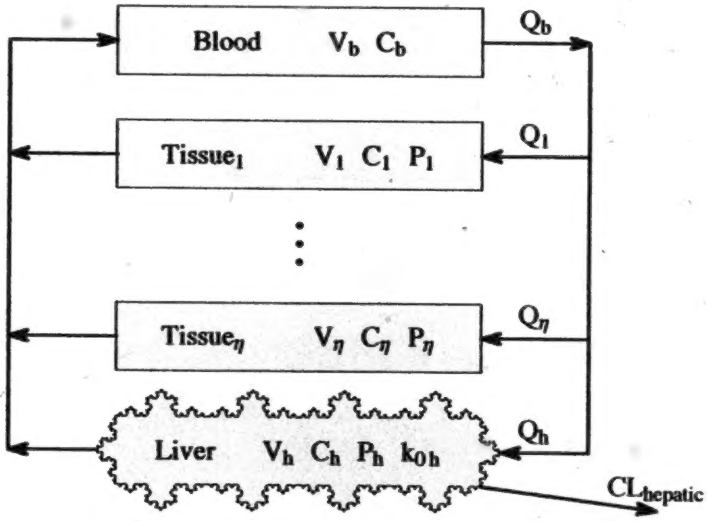
Blood V_b C_b
Q_b
Tissue$_1$ V_1 C_1 P_1
Q_1
Tissue$_\eta$ V_η C_η P_η
Q_η
Liver V_h C_h P_h k_{0h}
Q_h
$CL_{hepatic}$

Figure 5.1: A simple flow limited Physiologically-Based Pharmacokinetic (PBPK) Model where clearance of the drug occurs only in the liver by fractal kinetics.

Let there be a defined total blood flow ⟨34⟩, such that

$$Q_b = Q_h + \sum_{i=1}^{\eta} Q_i ,$$

where Q_h is the blood flow into the liver and Q_i is the blood flow into a non-eliminating tissue. Let the blood:tissue partition coefficient be a constant for each compartment, such that $P_i = C_i / C_b$, $i = h, 1, \ldots, \eta$. Let any drug binding that occurs in the blood or a tissue be linear and independent of time, such that, $C_b = \mathcal{B} C_f$, where C_f is the concentration of the free unbound drug ⟨24⟩, and the following mass balance equations may only be incidentally affected by a constant term, $\mathcal{B}$.

Let the drug mass balance differential equation for the blood compartment be

$$\frac{dX_b}{dt} = -Q_b C_b + \sum_{i=1}^{\eta} \frac{Q_i}{R_i} C_i + \frac{Q_h}{R_h} C_h ,$$

where X_b is the amount of drug in the blood and C_i, $i = h, 1, \dots, \eta$ are the tissue drug concentrations. Let the drug mass balance differential equations for the non-eliminating tissue compartments be

$$\frac{dX_i}{dt} = Q_i\, C_b - \frac{Q_i}{R_i}\, C_i \ ,$$

and for the metabolizing liver compartment be

$$\frac{dX_h}{dt} = Q_h\, C_b - \frac{Q_h}{R_h}\, C_h - CL_h\, C_h \ ,$$

where CL_h is the hepatic clearance ⟨80⟩.

Consider the pharmacokinetics of the model after an i.v. bolus injection into the blood, such that $X_b[0] = X_b^o = \text{dose}$ and $X_i[0] = 0 \ \forall \ i \neq b$, are the initial conditions of the system. Let the hepatic clearance be described as $CL_h C_h = k C_h$, accepting that the metabolism of the drug is a first order process in C_h as a trap annihilation reaction described by (1.1), where k is the first-order rate coefficient. Let the rate coefficient be time dependent of the form $k = k[t] = \kappa t^{-\zeta}$, assuming that the metabolism transpires within a fractal environment, where κ is constant in time and $\zeta \in [0,1)$. Now the mass balance differential equation for the metabolizing liver adopts the form

$$\frac{dX_h}{dt} = Q_h\, C_b - \left(\frac{Q_h}{R_h} + \kappa\, t^{-\zeta}\right) C_h \ .$$

The set of homogeneous linear first-order differential equations may be described with a concise vector notation similar to (1.9):

$$\begin{aligned} \vec{X}' &= \mathbf{A}[t]\,\vec{X}, \quad \vec{X}[0] = \hat{X} \\ \vec{C} &= \mathbf{V}^{-1}\,\vec{X}, \end{aligned} \tag{5.1}$$

where $\vec{X} = [X_b, X_1, \dots, X_\eta, X_h]^{\mathrm{T}}$ is a $(\eta+2)$-dimensional column vector of the dependent state variables, $\hat{X} = [X_b^o, 0, \dots]^{\mathrm{T}}$ is a $(\eta+2)$-dimensional column vector of constnats describing the initial conditions, $\mathbf{V} = \delta_{ij} V_i$, $i = b, 1, \dots, \eta, h$, is a constant matrix of the compartment volumes, and $\mathbf{A}[t]$ is a matrix describing drug pharmacokinetics with at least one time variable component (see Appendix 5 for an explicit statement), and $C_i = X_i/V_i$ are compartment concentrations.

Since a system of (η+2) first-order equations with at least one variable coefficient is equivalent to a general (η+2)th-order differential equation, for which exact closed-form solutions exist only rarely when the order is greater than or equal to two ⟨81⟩, solutions for (5.1) typically remain elusive. Considering that for a PBPK model there may be any natural number, η, of non-eliminating tissues and that the unknown parameter, ζ, may have a range of fractional values, a general closed form exact solution is impossible because $\mathbf{A}$ will be a nonconstant matrix of differing sizes. Now, while systems of differential equations may be solved numerically, exempli gratia by Gear's method for stiff differential equations ⟨80⟩, said techniques depend on input values for all of the parameters, some of which may not be known. These numerical techniques do not allow for unknown parameters, such as ζ, to remain for subsequent fitting directly from the data. Moreover, analytical solutions better lend themselves to teaching and understanding of pharmacokinetic models and their implications compared to obfuscating numerical methods. Therefore, it remained a major objective of the report to describe solutions to the PBPK model analytically and provide an objective estimate of the spectral dimension of the liver.

An Approximate Analytical Solution by Pertubation Methods

If the influences of fractal kinetics in the liver are minor, then ζ will be a small parameter, such that in the limit as $\zeta \rightarrow 0$, familiar classical annihilation kinetics are restored since $\kappa t^{-\zeta} \rightarrow \kappa$, a constant. With this view, fractal kinetics within the dog model liver can be considered as a slight alteration or pertubation of classical kinetics. Pertubation theory is a collection of iterative methods of dilute rigor, by mathematical standards, for slyly obtaining approximate solutions to problems involving small free parameters, as ζ is presumed to be for the remainder of this report. Following attested pertubation approaches ⟨81⟩, the solution of the pharmacokinetic system was assumed to be of the form

$$\vec{X}[t] = \sum_{n=0}^{\infty} \zeta^n \vec{X}_n \,, \tag{5.2}$$

for the initial conditions $\vec{X}_0[0] = \hat{X}$ and $\vec{X}_n[0] = \hat{0} \ \forall \, n \geq 1$, where the zero-order term, $\vec{X}_0$, fullfills the original initial conditions alone and all terms must submit to the physical boundry condition of $\vec{X}_n[t \rightarrow \infty] = \hat{0} \ \forall \, n$. Because ζ is a small number, larger powers of ζ and the corresponding higher terms of the above summation are expected to have relatively small magnitudes. Unlike local analysis of differential equations by series substitutions, pertubation techniques are global in the sense that if the pertubation series converges, then it does so for all finite values of t, not just for the abscissal domain within a radius of convergence around some time, t_0 ⟨81⟩.

Notice that since ζ is a free parameter independent of t, after the substitution of (5.2) into (5.1), such that

$$\sum_{n=0}^{\infty} \zeta^n \vec{X}'_n = \mathbf{A}[t, \zeta] \sum_{n=0}^{\infty} \zeta^n \vec{X}_n, \tag{5.3}$$

an equivalence of terms for each power of ζ between the left and right sides of (5.3) is implied. But with the coefficient matrix, $\mathbf{A}[t,\zeta]$, harboring a term with the form of $t^{-\zeta}$, the aforementioned equivalences are obscured. Using an approach unobserved in any literature to solve similar problems, the recalcitrant term implied by fractal kinetics was approximated as a Maclaurin series expansion in the variable ζ, with results useful for insertion into pertubative methods. Since, $f[x]=\sum_{n=0}^{\infty} a_n x^n$, where $a_n = f^{(n)}[0]/n!$ by Maclaurin series, if $f[\zeta]=t^{-\zeta}$ and because $dt^{-\zeta}/d\zeta=t^{-\zeta}\ln[t](-1) \Rightarrow$ $f^{(n)}[\zeta]=(-1)^n(\ln[t])^n t^{-\zeta}$ then $a_n=(-\ln[t])^n/n!$, such that

$$t^{-\zeta} = \sum_{n=0}^{\infty} \frac{(-1)^n}{n!} (\ln[t])^n \zeta^n = 1 - \ln[t]\,\zeta + \frac{1}{2} (\ln[t])^2 \zeta^2 - \ldots \, . \tag{5.4}$$

Like the pertubation expansion of $\vec{X}[t]$, this expansion of $t^{-\zeta}$ is local in ζ (around $\zeta=0$) but global in t (see Figure 5.2).

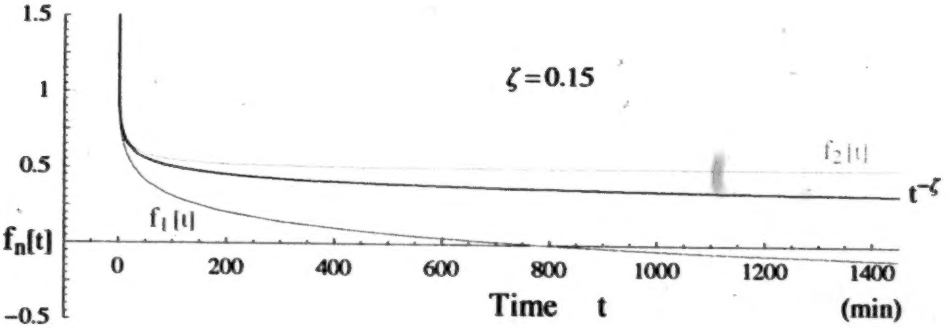

Figure 5.2: A comparative graph indicating that the series expansion (5.4) rapidly converges over the domain of t spanning the experimental abscissal data for an experimentally relevant value of ζ.

After substitution of the series expanasion of $t^{-\zeta}$, the coefficient matrix was

$$\begin{aligned} &\mathbf{A}[t,\zeta] = \sum_{n=0}^{\infty} \frac{(-1)^n}{n!} (\ln[t])^n \mathbf{A}_c \zeta^n = \mathbf{A}_0 - \ln[t]\, \mathbf{A}_c \zeta + \frac{1}{2} (\ln[t])^2 \mathbf{A}_c \zeta^2 - \ldots \\ &\Rightarrow \mathbf{A}[t,\zeta] = \mathbf{A}_0 + \zeta^1 \mathbf{A}_1[t] + \zeta^2 \mathbf{A}_2[t] + \ldots, \end{aligned} \tag{5.5}$$

where $\mathbf{A}_c \propto \delta_{bb}$ is a constant matrix containing a single nonzero component, and $\mathbf{A}_0$ is a constant matrix of the form to be expected if classical kinetics alone was occuring in the liver (see Appendix 5 for explicit statements). The substitution of the series form of the coefficient matrix (5.5) into (5.3) establishes the equivalence of terms for each power of ζ between the left and right sides, such that

$$\sum_{n=0}^{\infty} \zeta^n \vec{X}'_n = \sum_{n=0}^{\infty} \frac{(-1)^n}{n!} (\ln[t])^n \mathbf{A}_c \zeta^n \sum_{n=0}^{\infty} \zeta^n \vec{X},$$

which allows the following important statements of equality:

$$\begin{aligned} &\zeta^0: \quad \vec{X}'_0 = \mathbf{A}_0 \vec{X}_0 \\ &\zeta^1: \quad \vec{X}'_1 = \mathbf{A}_0 \vec{X}_1 + \mathbf{A}_1 \vec{X}_0 \\ &\zeta^2: \quad \vec{X}'_2 = \mathbf{A}_0 \vec{X}_2 + \mathbf{A}_1 \vec{X}_1 + \mathbf{A}_2 \vec{X}_0 \\ &\qquad\quad \vdots \\ &\zeta^n: \quad \vec{X}'_n = \sum_{i=0}^{n} \mathbf{A}_i \vec{X}_{n-i} \\ &\qquad\quad \vdots \end{aligned} \tag{5.6}$$

The zeroth-order pertubation equation from (5.6), describing a system of homogeneous first-order linear differential equations, incorperates all of the pharmacokinetic information of the PBPK model if the drug kinetics within the liver were assumed to be classical. Because $\mathbf{A}_0$ is a matrix with constant coefficients and the initial conditions are known, a solution may be realized, analogous to a single homogeneous first-order linear differential equation, of the form ⟨82⟩,

$$\vec{X}'_0 = \mathbf{A}_0 \vec{X}_0 \wedge \vec{X}_0[0] = \hat{X} \quad \Rightarrow \quad \vec{X}_0[t] = e^{\mathbf{A}_0 t} \hat{X}, \tag{5.7}$$

where a term of the form $e^{\mathbf{U}}$ is called a matrix exponential (see Appendix 5). The acheivable solution to the zeroth-order pertubation equation in turn renders higher-order pertubation equations assailable. After substitution of (5.7) into the first-order pertubation equation of (5.6), a nonhomogeneous first-order linear differential equation, $\mathbf{A}_1 \vec{X}_0$ being the inhomogeneity, most importantly with constant coefficients, that is susceptible to solution by the method of variation of parameters as defined in equation (a.3), results:

$$\vec{X}_1' = \mathbf{A}_0 \vec{X}_1 + \mathbf{A}_1 \vec{X}_0 \quad \Rightarrow \quad \vec{X}_1[t] = e^{\mathbf{A}_0 t} \int e^{-\mathbf{A}_0 t} \mathbf{A}_1[t] \vec{X}_0[t] \, dt, \quad \vec{X}_1[0] = \hat{0}.$$

The iterative process of pertubation theory replaces the original intractable differential system (5.1) with a sequence of amenable inhomogeneous equations. Generally, the *n*th-order pertubation equation has a solution based on the solutions of all the previous pertubation equations, such that

$$\vec{X}_n' = \sum_{i=0}^{n} \mathbf{A}_i \vec{X}_{n-i} \Rightarrow \vec{X}_n[t] = e^{\mathbf{A}_0 t} \int e^{-\mathbf{A}_0 t} \left(\sum_{i=1}^{n} \mathbf{A}_i[t] \vec{X}_{n-i}[t] \right) dt, \quad \vec{X}_n[0] = \hat{0}.$$

The final, closed form analytical desription of the proposed PBPK model describing the amount of drug in each compartment in terms of pharmacokinetic parameters, which may remain as unknowns for subsequent direct estimation by comparison to experimental data, is established by correct insertions into (5.3), such that

$$\vec{X}[t] \approx \vec{X}_0 + \zeta \vec{X}_1 + \zeta^2 \vec{X}_2 + \ldots + \zeta^n \vec{X}_n .$$

By a consideration of the uncertainty of the experimental data, a rational decision regarding the maximum order, *n*, of the pertubation term that is warrented for inclusion may be reached.

Chapter Six

Model Predictions & Comparison to Data

> However, a given theory may have been conceived as nothing more than an intellectual exercise with no pressing motivation and with little concern for its possible truth or usefulness.
>
> -William S. Hatcher

Because of the heuristic intent of the paper, its theoretical emphasis, and limited familiarity of the author regarding current practical implementation of clinical PBPK models, a mathematically analogous two compartment model will be used for further analysis. Given the complexity and the large number of nonphysics assumptions and input required for a PBPK model, all upon which the author remains too ignorant of, it is surmised that any results obtained by use of an ill-executed PBPK model would be less meaningful than what is achieved below. Besides, there exists, in my opinion, a kind of denial amongst many Pharmacokinetic researchers regarding either the continued relevance of, or the similarity of their own models to, classical multicompartmental models. It is rarely observed that the mathematical structure of most PBPK models is very similar to that of a similarly complicated classical multicompartmental model. At its core the argument is primarily one of philosophical foundations rather than practical capabilities, since both methods can be used for most clinical pharmacokinetic applications ⟨17⟩ and a rationally designed classical multicompartmental model may have some theoretical ramifications ⟨84⟩. Therefore, I establish a classical two-compartment open model as a test case by kinetically discriminating between a fractal and non-fractal processes of drug disposition and elimination. Let the liver, and therefore the elimination of mibefradil, be contained within the fractal compartment and the concentration measurements be taken from the nonfractal compartment as shown in Figure 6.1.

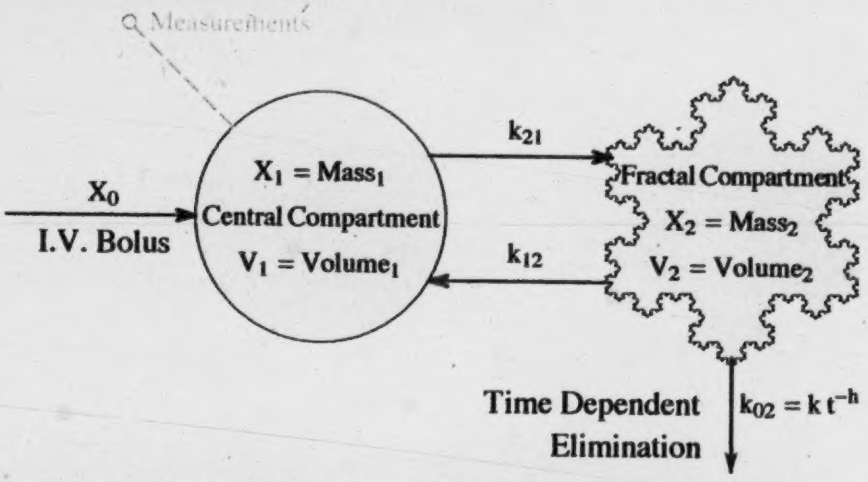
Measurements
X_1 = Mass$_1$
Central Compartment
V_1 = Volume$_1$
X_0
I.V. Bolus
k_{21}
k_{12}
Fractal Compartment
X_2 = Mass$_2$
V_2 = Volume$_2$
Time Dependent Elimination
$k_{02} = k\,t^{-h}$

Figure 6.1: A diagram of a 2-compartment model where the i.v. bolus source enters, and measurements are taken from, the central compartment. The secondary compartment is considered fractal with a time dependent rate of elimination. Compare to Figure 1.3.

Let the drug mass balance differential equation for the central compartment be

$$\frac{dX_1}{dt} = -k_{21}X_1 + k_{12}X_2\,,\quad X_1[0] = \mathfrak{X} = \text{dose.} \tag{6.1}$$

Let the drug mass balance differential equation portraying the fractal compartment be

$$\frac{dX_2}{dt} = k_{21}X_1 - k_{12}X_2 - k_{02}X_2\,,\quad X_2[0] = 0, \tag{6.2}$$

where $C_i = X_i/V_i$, k_{21} and k_{12} are positive first-order transfer rate constants, and k_{02} is an elimination coefficient. Let the elimination coefficient be time dependent as implied by fractal kinetics, such that

$$k_{02} = kt^{-\zeta}\,,\quad k > 0$$

where $\zeta \in (0,1]$. Since concentration measurements were drawn from the central compartment, only a solution for that space need be elucidated. By isolating for X_2

in (6.1), calculating its derivative, and substituting both results into (6.2), a generally cantankerous homogeneous second order linear differential equation with variable coefficients describing the drug concentration in the central compartment is caused:

$$X_1'' + (k_{21} + k_{12} + kt^{-\zeta})X_1' + k_{21}\,kt^{-\zeta}X_1 = 0\,. \qquad (6.3)$$

Initial conditions are $X_1[0]=\mathfrak{X}$ and, by substitution of $X_1[0]$ and $X_2[0]$ into (6.1), $X_1'[0]=-k_{21}\mathfrak{X}$, while an additional physical requirement is $\lim_{t\to\infty} X_1[0]=0$. Now, a cursory glance at equation (6.3) ostensibly reveals an potential singularity when $t=0$, but a phase portrait of the corresponding system of first-order differential equations, (6.1) and (6.2), indicates a stable trajectory for the solution towards a nodal sink at the origin for $t\to\infty$ as yielded by the particular initial conditions for this model (see Figure 6.2).

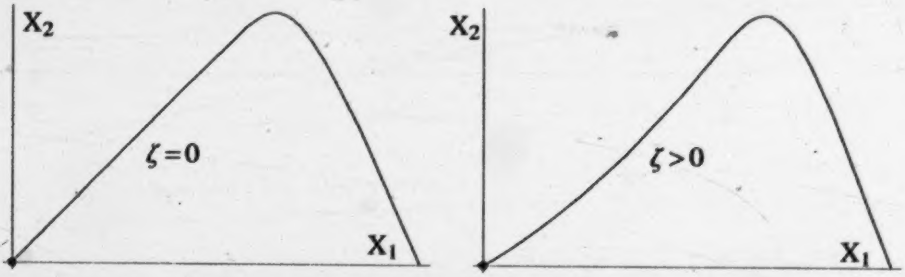

Figure 6.2: A numerical plot sketch using experimentally relevant numerical values for the parameters to qualitatively suggest the perturbative affects of fractal kinetics on the trajectory in the phase plane for the model system using equations (6.1) and (6.2) ⟨Dr. Li, Associate Professor of Mathematics, University of Alberta, personal communication, 10 September, 2001⟩.

To expunge superfluous subscripts and to stress the unspecific mathematical applicability of the following method for solution of equation (6.3), not quite in its most generic form, accede the temporary substitutions of ϕ for X_1, a for k_{21}, and b for k_{12}, such that

$$\phi'' + (a + b + kt^{-\zeta})\phi' + akt^{-\zeta}\phi = 0\,. \qquad (6.4)$$

Now, congruous with the previously described perturbative approach within the PBPK model, let the influences of fractal kinetics in the fractal compartment be diminutive, so ζ will be a small parameter and the solution of the pharmacokinetic system can be assumed to be of the form

$$\phi[t] = \sum_{n=0}^{\infty} \zeta^{n} \phi_{n}[t], \tag{6.5}$$

such that

$$\phi'[t] = \sum_{n=0}^{\infty} \zeta^{n} \phi'_{n}[t] \quad \bigwedge \quad \phi''[t] = \sum_{n=0}^{\infty} \zeta^{n} \phi''_{n}[t]. \tag{6.6}$$

After substitutions of terms of the differential equation (6.4) with the expansions (5.4), (6.5), and (6.6), and following some subsequent sorting, an equivalence of terms for each power of ζ may be recognized which requires the following series of statements of equality:

$$\begin{aligned}
\zeta^{0}:&\quad \phi''_{0} + (a+b+k)\phi'_{0} + ak\phi_{0} = 0\,, \quad \phi_{0}[0] = \mathcal{X}, \ \phi'_{0}[0] = -a\mathcal{X} \\
\zeta^{1}:&\quad \phi''_{1} + (a+b+k)\phi'_{1} + ak\phi_{1} = k\ln[t]\phi'_{0} + ak\ln[t]\phi_{0}, \\
&\qquad\qquad\qquad\qquad \phi_{1}[0] = 0\,, \ \phi'_{1}[0] = 0 \\
\zeta^{2}:&\quad \phi''_{2} + (a+b+k)\phi'_{2} + ak\phi_{2} = k\ln[t]\phi'_{1} + ak\ln[t]\phi_{1} \\
&\qquad - \frac{1}{2}k(\ln[t])^{2}\phi'_{0} - \frac{1}{2}ak(\ln[t])^{2}\phi_{0}, \ \phi_{2}[0] = 0\,, \ \phi'_{2}[0] = 0 \\
&\qquad \vdots \\
\zeta^{n}:&\quad \phi''_{n} + (a+b+k)\phi'_{n} + ak\phi_{n} = \sum_{i=1}^{n} \frac{(-1)^{i+1}}{i!} k(\ln[t])^{i}\left(\frac{d}{dt} + a\right)\phi_{n-i}\,, \\
&\qquad\qquad\qquad\qquad \phi_{n}[0] = 0\,, \ \phi'_{n}[0] = 0 \\
&\qquad \vdots
\end{aligned} \tag{6.7}$$

The zeroth-order perturbation equation from (6.7), describes a classical two compartment open model if the elimination kinetics within the secondary compartment were assumed to be classical. The solution is of the form of a sum of exponentials of equation (1.10):

$$\phi_0[t] = \vartheta_1 e^{s_1 t} + \vartheta_2 e^{s_2 t} \tag{6.8}$$

where s_1 and s_2 are negative coefficients that are a function of a, b, and k, while ϑ_1 and ϑ_2 are real coefficients that are functions of a, b, k, and Ӿ (see Appendix 6 for explicit statements).

Contingent upon the successful simple solution to the zeroth-order equation, as (6.9) is, the contributions from the second and all higher order equations are calculated. Success of the method of integration by the variation of parameters used for the post-zero terms, depends on at least solutions to integrals of the form

$$I_n = \int (\ln[t])^n e^{\theta t} dt,$$

where $\theta[a,b,k]$ is some constant. While these solutions and their derivatives exist, their account requires the special functions: Euler gamma function $\Gamma[\theta t]$, exponential integral function $\mathrm{Ei}[\theta t]$, and the generalized hypergeometric function ${}_pF_q[\overline{\alpha};\overline{\beta};\theta t]$ (see Appendix 6 for explicit statements). Finally, compliance to the initial conditions depends on terms behaving asymptotically like

$$\lim_{t \to 0} \ln[t]\,(e^{\theta_1 t} - e^{\theta_2 t}) = 0$$

occurring at each step of the perturbation.

It is disappointing that the analytical solution to the fractal compartmental model, assembled with the perturbation terms acquired from (6.7), quickly becomes complicated because this blunts a touted advantage of this approach - that it is a teaching tool and a method for physical and pharmacokinetic insight superior to strictly numerical methods. The behaviors of the first three perturbation terms are shown in Figure 6.3. Also, the variable, ϕ, introduced in (6.4), may just as well be interpreted as a concentration of the drug in the central compartment for the remainder of the report since $C_1 = X_1 / V_1$.

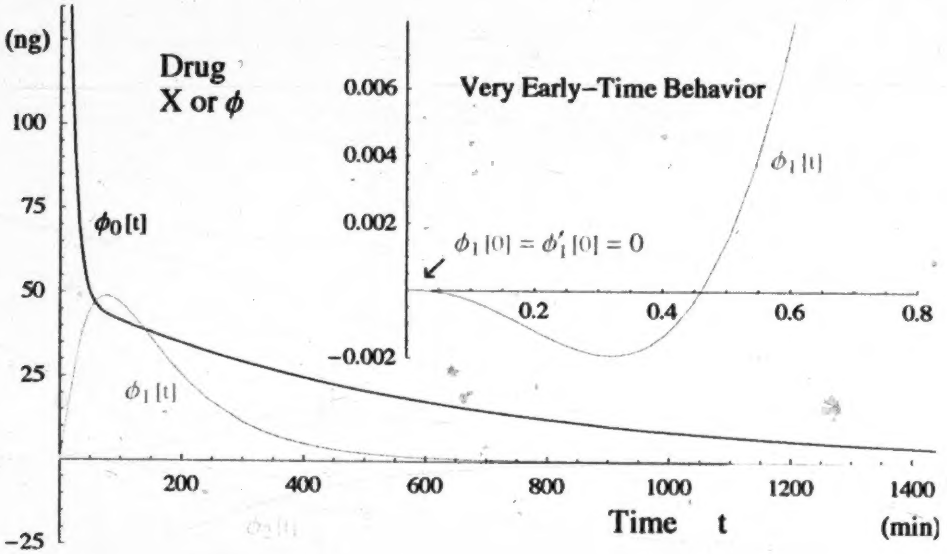

Figure 6.3: Comparative graphs of the first three terms impelled by the series of equalities in (6.7) for the pharmacokinetic model employing illustrative values of a, b, k, and $\mathfrak{X}$. Notice that the initial conditions for the higher order perturbation terms are met at the origin (↙). The solution implied is $\phi[t] \approx \phi_0[t] + \zeta \phi_1[t] + \zeta^2 \phi_2[t]$.

The Spectral Dimension of the Dog Liver

A three term perturbation expansion approximation to the solution of the differential equation (6.4) was adopted of the form

$$\phi[t] \approx \phi_0[t] + \zeta \phi_1[t] + \zeta^2 \phi_2[t] \,, \quad \zeta \ll 1 \,, \tag{6.9}$$

per (6.5), and compared to the pharmacokinetic data using the techniques of nonlinear fits with a global optimization method as previously described in chapter three (see Figure 6.4 for an example). The best-fit values for the small parameter, ζ, were: $\zeta_{D1}=0.084$, $\zeta_{D2}=0.092$, $\zeta_{D3}=0.111$, and $\zeta_{D4}=0.043$, for dogs one to four respectively. The absolute discrepancy was estimated by the chi-squared function to be: $\chi^2_{D1}\approx 17$, $\chi^2_{D2}\approx 10$, $\chi^2_{D3}\approx 14$, and $\chi^2_{D4}\approx 23$.

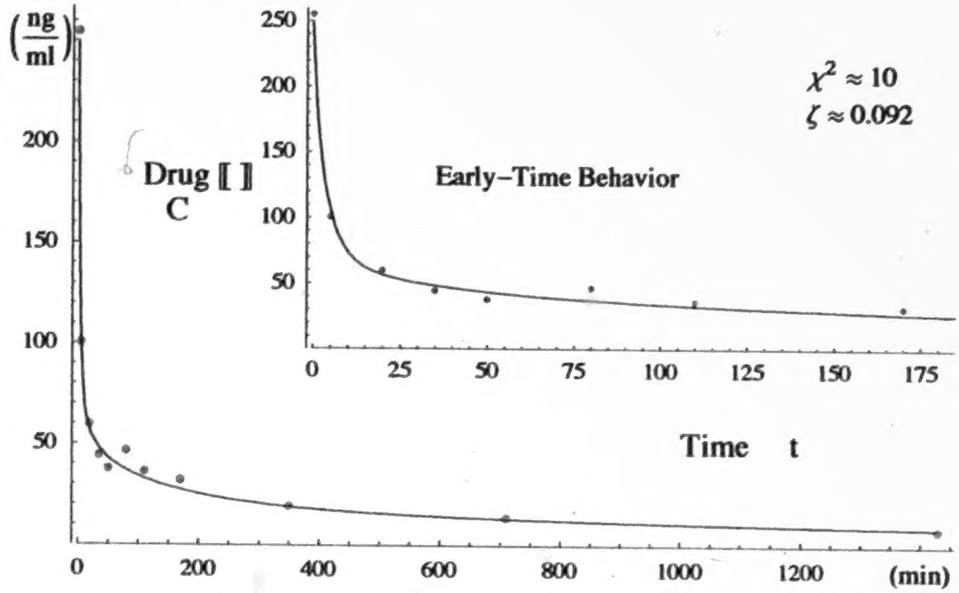

Figure 6.4: Mibefradil time course data fit with a three term perturbation series implied by a 2-compartment model with fractal kinetics in the eliminating compartment for trial IV-PV-D2.

Because the pharmacokinetic model (6.5) is nonlinear with respect to the unknown parameters, to establish the variance of the fitted small parameter zeta, synthetic sets of data via Monte Carlo methods were fabricated. While a standard Bootstrap approach ⟨85⟩ is based on resampling methods whereby sets of N datum points are randomly selected with replacement from the original set of data, ${}^{0}\mathcal{Z}$ (see Figure 2.3), this technique is troublesome for the pharmacokinetic data studied in this report. Since the data sets are rather small and with a particular lack of sampling at early times when rapid changes in concentration occur, and a data set missing influential datum points would prejudice calculations (consider Figure 6.4 with either the first or last datum point missing), synthetic data sets more reflective of the experimental data sets were devised. A Gaussian distribution centered at each point in ${}^{0}\vec{Z}$, with a standard deviation, $\sigma_i = 0.09\,C_i$, $i = 1, \ldots, N$, allows for new data sets, still possessing the inherent uncertainties but without duplications or omissions, to be created ⟨Dr. Lele, Associate Professor of Statistics, University of Alberta, personal communication, 20 August, 2001⟩.

A statistically suspect but practically manageable number, $N = 300$, of synthetic data sets, ${}^{i}_{S}\vec{Z}$, $i = 1, \ldots, N$, were pseudorandomly generated by computer for each dog and fit. A resulting M-dimensional distribution of fitted parameters, ${}^{i}_{S}\vec{a}$, $i = 1, \ldots, N$, corresponding to different chi-squared values can be observed over one intersecting plane in Figure 6.5. The one dimensional confidence intervals for the parameters are indicated by the appropriate projections of the region onto the axes ⟨93⟩.

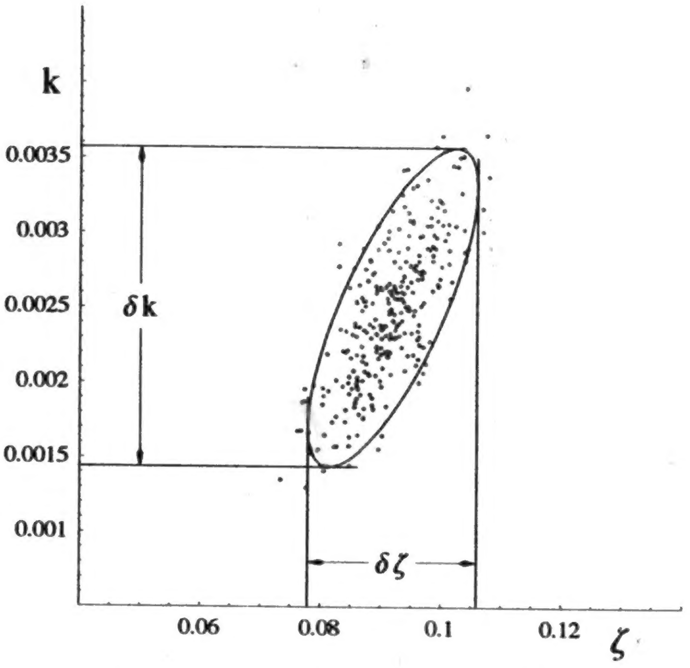

Figure 6.5: The confidence region intersecting the *k*-ζ plane in parameter space for trial IV-PV-D2, indicating an ellipse of 90% confidence.

The best-fit values for the small parameter, ζ, including uncertainties, were: $\zeta_{D1} = 0.084 \pm 0.020$, $\zeta_{D2} = 0.092 \pm 0.014$, $\zeta_{D3} = 0.111 \pm 0.016$, and $\zeta_{D4} = 0.043 \pm 0.028$, for dogs one to four respectively. This implies, by (4.7), calculated values of the spectral dimension for each of the dog livers are: $d_s^{D1} = 1.832 \pm 0.040$, $d_s^{D2} = 1.816 \pm 0.028$, $d_s^{D3} = 1.778 \pm 0.032$, and $d_s^{D4} = 1.914 \pm 0.056$. A comparison indicates that there is not agreement amongst all of the results to within experimental and theoretical uncertainty, but a mean value of the spectral dimension for some imaginary average dog, by the basic methods of error propagation, is $d_s^{\text{average}} = 1.84 + 0.04$.

Model Adequacy

Lastly, the goodness-of-fit of the model, as described in chapter two, may be reckoned by concocting a last data set useful for establishing a meaningful comparison of the model to the real data. Using the model equation (6.9) itself, a Gaussian distribution is centered at each point $(t_i, \phi[t_i])$, $i=1,\ldots,N$, with the standard deviation, $\sigma_i = 0.09\,C_i$. Analogous to the previous procedures, a series of new synthetic data sets, $N=300$, are made, via a pseudorandom number generator over the Gaussian distribution, and fit, via the chi-squared figure-of-merit function, to the same model from whence they originated. This establishes an ad hoc distribution of the chi-squared function around the model based on (pseudo) random fluctuations of the data as managed by the expected Gaussian distribution at each point. Finally, a meaningful statistic may be calculated comparing the model to the real data: the probability that a data set, exhibiting at least as much disagreement with the model as the real data set does, could arise from the model, assuming it is correct, given the expected random noise as observed from the experiment (see Figure 6.6).

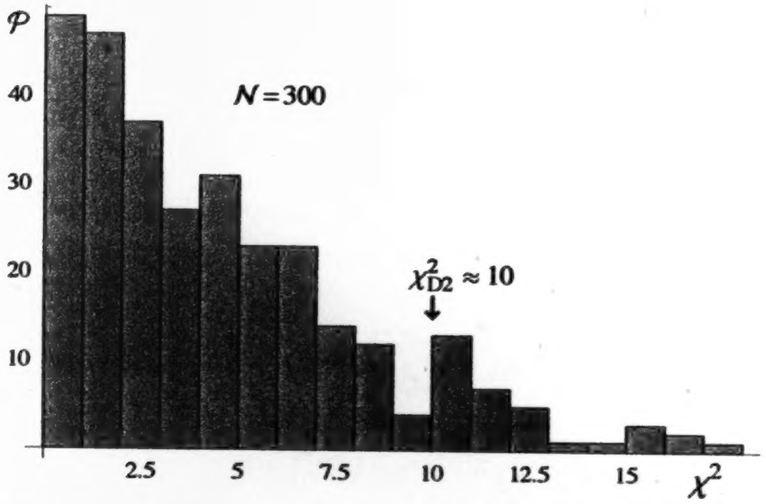

Figure 6.6: The ad hoc chi-square distribution for the model to which a chi-square value may be compared to estimate the probability that such a model could give rise to that data set or to one that fits at least as poorly. The probability is simply the ratio of the statistical weight of the bins to the right of the observed chi-square value to the total number of all observations ($N = 300$). Relevant to IV-PV-D2.

Following said procedure, the calculated chi-square probability for each set of dog data was: $\mathcal{P}_{D1} \approx 0$, $\mathcal{P}_{D2} \approx 0.11$, $\mathcal{P}_{D3} \approx 0.02$, and $\mathcal{P}_{D1} \approx 0$. Thus it seems that a at least half of the trials do not support the model given the experimental uncertainty.

Chapter Seven

Discussion

Subjective reality has the capacity to create abstract internal mental models of phenomena, and it is these mental representations that are really 'known'. They become the object of our scrutiny, contemplation, and social discourse.

-William S. Hatcher

Upon reflection on the results of fitting the new theoretical model to the data sets, despite the apparent lack of approval indicated by the statistical tests used, there were some tantalizing possibilities for a positive interpretation. An improved fit, as measured by the chi-square values, compared to a corresponding classical model was observed (compare Figure 6.4 to Figure 3.9). Unlike the negative indications from the data of any effects due to Michaelis-Menten kinetics, the calculated values of ζ, between 0.043 and 0.111, do not agree with the null hypothesis, that $\zeta=0$, within experimental uncertainties.

It may also be the case that the adopted experimental uncertainty of 9% was too conservative or that it was not normally distributed. Indeed, a further consideration of the uncertainties of the data is warranted. For example, since the slope is so steep during the initial peak phase of the experiment, $t<25$ min., even small uncertainties in the measurement times, which were assumed to be zero, would produce large uncertainties in the concentration measurements. Additionally, the intrinsic uncertainties of the biological model systems are likely to produce outlying data points that conspire to indicate low goodness-of-fit tests. This lack of predictability may arise form different sources; these include system instability (perhaps due to chaos), environmental fluctuations due to effects outside of the systems modeled, and measurement uncertainties (especially in time). Besides containing mundane signal and noise, irregular time series may be chaotic - irregularities produced by the intrinsic deterministic dynamics of a nonlinear biological system. ⟨88⟩ The least-squares fitting, linear or nonlinear, is a maximum likelihood estimation of the fitted parameters if the measurement errors are independent and Gaussianly distributed and may not have been ideal for the data sets provided. Perhaps a reanalysis of the data is justified within the context of robust statistics - statistics that are less sensitive to noise within the data ⟨96,97,98,99⟩.

Evidence that the data sets may not be well behaved is the simple observation that the peak concentration for two of the three concentration-time course curves occurred before the end of the intravenous infusion dose at ten minutes. The only way this can occur is if the rate of removal of drug from the blood was greater than the zero-order rate of the intravenous dose - an impossibility within the context of classical kinetics or its extensions such as Michaelis-Menten kinetics. This observation may also imply a time dependent rate coefficient, even a reactivity of the system to an input of drugs.

Considering that this report favors the interpretation that the kinetics of mibefradil are affected by the fractal structure of the liver that consequently reduces the rate of metabolism and clearance of drug over time, the question of why nature would design the liver in such a way is raised. Now while there is no performance advantage over a well stirred classically imagined compartment, one with a rate constant due to a uniformly random distribution of drug and enzyme, such a compartment may well be impossible to achieve under biological designs and the implied comparison is therefore an ill posed one. It may be that the fractal liver design is the best design possible, such that comparisons against non-ideal theoretical models, like a poorly stirred sphere with enzyme adhered along the inner wall, are favorable. For example, the fractal structure, with may layers of membrane at its interface, allows the organ to possess a high number (concentration) of enzymes, thus giving it a high reaction rate despite time dependent (decay) fractal kinetics. Indeed, the intricate interlacing of a stationary, catalytic phase of the hepatocytes, with a liquid phase of the drug dissolved in blood, along a fractal boarder is what reduces the required diffusional distances for reactions to take place with any appreciable celerity. Moreover, the complicated structure of the liver which provides for a huge interface between drug and hepatocytes, despite, may be generated quite simply during the growth of the liver (see Figure 4.6). The fractal form may be parsimoniously encoded in the DNA, indirectly specified by means of a simple recursive algorithm that instructs the biological machinery how to construct the liver. In this way, a vascular system made up of fine tubing with an effective topological dimension of one may fill the three dimensional embedding space of the liver. These possibilities reveal that the structure of the liver may necessarily be that of a fractal.

Finally, it is suggested that the often reported ⟨87⟩, poor correlation between in vivo and in vitro effects of drugs may be explained by the difference in the physical environments the two situations provide. I assume that most in vitro experiments of enzyme performance are made under the standard laboratory the conditions that satisfy classical kinetic assumptions. It is suggested that if the in vivo tests on hepatically metabolized drugs were made while attempting to reproduce the dimensionally restricted conditions of the liver, such as within a porous medium, the results may more closely match the results from in vivo experiments.

Chapter Eight

Conclusions

> **Even if we have so far been unsuccessful in fulfilling some individual need, we can always hope that we will in the future discover some heretofore unknown resource or power that can engender success.**
>
> **-William S. Hatcher**

The pharmacokinetics of mibefradil in a dog model system was scrutinized. En route, the basic principals of kinetics, pharmacokinetics, and scientific modeling, philosophy, and statistics were contemplated.

Experimental pharmacokinetic data sets were first addressed by empirical means. The unknown experimental uncertainty was estimated to be 9% and was assumed to be Gaussianly distributed. Pure power functions seemed to be the most efficient basis set with which to fit the data. Phenomenological evidence did not support the notion that Michaelis-Menten kinetics occur in the liver at the dosages studied. Mibefradil is likely to be eliminated in an annihilating trap reaction with liver enzymes. An improved, weighted Prony's method was observed to be problematic for construing Pharmacokinetic data because it generally implies that the drug levels in a compartment are oscillatory to some extent. Interpretation of this phenomena within the context of biological signal and control systems is possible and may be a topic for further research outside of this report.

The physiology of the liver supported the hypothesis that mibefradil may experience a fractal like environment within. Fractal kinetic theory suggested the adoption of a time dependent rate constant, with power law form, monitored by the spectral dimension. A general PBPK model was proposed and elucidated incorporating at least one heterogeneous compartment following fractal kinetics. After a local series expansion of the time dependent rate constant around $\zeta=0$, assuming that the fractal effects on the time dependent rate constant were small, approximate analytical solutions to the model differential mass balance equations were derived by purturbative techniques.

Mibefradil concentration-time course data were analyzed with a mathematically analogous multicompartmental model with the goal of measuring the effective spectral dimension of the dog liver. Estimates were: $d_s^{\mathrm{D1}}=1.832\pm0.040$, $d_s^{\mathrm{D2}}=1.816\pm0.028$, $d_s^{\mathrm{D3}}=1.778\pm0.032$, and $d_s^{\mathrm{D4}}=1.914\pm0.056$, for the four dogs, though these results are not enthusiastically endorsed by the chi-squared test statistic for the adopted experimental uncertainty. Yet, it is proffered that heterogeneous processes of drug distribution and reaction in the liver can obey the principles of fractal kinetics. Elaboration of present PBPK and multicompartmental models to include fractal kinetics should be considered.

References

> . . . whereas determining truth through multisubjective confirmation and verification is accessible only by means of highly complex forms of social organization and information exchange.
>
> -William S. Hatcher

1. E. Gladtke & H. M. von Hattingberg. *Pharmacokinetics: An Introduction.* (Springer-Verlag, Berlin, 1979).

2. A. Rescigno & B. Bocchialini. Pharmacokinetics: Unfolding of a Concept, in: *New Trends in Pharmacokinetics.* (NATO Science Series, Plenum Press, London, 1992).

3. T. L. Schwinghammer & P. D. Kroboth. Basic Concepts in Pharmacodynamic Modeling. *Journal of Clinical Pharmacology,* **28**, 388-394 (1988).

4. Wayne. A. Colburn et alia. Controversy III: To Model or Not to Model. *Pharmacokinetics,* **28**, 879-888 (1988).

5. Michael E. Winters. *Basic Clinical Pharmacokinetics.* (Applied Therapeutics, Inc., Vancouver, WA, 1994).

6. Milo Gibaldi & Donald Perrier. *Pharmacokinetics,* 2nd. (Marcel Dekker, Inc., New York, 1982).

7. W. Evans, J. Schentag, & W. Jusko (editors). *Applied Pharmacokinetics: Principles of Therapeutic Drug Monitoring,* 3rd.. (Applied Therapeutics, Inc., Vancouver, WA, 1992).

8. R. Marsh. Fractal Theory Applied to Pharmacokinetics. Unpublished undergraduate report. Edmonton, AB, 1997. Available from: Dr. Tuszynski, Department of Physics, University of Alberta.

9. Raoul Kopelman. Fractal Reaction Kinetics. *Science.* Vol. 241, pp. 1620-1626 (1988).

10. D. Calef & J. Deutch. Diffusion-Controlled Reactions. *Annual Review of Physical Chemistry.* **34**, pp. 493-524 (1983).

11. Joel Keizer. Nonequilibrium Statistical Thermodynamics and the Effect of Diffusion on Chemical Reaction Rates. *Journal of Physical Chemistry,* **86**, 5052-5067 (1982).

12. J. D. Murray. *Mathematical Biology,* 2nd.. (Springer-Verlag, Berlin, 1993).

13. Christopher K. Mathews & K. E. van Holde. *Biochemistry.* (The Benjamin/Cummings Publishing Company, Inc., Redwood City, CA, 1990).

14. G. G. Gibson & P. Skett. *Introduction to Drug Metabolism,* 2nd.. (Blackie Academic & Professional, an imprint of Chapman & Hall, Glasgow, 1994).

15. James S. Beck. Epistemology in Pharmacokinetics, in: *New Trends in Pharmacokinetics.* (NATO Science Series, Plenum Press, London, 1992).

16. J. J. DiStefano & E. M. Landaw. Multiexponential, multicompartmental, and noncompartmental modeling I. Methodological limitations and physiological interpretations. *American Journal of Physiology,* **246**, R651-R664 (1984).

17. William R. Gillespie. Noncompartmental Verses Compartmental Modelling in Clinical Pharmacokinetics. *Clinical Pharmacokinetics,* **20**(4), 243-262 (1991).

18. K. F. O'Grady & D. J. Doyle. Compartmental Modeling in Clinical Pharmacokinetics. *Journal of Clinical Engineering*, Vol. 20, No. 2, 156-170 (1995).

19. Earvin Liang & Hartmut Derendorf. Pitfalls in Pharmacokinetic Multicompartment Analysis. *Journal of Pharmacokinetics and Biopharmaceutics*, Vol. 26, No. 2, 247-260 (1998). (Though the title implies a negativity towards multicompartmental analysis, the article is a constructive critism of the topic with the aim of imparting useful knowledge to improve the skills and interpretations of those who use the technique.)

20. M. R. Rowland & A. M. Evans. Physiologic Models of Hepatic Drug Elimination, in: *New Trends in Pharmacokinetics*. 83-115 (NATO Science Series, Plenum Press, London, 1992).

21. D. Krewski, Y. Wang, S. Bartlett, & K. Krishnan. Uncertainty, Variability, and Sensitivity Analysis in Physiological Pharmacokinetic Models (preliminary publication). *Technical Report Series of the Laboratory for Research in Statistics and Probability*, No. 252, (1994).

22. L. Kedderis, J. Mills, M. Andersen, & L. Birnbaum. A Physiologically Based Pharmacokinetic Model for 2,3,7,8-Tetrabromodibenzo-*p*-dioxin (TBDD) in the Rat: Tissue Distribution and CYP1A Induction. *Toxocology and Applied Pharmacology*, 121, 87-98 (1993).

23. L. C. W. Dixon, E. Spedicato, & G. P. Szego (editors). *Nonlinear Optimization: Theory and Algorithms*. (Birkhauser, Boston, 1980).

24. Kim-Chi T. Hoang. Physiologically based pharmacokinetic models: mathematical fundamentals and simulation implementations. *Toxicology Letters*, 79, pp. 99-106 (1995).

26. H. Boxenbaum. Pharmacokinetics: Philosophy of Modeling. *Drug Metabolism Reviews*, 24(1), pp. 89-120 (1992).

27. L. Gerlowski & R. Jain. Physiologically Based Pharmacokinetic Modeling: Principles and Applications. *Journal of Pharmaceutical Sciences*. Vol. 72, No. 10, pp. 1103- (1983).

28. W. S. Hatcher. *Logic and Logos: Essays on Science, Religion, and Philosophy*. (George Ronald, Oxford, 1990).

29. B. Alberts, D. Bray, J. Lewis, M. Raff, K. Roberts, & J. Watson. *Molecular Biology of the Cell*, 3rd., (Garland Publishing, Inc., London, 1994).

30. C. J. Puccia & R. Levins. *Qualitative Modeling of Complex Systems*. (Harvard University Press, Cambridge, MA, 1985).

31. J. C. Fleishaker & R. B. Smith. Compartmental Model Analysis in Pharmacokinetics. *Journal of Clinical Pharmacology*, 27, 922-926 (1987).

32. W. H. Press, S. A. Teukolsky, W. T. Vetterling, & B. P. Flannery. *Numerical Recipes in Fortran: The Art of Scientific Computing*, 2nd. (Cambridge University Press, Cambridge, 1992).

33. John R. Taylor. *An Introduction to Error Analysis: The Study of Uncertainties in Physical Measurements*. (University Science Books, Mill Valley, CA, 1982).

34. David W. A. Bourne. *Mathematical Modeling of Pharmacokinetic Data*. (Technomic Publishing Company, Inc., Lancaster, PA, 1995).

35. Franklin A. Graybill. *Theory and Application of the Linear Model*. (Duxbury Press, North Scituate, MA, 1976).

36. Thomas P. Ryan. *Modern Regression Methods*. (John Wiley & Sons, Inc., New York, 1997).

37. M. Abramowitz & I. Stegun (editors). *Handbook of Mathematical Functions with Formulas, Graphs, and Mathematical Tables*, 9th. (Dover Publications, Inc., New York, 1970).

38. C. Loehle (editor). *Global Nonlinear Optimization Using Mathematica*, 3rd. (Loehle Enterprises, Naperville, IL, 2000).

39. H. Wiltshire, B. Sutton, G. Heeps, A. Betty, D. Angus, S. Harris, E. Worth, and H. Welker. Metabolism of the calcium antagonist, mibefradil (POSICOR^{TM}, Ro 40-5967). *Xenobiotica*, Vol. 27, No. 6, 557-571 (1997).

40. Horst A.Welker. Single- and Multiple-dose Mibefradil Pharmacokinetics in Normal and Hypertensive Subjects. *Journal of Pharmacy and Pharmacology*. **50**, pp. 983-987 (1998).

41. A. Skerjanec. *Mechanisms of Nonlinear Pharmacokinetics of Mibefradil*. Edmonton, Alberta: University of Alberta; 1995. Thesis. 1-108.

42. A. Skerjanec, S. Tawfik, & Y. K. Tam. Nonlinear Pharmacokinetics of Mibefradil in the Dog. *Journal of Pharmaceutical Science*, Vol. 85, No. 2, 189-192 (1995).

43. L. Y. (Stella) Ngo. *A Study on the Time-Dependent Kinetics of Lidocaine*. Edmonton, Alberta: University of Alberta; 1997. Thesis. 1-171.

44. M.E. Wise & G.J. Borsboom. Two Exceptional Sets of Physiological Clearance Curves and Their Mathematical Form: Test Cases?. *Bulletin of Mathematical Biology*. Vol. 51, No. 5, pp. 579-596 (1989).

45. F. B. Hildebrand. *Introduction to Numerical Analysis*, 2nd. (Dover Publications, Inc., New York, 1987).

46. Giorgio Segre. Relevance, Experiences, and Trends in the Use of Compartmental Models. *Drug Metabolism Reviews*, **15** (1&2), 7-53 (1984).

47. R. Khorsravan, M. Gray, & Y. K. Tam. The Effects of Early Blood Sampling and Different Sampling Sites on Estimation of Pharmacokinetic Pamameters: An Evaluation Using a Physiological Model. *Unpublished Document?*, Vol. 20, No. 2, 156-170 (1995).

48. R. Horst & H. Tuy. *Global Optimization: Deterministic Approaches*, 3rd. (Springer-Verlag, Berlin, 1996).

49. E. Weisstein (editor). (2000) *Mathworld*. Lambert's *W*-Function [On Line], Available: mathworld.wolfram.com/LambertsW-Function.html

50. Stephen Wolfram. *The Mathematica Book*, 4th. (Cambridge University Press, Cambridge, 1999).

51. K. H. Norwich & S. Siu. Power Functions in Physiology and Pharmacology. *Journal of Theoretical Biology*, **95**, 387-398 (1982).

52. M.E. Wise. Negative Power Functions of Time in Pharmacokinetics and Their Implications. *Journal of Pharmacokinetics and Biopharmaceutics*. Vol. 13, No. 3, pp. 309-346 (1985).

53. C. Goresky & A. Groom. Microcirculatory Events in the Liver and the Spleen, in: *Handbook of Physiology~Cardiovascular System IV*, 689-703, (???, ???, 197?).

54. J. L. Campra & T. B. Reynolds. The Hepatic Circulation, in: *The Liver: Biology and Pathology*, 2nd., 911-930, (Raven Press, New York, 1988).

55. W. W. Loutt & M. P. Macedo. Hepatic Circulation and Toxicology. *Drug Metabolism Reviews*, **29** (1&2), 369-395 (1997).

56. Jorge Marquez. (1992) *Fractal Tutorial*. II International Image Processing Workshop [On Line], Available: www.tsi.enst.fr/~marquez/fractals.html

57. J. Bassingthwaighte, L. Liebovitch, & B. West. *Fractal Physiology*, (Oxford University Press, Oxford, 1994).

58. T. Nonnenmacher, G. Losa, & E. Weibel (editors). *Fractals in Biology and Medicine*, (Birkhauser Verlang, Basel, 1994).

59. J. Bassingthwaighte, R. King, & S. Roger. Fractal Nature of Regional Myocardial Blood Flow Heterogeneity. *Circulation Research*, Vol. 65, No. 3, 578-590, (1989).

60. C. Javanaud. The Application of a Fractal Model to the Scattering of Ultrasound in Biological Media. *Journal of the Acoustical Society of America*, **86** (2), 493-496, (1989).

61. Panos Macheras. A Fractal Approach to Heterogeneous Drug Distribution: Calcium Pharmacokinetics. *Pharmaceutical Research*. Vol. 13, No. 5, pp. 663-670 (1996).

62. H. Koch. The Concept of Fractals in the Pharmaceutical Sciences. *Pharmazie*, **48**, 643-659, (1993).

63. B. B. Mandelbrot. A Fractal's Lacunarity, and how it can be Tuned and Measured, in: *Fractals in Biology and Medicine*, 8-21, (Birkhauser Verlang, Basel, Switzerland, 1993).

64. Robert P. Munafo. (2000) *Fractal, Definition of.* Mandelbrot Set Glossary and Encyclopedia [On Line], Available: home.earthlink.net/~mrob/pub/muency/fractaldefinitionof.html

65. P. Macheras, P. Argyrakis, & C. Polymilis. Fractal geometry, fractal kinetics and chaos en route to biopharmaceutical sciences. *European Journal of Drug Metabolism and Pharmacokinetics*. Vol. 21, No. 2, pp. 77-86 (1996).

66. Muhammad Sahimi. Linear and Nonlinear, Scalar and Vector Transport Processes in Hetrogeneous Media: Fractals, Percolation, and Scaling Laws. *The Chemical Engineering Journal*, **64**, 21-44, (1996).

67. Raffaella Burioni & Davide Cassi. (1995) Universal Properties of Spectral Dimension [On Line], Available: www.pr.infn.it/preprints/1995/uprf-95-430.ps.gz

68. Massimiliano Giona. First-Order Reaction-Diffusion Kinetics in Complex Fractal Media. *Chemical Engineering Science*. Vol. 47, No. 6, pp. 1503-1515 (1992).

69. Shlomo Havlin & Daniel Ben-Avraham. Diffusion in Disordered Media. *Advances in Physics*. Vol. 36, No. 6, pp. 695-798 (1990).

70. A. Bunde & S. Havlin. *Fractals and Disordered Systems*, 2nd. (Springer-Verlag, Berlin, 1996).

71. P. Argyrakis, G. Duportail, & P. Lianos. Behavior of the Rate Constant for Reactions in Restricted Spaces: Flourescence Probing of Lipid Vesicles. *J. Chem. Phys*. **95** (5), pp. 3808-3814 (1991).

72. Raoul Kopelman. Rate Processes on Fractals: Theory, Simulations, and Experiments. *Journal of Statistical Physics*. Vol. 42, No. 1/2, pp. 185-201 (1986).

73. K. Lindenberg, P. Argyrakis, & R. Kopleman. Reaction-Diffusion Model for A+A Reaction. *Journal of Physical Chemistry*, **99**, 7542-7556 (1995).

74. Yong-Eun Koo & R. Kopelman. Space- and Time-Resolved Diffusion-Limited Binary Reaction Kinetics in Capillaries: Experimental Observation of Segregation, Anomalous Exponents, and Depletion Zone. *Journal of Statistical Physics*. Vol. 65, No. 5/6, pp. 185-201 (1986).

75. R. Kopelman, A. Lin, & P. Argyrakis. Non-Classical Kinetics and Reactant Segregation in D-Dimensional Tubular Spaces. *Physics Letters A*. **232**, pp. 34-40 (1997).

76. E. Clement, R. Kopelman, & L. Sander. Trapping Reaction in Low Dimensions: Steady-State Self-Organization. *Europhysics Letters*. **11** (8), pp. 707-712 (1990).

77. R. Kopelman, L. Anacker, E. Clement, L. Li, & L. Sander. Low Dimensional Reaction Kinetics. *Chemometrics and Intelligent Laboratory Systems*. **10**, pp. 127-132 (1991).

78. E. Clement, R. Kopelman, & L. Sander. Bimolecular Reaction $A+B\rightarrow 0$ at Steady State on Fractals: Anomolous Rate Law and Reactant Self-Organization. *Chemical Physics*. **146**, pp. 343-350 (1990).

79. K. F. Eckerman, R. W. Leggett, & L. R. Williams. An Elementary Method for Solving Compartmental Models with Time-Dependent Coefficients. *Radiation Protection Dosimetry*, Vol. 41, No. 2/4, pp. 257-263 (1992).

80. F.Farris, R. Dedrick, P. Allen, & J. Smith. Physiological Model for the Pharmacokinetics of Methyl Mercury in the Growing Rat. *Toxocology and Applied Pharmacology*, **119**, 74-90 (1993).

81. C. Bender & A. Orszag. *Advanced Mathematical Methods for Scientists and Engineers: AsymptoticMethod and Perturbation Theory*, (Springer-Verlag, Berlin, 1999).

82. Ray Redheffer. *Differential Equations: Theory and Applications*, Chapter 17, (Jones & Bartlett, Boston, 1991).

83. R. Kopelman & Yong-Eun Koo. Reaction Kinetics in Restricted Spaces. *Israel Journal of Chemistry*. Vol. 31, pp. 147-157 (1991).

84. W. L. Roth, L. W. Weber, & K. K. Rozman. Incorporation of First-Order Uptake Rate Constants form Simple Mammillary Models into Blood-Flow Limited Physiological Pharmacokinetic Models via Extraction Efficiencies. *Pharmaceutical Research*, Vol. 12, No. 2, pp. 263-269 (1995).

85. S. Huet, A. Bouvier, M.-A. Gruet, & E. Jolivet (all women). *Statistical Tools for Nonlinear Regression*. (Springer-Verlag, New York, 1996).

86. I. Gradshteyn & I. Ryzhik. *Table of Integrals, Series, and Products*, 5th. (Academic Press, London, 1994).

87. Michael A Savageau. Michaelis-Menten Mechanism Reconsidered: Implications of Fractal Kinetics. *Journal of Theoretical Biology*. **176**, pp. 115-124 (1995).

88. B. West, W. Zhang, & H. Mackey. Chaos, Noise, and Biological Data, in: *Fractals in Biology and Medicine*, 38-54, (Birkhauser Verlang, Basel, Switzerland, 1993).

89. Peter Veng-Pedersen. System Approaches in Pharmacokinetics: II. Applications. *Journal of Clinical Pharmacolog*, **28**, 97-104 (1988).

90. Kim-Chi T. Hoang. Physiologically based pharmacokinetic models: mathematical fundamentals and simulation implementations. *Toxicology Letters*. **79**, pp. 99-106 (1995).

91. Horst A. Welker. Single- and Multiple-dose Mibefradil Pharmacokinetics in Normal and Hypertensive Subjects. *Journal of Pharmacy and Pharmacology*. **50**, pp. 983-987 (1998).

92. S. Huet, A. Bouvier, M.-A. Gruet, & E. Jolivet (all women). *Statistical Tools for Nonlinear Regression*. (Springer-Verlag, New York, 1996).

93. G. A. F. Seber & C. J. Wild. *Nonlinear Regression*. (John Wiley & Sons, Inc., New York, 1989).

94. L. Anacker & R. Kopelman. Steady-State Chemical Kinetics on Fractals: Geminate and Nongeminate Generation of Reactants. *J. Chem. Phys*. **91**, pp. 5555-5557 (1987).

95. L. Li & R. Kopelman. Influence of External Steady Source Structure on Particle Distributions and Kinetics of Diffusion-Limited Reactions I: A+A→0 Simulations. *J. Phys. Chem*. **96**, pp. 8079-8084 (1992).

96. G. A. Milliken & D. E. Johnson. *Analysis of Messy Data*, Vol. I. (Chapman & Hall, London, 1992).

97. D. C. Hoaglin, F. M. Mosteller, & J. W. Tukey. *Understanding Robust and Exploratory Data Analysis*. (John Wiley & Sons, Inc., New York, 1983).

98. P. J. Rousseeuw & A. M. Leroy. *Robust Regression and Outlier Detection*. (John Wiley & Sons, Inc., New York, 1987).

99. A. Atkinson & M. Riani. *Robust Diagnostic Regression Analysis*. (Springer-Verlag, New York, 2000).

Other Important Sources

Ray Redheffer. *Differential Equations: Theory and Applications*, (Jones & Bartlett, Boston, 1991).

Robert Audi (editor). *The Cambridge Dictionary of Philosophy*,
(Cambridge University Press, Cambridge, 1999).

A. D. Smith (managing editor). *The Oxford Dictionary of Biochemistry and Molecular Biology*,
(Oxford University Press, Oxford, 2000).

Y. K. Tam, B. A. Saville, & M. R. Gray. Models of Hepatic Drug Elimination.
Drug Metabolism Reviews, **24** (1), 49-88 (1992).

Appendix

> The world is full of obvious things which nobody by any chance ever observes.
> -Sherlock Holmes, *The Hound of the Baskervilles*
> Sir Arthur Conan Doyle

A1. An Introduction to Lambert's W Function

The omega function, product log function, ProductLog[x] in *Mathematica* notation, or Lambert's W-function, is a generalization of the natural log function, and a comparison has heuristic value:

$$\text{natural logarithm}: x = e^y \iff \ln[x] = \ln[e^y] = y, \text{ while}$$

$$\text{product log}: z = \omega e^\omega \iff W[z] = W[\omega e^\omega] = \omega.$$

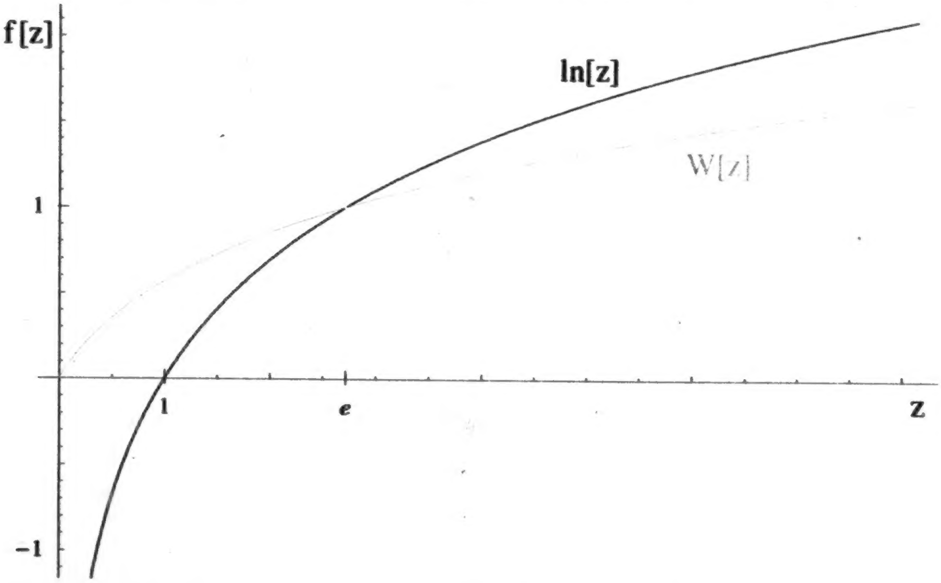

Figure a.1: A graphical comparison of the obscure product log function, *W*[*z*], with the related ubiquitous natural logarithm function, ln[z].

The derivative of *W* is

$$W'[z] = \frac{1}{(1+W[z])\,e^{W[z]}} = \frac{W[z]}{z(1+W[z])}, \quad z \neq 0.$$

The omega function satisfies the differential equation

$$\frac{df}{dz} = \frac{f}{z(1+f)}.$$

Lambert's W-function has the series expansion

$$W[z] = \sum_{i=1}^{\infty} \frac{(-1)^{i-1}\, i^{i-2}}{(i-1)!} z^i.$$

W(1) is called the "omega constant" and can be considered a sort of "golden ratio" of exponentials since

$$e^{-W[1]} = W[1] \Rightarrow \ln\left[\frac{1}{W[1]}\right] = W[1].$$

A2. A Recapitulation of the Method of Least-Squares Approximation Over Discrete Sets of Points

Consider the case when the data comprise a discrete set of *N* points, (t_1, C_1), (t_2, C_2), …, (t_N, C_N). Let the approximation of the data at any of the points be a sum of basis functions, ϕ_j, linear in the parameters, a_j, of the form

$$C_i \approx \sum_{j=1}^{M} a_j\, \phi_j[t_i] \equiv C[t_i; a_1, \ldots, a_M], \tag{a.1}$$

where $M<N$. Now the best approximation in the least-squares sense for the above equation is defined to be that for which the parameters are determined so that the magnitude of the chi-squared function is at its nadir:

$$\text{minimize}\,\chi^2 \equiv \sum_{i=1}^{N} w_i[t_i]\,(C_i - C[t_i; a_1, \ldots, a_M])^2 ,$$

where $w_i[t_i]$ is the weight assigned to that datum point, such that often $w_i[t_i]$ is a function of C_i, and C_i-$C[t_i]$ is called the residual at t_i. This requirement imposes the necessary conditions

$$\frac{\partial}{\partial a_r} \sum_{i=1}^{N} w_i[t_i]\,(C_i - C[t_i; a_1, \ldots, a_M])^2 = 0, \qquad (r = 1,\ 2,\ \ldots,\ M),$$

that lead to the exactly solvable M simultaneous linear equations in the M unknown parameters $a_1, a_2, \ldots, a_M$. These important "normal equations" of the method of least-squares can be obtained ⟨45⟩ through an elementary process by first writing down the N equations which would require that (a.1) be an equality at the N points t_i by direct substitution. The rth normal equation is obtained by multiplying each equation by the coefficient of a_r, that being $\phi_r[\_]$ for this set of equations, and by the weight associated with that equation, and summing the results, as follows:

$$\begin{array}{l l}
\phi_1[t_1]\,a_1 + \phi_2[t_1]\,a_2 + \cdots + \phi_M[t_1]\,a_M = C_1 & \times\phi_r[t_1] \quad \times w[t_1] \\
\phi_1[t_2]\,a_1 + \phi_2[t_2]\,a_2 + \cdots + \phi_M[t_2]\,a_M = C_2 & \times\phi_r[t_2] \quad \times w[t_2] \\
\qquad\qquad \vdots & \qquad \vdots \\
\phi_1[t_N]\,a_1 + \phi_2[t_N]\,a_2 + \cdots + \phi_M[t_N]\,a_M = C_N & \times\phi_r[t_N] \quad \times w[t_N] \\
+ \overline{\qquad\qquad\qquad\qquad\qquad\qquad\qquad\qquad} & \\
\quad \varsigma_{r,1}\,a_1 + \varsigma_{r,2}\,a_2 + \cdots + \varsigma_{r,M}\,a_M = \xi_r \quad (r\text{th normal equation}), &
\end{array} \tag{a.2}$$

where $\varsigma_{r,j}$ are the constant coefficients of the unknown parameter variables a_j described by

$$\varsigma_{r,j} = \sum_{i=1}^{N} w[t_i]\,\phi_r[t_i]\,\phi_j[t_i]$$

and ξ_r are constants described in terms of known values by

$$\xi_r = \sum_{i=1}^{N} w[t_i]\,\phi_r[t_i]\,C_i\,.$$

A3. A Brief Definition of the Gaussian Distribution

The normalized Gaussian distribution is a probability density function

$$f_{X,\sigma}[x] = \frac{1}{\sigma\sqrt{2\pi}}\,e^{-\frac{(x-X)^2}{2\sigma^2}}\,,$$

where X is the center (the mean), and σ is the width (standard deviation) of the distribution, while x is the independent variable. The function describes the limiting distribution of results in an independently repeated measurement of a quantity x whose true value is X, if the measurement is subject only to random errors ⟨33⟩.

A4. Coda of Pharmacokinetic Concepts

Volume of Distribution

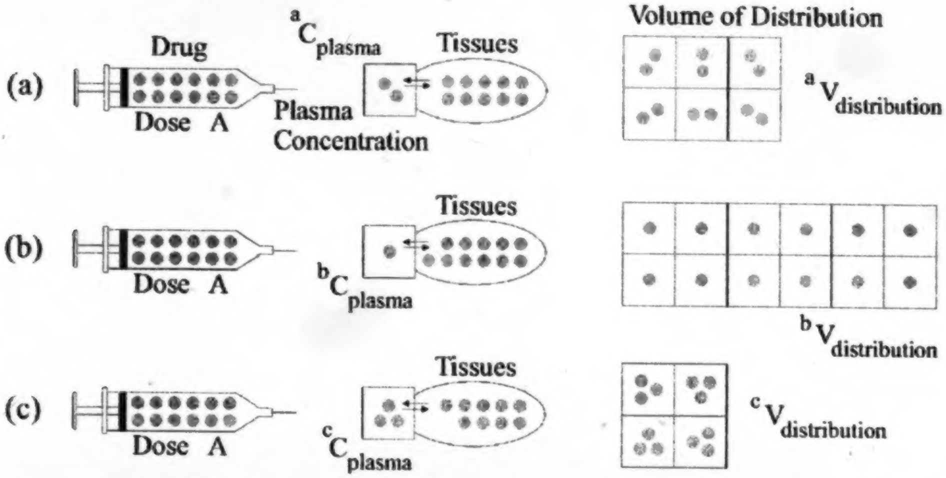
Volume of Distribution
(a)
Drug
Dose A
${}^{a}C_{plasma}$
Tissues
Plasma Concentration
${}^{a}V_{distribution}$
(b)
Dose A
Tissues
${}^{b}C_{plasma}$
${}^{b}V_{distribution}$
(c)
Dose A
Tissues
${}^{c}C_{plasma}$
${}^{c}V_{distribution}$

Figure a.2: (a) The administration of a drug into the body produces a specific plasma concentration. The apparent volume of distribution, $V_{distribution}$, is the volume that accounts for the total dose administered based upon the observed plasma concentration, $C_{concentration}$. (b) Any factor that suppresses the drug plasma concentration will increase the apparent volume of distribution. (c) Conversely, any factor that increases the plasma concentration will decrease the apparent volume of distribution ⟨5⟩.

Drug located outside of the plasma is present in the tissues. The apparent volume of a tissue compartment has two basic determinants: physiologic weight or volume of each tissue (V_i) and partition or distribution factors (K_i). Whenever tissues are grouped together for analysis their apparent volumes are combined

$$V_{tissues} = \sum_{i} K_i V_i$$

and the volume at steady state is $V_{ss} = V_{plasma} + V_{tissues}$.

Additional Noncompartmental Analysis Formulas - Statistical Moments

The time course of drug concentration in plasma can at times be regarded as a statistical distribution curve ⟨6⟩. Irrespective of the route of administration, the zero and second moments are defined as follows:

$$\mathrm{AUC} = \int_0^{\infty} \mathrm{C}[\mathrm{t}]\, d\mathrm{t} \quad \wedge \quad \mathrm{MRT} = \frac{\int_0^{\infty} \mathrm{C}[\mathrm{t}]\, d\mathrm{t}}{\int_0^{\infty} \mathrm{C}[\mathrm{t}]\, d\mathrm{t}} = \frac{\mathrm{AUMC}}{\mathrm{AUC}},$$

where MRT is the mean residence time of the drug in the body and AUMC stands for Area Under the first Moment Curve. With the above values, estimates for the Pharmacokinetic parameters of drug bioavailability, clearance, half-life, volume of distribution, mean absorption time, and fraction metabolized can be simply calculated ⟨89⟩.

A5. Expounders of the Developement of the PBPK Mathematical Model

The $(\eta+2)\times(\eta+2)$ coeifficient matrix, $\mathbf{A}[t]$, of (5.1) characterizes the pharmacok inetic intercourse between compartments of the PBPK model.

$$\mathbf{A}[\mathrm{t}] = \begin{bmatrix} -\frac{Q_b}{V_b} & \frac{Q_1}{R_1 V_1} & \frac{Q_2}{R_2 V_2} & \cdots & \frac{Q_\eta}{R_\eta V_\eta} & \frac{Q_h}{R_h V_h} \\ \frac{Q_1}{V_b} & \frac{-Q_1}{R_1 V_1} & 0 & \cdots & 0 & 0 \\ \frac{Q_2}{V_b} & 0 & \frac{-Q_2}{R_2 V_2} & 0 & \cdots & 0 \\ \vdots & \vdots & 0 & \ddots & 0 & 0 \\ \frac{Q_\eta}{V_b} & 0 & \vdots & 0 & \frac{-Q_\eta}{R_\eta V_\eta} & 0 \\ \frac{Q_h}{V_b} & 0 & 0 & 0 & 0 & -\left(\frac{-Q_h}{R_h V_h} + \frac{\kappa}{V_h} \mathrm{t}^{-\zeta}\right) \end{bmatrix}$$

After substitution of the series expanasion of $t^{-\zeta}$, the coefficient matrix could be expressed as the series,

$$\mathsf{A}[t, \zeta] = \mathsf{A}_0 - \ln[t]\, \mathsf{A}_c\, \zeta + \frac{1}{2} (\ln[t])^2\, \mathsf{A}_c\, \zeta^2 - \dots \, .$$

The first term of the coefficient matrix series was

$$\mathsf{A}_0 = \begin{bmatrix} -\frac{Q_b}{V_b} & \frac{Q_1}{R_1\,V_1} & \frac{Q_2}{R_2\,V_2} & \cdots & \frac{Q_\eta}{R_\eta\,V_\eta} & \frac{Q_h}{R_h\,V_h} \\ \frac{Q_1}{V_b} & \frac{-Q_1}{R_1\,V_1} & 0 & \cdots & 0 & 0 \\ \frac{Q_2}{V_b} & 0 & \frac{-Q_2}{R_2\,V_2} & 0 & \cdots & 0 \\ \vdots & \vdots & 0 & \ddots & 0 & 0 \\ \frac{Q_\eta}{V_b} & 0 & \vdots & 0 & \frac{-Q_\eta}{R_\eta\,V_\eta} & 0 \\ \frac{Q_h}{V_b} & 0 & 0 & 0 & 0 & \frac{Q_h}{R_h\,V_h} - \frac{\kappa}{V_h} \end{bmatrix};$$

the same matrix to be expected if the physiological model implemented only classical kinetics. For the remainder of the matrix series, only a simple $(\eta+2)\times(\eta+2)$ constant matrix appears

$$\mathsf{A}_c = \frac{-\kappa}{V_b}\,\delta_{bb} = \frac{-\kappa}{V_b}\begin{bmatrix} 0 & 0 & 0 & 0 \\ 0 & 0 & 0 & 0 \\ 0 & 0 & 0 & 0 \\ 0 & 0 & 0 & 1 \end{bmatrix}.$$

The coefficient matrix, $\mathsf{A}[t,\zeta]$, can also be expressed as the series

$$\mathsf{A}[t, \zeta] = \mathsf{A}_0 + \zeta \mathsf{A}_1[t] + \zeta^2\, \mathsf{A}_2[t] + \dots \, ,$$

where

$$\mathsf{A}_n[t] = \frac{(-1)^n}{n!} (\ln[t])^n\, \mathsf{A}_c \, , \; n \geq 1.$$

An Introduction to the Matrix Exponential ⟨82⟩

Let the $n \times n$ constant matrix A have n distinct eigenvalues, λ_j, and a characteristic polynomeal $P[s] = (s-\lambda_1)(s-\lambda_2)\dots(s-\lambda_n)$. A matrix exponential form with A is

$$e^{\mathsf{A}t} = \mathsf{M}_1\, e^{\lambda_1 t} + \mathsf{M}_2\, e^{\lambda_2 t} + \dots + \mathsf{M}_n\, e^{\lambda_n t} \, ,$$

possessing the same behavior of the exponential function under derivation: $(d/dt)e^{\Lambda t}=e^{\Lambda t}\Lambda$. The square matrices of order n are given by $\mathbf{M}_j=L_j[\Lambda]$, where Lagrange polynomeals are designated to be $L_j[s]=(N_j[s])/N_j[\lambda_j]$, where $N_j[s]$ is obtained by omitting the factor $(s-\lambda_j)$ from $P[s]$.

The Definition of the Method of Variation of Parameters

$$\vec{Y}' = \Lambda\vec{Y}+\vec{f}[t] \quad \Rightarrow \quad \vec{Y}=e^{\Lambda t}\int e^{-\Lambda t}\,\vec{f}[t]\,dt \tag{a.3}$$

A6. Expounders of the Solution of the Multicompartmental Mathematical Model

The two zeroth order pertubation exponential coefficients have the explicit values of

$$s=\frac{-(a+b+k)\pm\sqrt{(a+b+k)^2-4ak}}{2}\ \text{(eigenvalues)}.$$

$\because a,b,k>0 \Rightarrow (a+b+k)^2\text{-}4ak<(a+b+k)^2 \Rightarrow s<0$, so $\exists$ real unequal eigenvalues of the same sign (-), such that the critical point $(X_1,X_2)\hat{=}(0,0)$ is called a nodal sink. The coefficients ϑ_1 and ϑ_2 take the values

$$\vartheta_1=\frac{\text{Ӿ}\left(-a+b+k+\sqrt{(a+b+k)^2-4ak}\right)}{2\sqrt{(a+b+k)^2-4ak}},$$

$$\vartheta_2=\frac{\text{Ӿ}\left(a-b-k+\sqrt{(a+b+k)^2-4ak}\right)}{2\sqrt{(a+b+k)^2-4ak}}.$$

The Euler gamma function is defined by the integral $\Gamma[z]=\int_0^\infty t^{z-1}\,e^{-t}\,dt$, and can be viewed as a generalization of the factorial function, valid for complex z.

The exponential integral is defined by $\mathrm{Ei}[z] = -\int_{-z}^{\infty} e^{-t}/t\,dt$.

The generalized hypergeometric function has a series expansion, ${}_pF_q[\overline{\alpha};\overline{\beta};z] = \sum_{k=0}^{\infty} (\alpha_1)_k \ldots (\alpha_p)_k / \{(\beta_1)_k \ldots (\beta_1)_q\} z^k / k!$.

Glossary of Scientific & Literary Vocabulary

Many of the following definitions are specific to this thesis, such that the words or phrases may have other, or more general, definitions in a different context.

aberrant - deviating from the ordinary, usual, or normal type; exceptional.

abscissa - Cartesian coordinate obtained by measuring parallel to the x-axis.

abstract - disassociation from any specific instance.

accede - to express approval or give consent.

ad hoc - for the particular end or case at hand without consideration of wider application: improvised.

ad libitum - in accordance with one's wishes; abbreviated as ad lib.

admonishment - to express warning or disapproval to especially in a gentle, earnest, or solicitous manner.

adscititious - derived or acquired from something extrinsic.

adsorbent - a solid that absorbs another substance from a gas or liquid phase.

aegis - control or guidance especially by an individual or, group, or system.

ameliorate - to make better or more tolerable; improve.

amenable - liable to be brought to account; capable of submission.

analytical chemistry - the branch of chemistry concerned with analyzing materials by chemical methods.

anatomy - the branch of biology concerning the structure of organisms.

angina pectoris - brief attacks of chest pain precipitated by insufficient oxygenation of the heart.

antagonist - a drug that reduces the action of another agent.

appertain - to belong as a part, right, possession, attribute, etcetera; relate.

a priori - relating to or derived by reasoning from self-evident propositions.

archetype - the original pattern or model of which all things of the same type are representations or copies.

arteriole - any of the small terminal twigs of an artery that ends in capillaries.

assay - the determination of the concentration of a drug in comparison with that of a standard preparation.

batch reaction - a reaction process where the reactants (drugs and enzymes for this paper) are introduced with some given initial concentration without any further introductions such that a nonzero steady state is never achieved.

begat - to sire or produce especially as an effect or outgrowth.

biliary - relating to bile-conveying structures.

bioavailability - the fraction of an oral dose that actually reaches the systemic circulation of the biological model system.

biochemistry - the branch of science dealing with the chemical compounds, reactions, and other processes that occur in living organisms.

biophysics - the application of physical techniques and physical methods of analysis to biological problems.

bolus - a large pill, as used in medicine.

calcium - Ca^{2+}; high intracellular $[\![Ca^{2+}]\!]$ causes smooth muscle contraction around blood vessels and contributes to high blood pressure.

canon - an accepted principal, rule, standard, or norm.

cantankerous - difficult or irritating to deal with.

capacitate - to make capable; enable.

capillary - any of the very fine blood vessels that form a network between the arterioles and the venules throughout the body.

celerity - rapidity of motion or action.

chromatogram - the result of a chromatographic separation that may be visible or that may take the form of a graph after processing of data.

chromatography - a group of analytical techniques for separating the components of a mixture by differential adsorption of compounds to adsorbents or other means.

chronic - marked by long duration and frequent or continuos recurrence.

clearance - a measurement of the body or an organ to remove drug from the plasma, measured as a volume per unit time (flow) of blood from which all drug is extracted and excreted or metabolized. In pharmacokinetic terms, clearance is the extraction rate divided by the plasma concentration of drug.

clinical pharmacokinetics - is a health sciences discipline that deals with the application of pharmacokinetics to optimize the pharmacotheraputic management of individual patients.

coda - something that serves to round out, conclude, or summarize and that has an interest of its own.

collagen - a group of insoluble fibrous proteins of very high tensile strength that form the main component of connective tissue.

compact set - a set E in a metric space (X, d) is compact $\Longleftrightarrow \forall$ sequence of points $\{p_n\} \subset E$, $\exists$ some subsequence $\{q_n\} \subset \{p_n\}$ which converges to a point $p_o \in E$.

concoct - to prepare by combining raw materials; devise; fabricate.

conduce - to lead or tend to a particular result.

congruous - being in agreement, harmony, or correspondence.

convolution - The expression $w[t] = (f*g)[t] = \int_0^t f[t']\, g[t-t']\, dt$ is called the convolution of f and g. It gives the response at the present time t as a weighted superposition over the inputs at times $t' \leq t$. The weighting factor $g[t-t']$ characterizes the system and $f[t']$ characterizes the past history of the input.

curt - short; shortened; brief; abrupt in manner.

demarche - a course of action; maneuver.

deportment - the manner of conduct.

didactic - designed or intended to teach.

diminutive - indicating small size.

disposition rate constant - in terms of classical compartmental models, it is the first order rate constant used to describe the concentration time-course data, expressible as a function of the individual intercompartmental transfer rate constants and elimination constants.

distributive phase - after a rapid i.v. injection of drug, the finite time for a drug to distribute fully throughout the available body space.

Dyson, Freeman J. - (1923-) physicist, Fellow of the Royal Society, London; Professor Emeritus, Princeton, NJ; never received a PhD.

ecological fallacy - invalid conclusions about causality may occur when relationships between variables measured at the group level are assumed to apply at the individual level.

embedding dimension - the dimension of the Euclidean space $\mathbb{R}^n$ in which a shape (fractal) F resides, thus $d_E \equiv n$. For a warped surface in $\mathbb{R}^3$, for example, $d_T = 2$, and $d_E = 3$.

endogenous - arising or developing within an organism, tissue, or cell, and excluding any consequences of externally added drugs.

endothelium - the single layer of thin, flattened cells that lines the blood vessels as in the liver.

entropic - chaotic, disorganized, and random.

enzyme - a biological macromolecular substance composed wholly or largely of protein, that catalyzes, more or less specifically, one or more biochemical reactions at relatively low temperatures.

epistemology - the study or a theory of the nature and grounds of knowledge, especially with reference to its limits and validity.

ergo - therefore; hence.

erythrocyte - red blood cell; hemoglobin-containing cells that carry oxygen to the tissues and are responsible for the red color of blood.

et alia - and others; abbreviated as et al.

evince - to constitute outward evidence of.

exemplar - serving as a pattern.

exempli gratia - for example; abbreviated as e.g..

exogenous - originating outside an organism, tissue, or cell.

expounder - the noun form of verb expound - to state; to explain in careful detail.

extraction ratio - the fraction of drug which is removed from the plasma as it passes through an eliminating organ.

extremum - the maximum or minimum of a mathematical function.

fact - an observed configuration.

fenestra - a small anatomical opening among the hepatic endothelial cells between the space of Disse and the sinusoidal lumen.

figure-of-merit function - a function that measures the degree to which a model approximates a data set.

first-order rate - the rate of change in drug concentration or amount of drug, is proportional to the drug concentration, such that, $dC/dt \propto [\![C]\!]$.

first-pass effect - since all the blood emerging from the intestines first passes through the liver, the fraction of drug reaching the systemic circulation is given by $1 - ER$, where ER is the extraction ratio of the liver. Therefore, the first-pass effect is a significant characteristic of drugs with a high hepatic extraction ratio.

fractal - any of various extremely irregular curves or shapes for which any suitably chosen part is similar in shape or statistical feature to a given larger or smaller part when magnified or reduced to the same size.

Gaussian distribution - a probability density function defined in Appendix 3; also called a normal distribution.

global optimization - the process of locating an extremum of an equation with perhaps more than one local extrema.

Golden ratio - often called φ; has the following properties: $\varphi^2 = \varphi + 1$, it is the limit of $F[i+1]/F[i]$ as $i \to \infty$ where F is the Fibonacci relationship $F[i+2] = F[i+1] + F[i]$, and finally, it can be expressed as a continued fraction $\varphi = 1+1/(1+1/(1+1/(1+\ldots)))$.

ground substance - a more or less homogeneous matrix that forms the background in which the specific differentiated elements of a system are suspended; the intercellular substance of tissues.

Hatcher, William S. - (1935-) Canadian philosopher and Professor of Mathematics at Laval University.

Hausdorff dimension - for a shape F imbedded in D-dimensional Euclidian space S_D, define the measure M_ε to be

$$M_\varepsilon = \varepsilon^D N_\varepsilon$$

where $\varepsilon \in \mathbb{R}$ and N_ε is the minimum number of points in the space S_D such that every point in F lies within a neighborhood of radius ε of at least on point.

The Hausdorff dimension of F would be

$$d_h = \lim_{\varepsilon \to 0} \frac{\ln[N_\varepsilon]}{\ln[\varepsilon]}.$$

A simple way of estimating the Hausdorff dimension for fractals is by calculating the box-counting dimension. First compute the box-counting dimension from a grid that is superimposed on a fractal image and count how many boxes in the grid contain part of the fractal. Then increase the number of boxes in the grid (but covering the same area: the boxes get smaller) and count again. If the number of boxes in the first and second grids are G_1 and G_2, and the counts are C_1 and C_2, then you compute a dimension by the formula: $d_h \approx \ln[C_2/C_1] / \ln[\sqrt{G_2/G_1}]$.

hepatocyte - the major cell type of the liver. They are arranged in folding sheets facing blood-filled spaces called sinusoids. Hepatocytes are responsible for the metabolism of a wide range of substances including mibefradil.

Hertzian distribution - a one sided distribution with maximum probability at $r=0$.

homomorphic - a structure preserving mapping from one structure to another, such that, if objects in the first structure bear a certain relationship to one another, then their images in the second structure under the mapping bear the corresponding relation to one another.

HPLC - High Performance Liquid Chromatography.

hypertension - abnormally high arterial blood pressure.

id est - that is; abbreviated as i.e..

illation - a conclusion inferred; the action of inferring.

inscrutable - not readily investigated, interpreted, or understood.

interface - a surface forming a common boundary of two bodies, spaces, or phases.

intersperse - to place something at intervals in or among.

interstitial fluid - the portion of the extracellular fluid, consisting mainly of water, that occurs outside the blood vessels and the lymphatics.

intravenous - within a vein; used especially of an injection, infusion, transfusion, or aspiration; abbreviated as IV or i.v..

in vitro - of any biological process occurring or made to occur outside an organism; "in glass".

in vivo - of any biological process occurring or made to occur within a living organism; "in life".

juxtaposed - to place side by side.

laudable - worthy of praise; commendable.

law of mass action - the rate of a simple process (reaction) is proportional the concentrations of each of the reactants under homogeneous conditions.

law of superposition - a model follows this law when its responses (outputs) to different test inputs (φ, ψ) are additive, such that $\mathcal{L}[a\varphi + b\psi] = a\mathcal{L}[\varphi] + b\mathcal{L}[\psi]$, where $\mathcal{L}$ is a linear operator and a and b are constants.

linearity - a word with multiple meanings: in pharmacokinetics, a biological model system is said to be linear if the systemic drug concentration at any time is a function of the unit impulse response and directly proportional to the dose, such that it obeys the law of superposition. A mathematical model is linear in its parameters when it can be expressed as a sum of products between a parameter and a basis function. A differential operator, T, is said to be linear if it is of the form $T[y] = y^{(n)} + p_{n-1}\, y^{(n-1)} + \ldots + p_1\, y' + p_0\, y$, where $y = y[x]$, and $p_i = f[x]$.

lobules - a fundamental histological unit containing a sinusoid plexus.

lumen - the cavity of a tubular organ space, exempli gratia, within the sinusoids.

lumped-parameter - adjective used to describe a compartment in a PBPK model wherein it is assumed that the drug concentration is homogeneous and the transport process is only time dependent.

macroconstant - in classical multicompartment analysis, the constants of the sum of exponentials that fit the data, A_i and a_i, of equation (1.10) that are functions of the microconstants, V_j and k_j, of the multicompartmental model.

mammillary system - a classical linear pharmacokinetic multicompartmental model designed with a central compartment on which drug concentration measurements are made, to which the drug is assumed to be administered, from which the drug is assumed to be eliminated, and with which secondary compartments exchange drug in parallel by first-order processes.

Matisse, Henri - (1869-1954) French painter and sculptor; studied under Moreau; influenced by Post-Impressionism; became a leader among the Fauvists; resident chiefly at Nice; probably knew very little about Pharmacokinetics.

matrix - a mass by which something is enclosed or in which something is embedded; a rectangular array of numbers or functions.

mean residence time - the average total time the drug molecules spend in the systemic circulation.

merit function - see figure-of-merit function.

metabolism - the totality of the chemical reactions and physical processes undergone by a drug in a living organism.

metabolite - any substance, such as a drug, that is formed or changed by metabolism.

metric space - is a pair (X,d) where X is a set and d is a function, which $\forall$ x,y,z $\in X$, satisfies: 1) $d[x,y] \neq 0$. 2) $d[x,y]=0 \Leftrightarrow x=y$. 3) $d[x,y]=d[y,x]$ (symmetry). 4) $d[x,z] \leq d[x,y]+d[y,z]$ (triangle law), where d is called a metric for X and $d[x,z]$ is the distance from x to y.

Michaelis-Menten kinetics - a model to explain the kinetics of a saturable enzyme.

microvascular - relating to the part of the circulatory system made up of minute vessels that average less than 0.3 mm in diameter.

microvillus - a microscopic projection of tissue, especially any of the finger-like outward projections of some cell surfaces.

model - a conceptual representation of a particular phenomenon, system, or set of experimental observations as an aid to understanding and as an object for test or for further experimentation.

model system - any biological or biochemical system (exempli grata a dog) that is used for study because it is considered to be representative of one or more other (often more complex) systems in which similar phenomena occur or are believed to occur.

nadir - the lowest point.

neighborhood - let $\varepsilon \in \mathbb{R} \wedge \varepsilon > 0$, then an open ε-neighborhood of a point $x^* \in \mathbb{R}^M$ is defined as the open ball

$$B[x^*] := \{x \in \mathbb{R}^M : \|x - x^*\| < \varepsilon\}$$

centered at x^* with radius ε.

noncompartmental - a class of pharmacokinetic models of data with generally simple assumptions providing efficient accurate empirical interpretations of data for clinical pharmacokinetics.

notional - speculative; existing in the mind only.

obfuscate - darken; to make obscure; confuse.

open cover - for a set E in a metric space (X, d), a collection $\{G_\alpha\}$ of open subsets of X is a cover if $E \subset \bigcup_\alpha G_\alpha$.

open set - for a metric space (X, d), a subset $U \subset X$ is open in X if $\forall\, x \in U, \exists\, \varepsilon > 0 \ni \mathrm{B}[x, \varepsilon] \subset U$.

ordinate - Cartesian coordinate obtained by measuring parallel to the y-axis.

ostensible - being such in appearance; plausible rather than demonstrably true or real.

paradigm - a philosophical and theoretical framework of a scientific school or discipline within which theories, laws, and generalizations and the experiments performed in support of them are formulated.

parsimony - economy in the use of means to an end.

partition coefficient - the ratio of the equilibrium concentrations of a pure substance dissolved in two phases that are in contact.

PBPK Models - Physiologically Based PharmacoKinetic Models.

pedantic - ostentatiously learned; making a show of knowledge.

penultimate - next to the last.

per - according to.

peri - near; around; enclosing; surrounding.

pharmacodynamics - the branch of pharmacology dealing with the effects of drugs on the body, id est, with the physiological, therapeutic, and toxicological responses to drugs with particular regard to the extent and time course of such effects; "power of drugs"

pharmacokinetics - the branch of pharmacology dealing quantitatively with the movement of drugs within the body, id est with the absorption, distribution, metabolism, and elimination of drugs; "movement of drugs"

pharmacology - the science or study of drugs - their origin, characteristics, identification, biological effects, and modes of action.

phenomenological - known through the senses rather than intuition; concerned with phenomena rather than hypotheses.

physical chemistry - the branch of chemistry concerned with the relationship between the physical properties of substances and their chemical properties, reactions, and structures.

physics - the science concerned with the properties of matter and of energy, and with the interactions and interconversions between matter and energy.

physiology - the science of dealing with the functioning of cells, tissues, organs, and organisms, and with the chemical and physical phenomena concerned.

plasma - the proteinaceous fluid in which the cells of blood are suspended and unbound drug is dissolved; plasma = serum + fibrin + fibrinogen.

plexus - a network of interlacing blood vessels.

portal vein - a large vein that is formed by fusion of other veins, that terminates in a capillary network, and that delivers blood to some area of the body other than the heart. Hepatic portal vein: a portal vein carrying blood from the capillaries of the stomach, intestine, spleen, and pancreas to the sinusoids of the liver.

posit - to purpose as an explanation.

precept - a principal intended as a general rule of action.

proem - a preliminary comment.

proffer - to put before a person for acceptance.

puissance - strength; power.

recalcitrant - difficult to manage; not responsive to treatment; resistant; unruly.

reductionism - a procedure or theory that reduces complex data or phenomena to simple terms; the attempt to explain all biological processes by the same explanations (as by physical laws) that chemists and physicists use to interpret inanimate matter.

reductionist fallacy - when relationships between variables measured at the level of individuals are assumed to apply at the group level.

renal - pertaining to, or of, the kidney.

replete - to fully or abundantly provide or fill; opposite of deplete.

residual - absolute difference between a measured value and a calculated value.

rubric - name; title; something under which a thing is classified: category.

secondary - immediately derived from something original, primary, or basic.

second order reaction - the rate of change in drug concentration or amount of drug, is proportional to the drug concentration and the concentration of another reactant, such that $dC/dt \propto [\![C]\!][\![E]\!]$.

self similarity - the common characteristic of fractals, whereby in statistical or qualitative terms, smaller parts of a fractal are related to larger parts.

sequester - separation, isolation.

serum - the watery portion of an animal fluid after coagulation.

simulation - a description of the experimental observations in a form concise or more evident, but neutral as to the causes involved.

singularity - the point at which the derivative of a given function does not exist but every neighborhood of which contains points for which the derivative exists.

sinusoid - a minute endothelium-lined space or passage for blood in the tissues of the liver.

solute - a dissolved substance (drug) in a solvent composing a solution.

spline function - a function used to specify a specific function on an interval consisting of pieces that are defined on subintervals, usually as polynomial or some other simple form.

steady state - a situation of unchanging drug concentration in a biological model system achieved when the rate of drug administration is equal to the rate of drug elimination.

substrate - a substance that is acted upon, especially by an enzyme.

sundry - various or diverse.

superfluous - exceeding what is sufficient or necessary.

systemic - concerning the whole of the body of an animal rather than an individual part.

tenet - a principal, belief, or doctrine generally held to be true.

topological dimension - This dimension is defined on local properties for all points in F, and corresponds to the intuitive notion of dimension $d=0$ for points, $d=1$ for lines and smooth curves, $d=2$ for surfaces, etcetera, without regard of how F is embedded in a higher dimensional space. A recursive definition can be given, such that (a) $d_T = 0$ if F is not connected (exempli gratia, points), and (b) $d_T = k$, $k \geq 1$ if any $p \in F$ has arbitrarily small neighborhoods $B[p]$ whose boundary has dimension $d_T = k\text{-}1$ and the intuitive notion follows, because for $k = 1$, all neighborhoods of points in a smooth curve is just an interval whose boundary consist of two points with dimension $d_T = k\text{-}1 = 0$. A closed curve may be the boundary of a point on a surface, and a closed surface defines a solid, etcetera. The topological dimension is preserved when an homeomorphism deforms the object.

topology - a branch of mathematics concerned with those properties of geometric configurations which are unaltered by elastic deformations that are homeomorphisms; configuration.

unctuous - revealing or marked by smug, exaggerated, assumed, or superficial earnestness or spirituality.

unit impulse response - the systemic drug concentration time-course resulting from the instantaneous input of a small unit of drug.

upshot - the gist as of an argument or thesis; final issue; end.

vascular - of or relating to a channel for the conveyance of a body fluid or to a system of such channels.

veracious - marked by conformity with truth or accuracy.

visceral - relating to the viscera - plural of viscus.

viscus - an internal organ of the body.

volume of distribution - the apparent volume required to account for all the drug in the body if it were present throughout the body in the same concentration as in the sample obtained from the plasma.

xenobiotic - of, or relating to, substances that are foreign to living systems.

zero order rate - a rate of change in drug concentration or amount of drug, that is independent of drug concentration, as is the case with a constant I.V. infusion, such that $dC/dt = \text{constant}$.